Conformation based *in vitro* selection of mammalian prion seeds – Propagation and characterization of prion strains

Von der Fakultät für Lebenswissenschaften

der Technischen Universität Carolo-Wilhelmina zu Braunschweig

zur Erlangung des Grades

eines Doktors der Naturwissenschaften

(Dr. rer. nat.)

genehmigte

D i s s e r t a t i o n

Felix Helge Deluweit
aus Wittmund

1. Referentin: Professor Dr. Christiane Ritter
2. Referent: Professor Dr. Martin Korte
eingereicht am: 27.02.2014
mündliche Prüfung (Disputation) am: 02.02.2015

Druckjahr 2015

Vorveröffentlichungen der Dissertation

Teilergebnisse der vorliegenden Arbeit wurden mit Genehmigung der Fakultät für Lebenswissenschaften, vertreten durch die Mentorin, in folgenden Beiträgen vorab veröffentlicht:

Tagungsbeiträge

Lührs, T.: Conformation selective prion amplification using specific shear fields, Konferenz Prion 2012, Amsterdam (2012).

Posterbeiträge:

Deluweit, F., Gupta, V., Lührs, T.: Optimal protein misfolding cyclic amplification of mammalian prions, Konferenz Amyloid, Halle (2011).

Danksagung

Ich möchte hiermit allen danken, die direkt oder indirekt an meiner Arbeit beteiligt waren.

Zunächst gilt mein Dank meiner Mentorin Prof. Dr. Christiane Ritter und Dr. Thorsten Lührs für die Förderung und das Ermöglichen dieser Arbeit.

Herrn Prof. Dr. Martin Korte vom Zoologischen Institut danke ich für die Übernahme des Koreferates und die Erstellung des Zweitgutachtens.

Herrn Prof. Dr. Michael Hust danke ich für die Übernahme des Prüfungsvorsitzes.

Dr. Verena Haist von der Tierärztlichen Hochschule Hannover danke ich für die Hilfestellung bei der intracerebralen Inokulation.

Prof. Dr. Michael Klein von Julius-Maximilans-Universität Würzburg gilt mein Dank für die Bereitstellung der verschiedenen Prionenstämme.

Ein ganz besonderer Dank geht an meine Arbeitsgruppe, besonders an Vandana Gupta, Jan Hellert und an Steffanie Loss.

Meinen Eltern möchte ich für Ihre stete Unterstützung danken.

Ein besonderes Dankeschön geht an Kathrin Fiege für all die Unterstützung.

Summary

Neurodegnerative disordes like Alzheimer disease, Parkinson disease and infectious prion diseases pose a significant threat to human health. Recent research associates these diseases with corruptive protein templating or seeding.[1] Interaction of protein monomers with their misfolded confomers, or seeds, induces a conformational alteration which resembles seeded crystallization.[2] The presumably self-perpetuating mechanism leads to seed amplification as the pathogenic aggregates corrupt more and more benign monomers over time. The first example of a self-templated protein misfolding was given by mammalian prion diseases, such as scrapie in sheep, BSE (bovine spongifrom encephalopathy) in cattle or new variant CJD (Creutzfeldt-Jakob disease) and kuru in humans.[3] It was demonstrated that prion infectivity can be maintained infinetely *in vitro* if periodic ultrasound pulses are used, a technique called Protein Misfolding Cyclic Amplification (PMCA).[4] In this context, it was proposed that prion amplifcation *in vitro* is promoted due to periodical fragmentation of the seeds.[5]

We successfully used PMCA to amplify Sc237 hamster prions, but also revealed the limitation of the method regarding its reproducibility. Based on conformation sensitive seed fragmentation we therefore developed the concept of Selective Shearing Amplification (SSA), which achieves seed fragmentation by fine-tuned shear forces *in vitro*. We hypothesized that conformational seed polymorphisms imply different structural stabilities. Thus, uniform seed populations might be conformationally selectable from natural, potentially mixed seed populations. Starting from a mixture SSA confers a selective advantage for optimally fragmented seeds which then become the dominant species. As opposed to this, seed populations which show a distinct mechanic fragmentability are suppressed. To validate the concept of SSA we surveyed the amplification of the closely related hamster prion strains Sc237 and 263K using a new ultrasonic as well as a mechanical approach. In ultrasonic SSA the shear forces are modulated by the distance of the reaction vials from the sound source. Furthermore the vibrational behavior of the used sonotrodes was considered. The experiments revealed that there is a clear distinction between both prion strains. In contrast to the ultrasonic approach, mechanical SSA is based on Couette-flow which generates a constant shear stress. Additionally, the technique makes it possible to test various parameters in parallel. Interestingly, the data showed to be in line with the results from ultrasonic SSA. While multiple seed conformations were detected in the Sc237 strain, mechanical SSA experiments with the cloned prion strain 263K revealed

only one detectable seed population. Furthermore, the presented method provides a way for kinetic seed amplification acquisition. Indeed, the kinetic seed amplification traces of the surveyed prion strains also showed clear differences. Thus, we concluded that the prion strain Sc237 is comprised of conformationally different seed populations.

Unfortunately, the underlying mechanisms of self-templated protein conversion remain elusive and the molecular structures of proteopathic seeds are still unknown. The concept of selective shearing amplification is not limited to prions and the identification and characterization of specific seed populations using SSA could provide a significant benefit to current research. The presence of more than one seed conformation, for example, might also be true for human neurodegenerative diseases like Alzheimer disease or Parkinson disease which have also been associated with proteopathic seeds. Using the conformation sensitive concept of SSA a future application could be the generation of kinetically selected, homogeneous seed preparations for detailed structural investigations.

Index

Summary **3**

1 Introduction **9**
1.1 Transmissible spoDeluweitngiform encephalopathies 9
1.2 The protein only hypothesis 13
1.3 Prion strains and transmission barriers 15
1.4 Protein misfolding 19
1.5 *In vitro* conversion of the prion protein 23
1.6 The cellular isoform of the prion protein (PrP^{C}) 27
1.6.1 The function of PrP^{C} 29

2 Objectives **31**

3 Materials and methods **32**
3.1 Materials 32
3.1.1 Chemicals 32
3.1.2 Enzymes 32
3.1.3 Size standards 32
3.1.4 Additional agents and materials 32
3.1.5 Bicellar mixtures 33
3.1.6 Instruments 36
3.1.7 Prion strains 37
3.1.8 Buffer solutions 37
3.2 Protein analytical methods 39
3.2.1 SDS-Polyacrylamid-gel electrophoresis (SDS-PAGE) 39
3.2.2 Prion sample proteinase K digest and western blotting 39
3.2.3 Quantification of prion samples by western blotting 41
3.3 Safety precautions for work with scrapie prions 41
3.4 *In vivo* prion propagation 42
3.5 Brain tissue homogenate 44
3.6 PrP^{Sc} amplification by ultrasonic processing 46
3.6.1 Protein Misfolding Cyclic Amplification (PMCA) 46
Reaction mix and preparation steps for PMCA 49
3.7 Selective Shearing Amplification (SSA) 51
3.7.1 Acoustic SSA 52
3.7.2 Test of the Acoustic SSA device 55
3.7.3 Mechanical Selective Shearing Amplification (SSA) 57

3.7.4 Mechanical SSA array 58
3.7.5 Proof of principle 59
3.7.6 Test of the SSA array 60
3.7.7 The kinetic buildup of PrP^{res} 60
Interprocessing delay 60
3.7.8 Non-processed reactions 61
3.7.9 Effect of seed and homogenate treatment 61
3.7.10 Effect of SDS 62
3.7.11 Reaction mix and preparation steps for mechanical SSA 62

4 Results 65
4.1 PrP^{Sc} amplification by ultrasonic processing 65
4.1.1 Protein Misfolding Cyclic Amplification (PMCA) 65
Conclusions 67
4.2 Acoustic SSA 68
Conclusions 69
4.3 Mechanical SSA 70
4.3.1 Proof of principle 70
Conclusions 71
4.3.2 Test of the SSA array 71
Conclusions 72
4.3.3 The kinetic buildup of PrP^{res} 73
Interprocessing delay 76
Conclusion 77
4.3.4 Non-processed reactions 78
Conclusion 78
4.3.5 Effect of seed and homogenate treatment 78
Conclusion 81
4.3.6 Influence of SDS 81
Conclusion 82

5 Discussion 83

6 Outlook 87

Appendix 90

Abbreviations 97

Bibliography 103

1 Introduction

1.1 Transmissible spongiform encephalopathies

Transmissible spongiform encephalopathies (TSEs) are infectious, progressive disorders that affect the central nervous system. These inevitable fatal diseases are characterized by long incubation times. The typical course of the disease is associated with a vacuolization of the grey matter. Beside astrogliosis – a proliferation of astrocytes – protein aggregates can be observed. Also neural cell loss, caused by apoptosis, and meningitis are described.[6–9] Distribution and intensity of histopathologic abnormalities strongly depend on cell tropism, toxicity, the hosts neural anatomy as well as its genetics.[7,10] Several examples for TSEs in human and animals are given in Table 1.1.

Table 1.1: Mammalian TSEs[11]

Disease	Abbrevation	Species	Incidence	Etiology
Creutfeldt-Jakob disease	fCJD	Human	Familial	*Prnp* mutation
	sCJD		Sporadic	?
	vCJD		iatrogenic	Infection
Gerstmann-Sträussler-Scheinker syndrome	GSS	Human	Familial	*Prnp* mutation
Fatal familial insomnia	FFI	Human	Familial	*Prnp* mutation
Bovine spongiform encephalopathy	BSE	Cattle	Iatrogenic	Infection
Scrapie		Sheep/goats	Iatrogenic	Infection
		Mouse (adapted)		Experiment
		Hamster (adapted)		Experiment
Chronic wasting disease	CWD	Elk/Mule deer	Iatrogenic	Infection

The Creutzfeldt-Jakob disease (CJD) is the most common TSE in human. However, only one incidence in a million occurs. It was discovered by H.G. Creutzfeldt in 1920. One year later several cases of the disease were described by A. Jakob. Four forms of CJD are known: The sporadic (sCJD), the familiar (fCJD), the iatrogen (iCJD) and the variant form (vCJD). About 85% of the CJD cases are sporadic and occur in human at the age of 50 to 75 years. Besides dementia the disease impairs the speaking ability, the movement and is often accompanied by muscle convulsions. First symptoms are usually forgetfulness, a loss of general interest and

social contacts as well as changes in eating and sleeping behavior. As the illness progresses, irregular walking, vision changes, slow talking and hallucinations can occur. Furthermore, incontinence and totally involuntary movements appear. Sporadic CJD usually leads to death one year after diagnosis.[12–15] The familial CJD, in contrast, is inherited and concerns only 10-15% of all CJD cases. Patients with fCJD are often younger than sCJD patients and carry specific mutations of the *Prnp* gene (cp. 1.6, p. 27 *et seqq.*).[16,17] The course of fCJD is longer compared to the sporadic form and the typical symptoms vary more. While sCJD and fCJD just appear or are genetically predisposed, iatrogen CJD is caused by contact with the infectious agent during medical procedures (gr. *iatr, iater* = doctor*; genes, genet* = genesis). Indeed, it was shown that contaminated surgical instruments pose a risk to patients and the effictivity of common decontamination techniques was questioned.[18,19,20,21,22]

In the year 1996, during the BSE-crisis, a new variant of CJD was firstly described[23] and until August 2012 173 cases were recorded.[24] Contrary to other CJD forms, the pathology of vCJD turned out to be considerably different: extensive amyloid plaque formation can be found in the cerebrum and the cerebellum.[23,25,26] The protein deposits are often surrounded by vacuoles, also referred to as florid plaques.[27] In sCJD and fCJD these protein plaques are rarer and occur in clusters of Purkinje cells. In contrast, the plaques in iCJD spread across the whole brain. Symptoms in vCJD can reach from lightly depressions and psychosis[28] to painful sensory abnormalities, ataxia and involuntary movements. Unlike sCJD the course of the disease is longer and the patients are younger – averaging out at 27 years. Based on the atypical clinical course of the diesase as well as other biomolecular evidences[25,29,30] it was proposed that vCJD is a direct consequence of BSE transmission via contaminated food sources. Indeed, transmission studies with macaques found evidence that BSE isolates can cause vCJD[31], while further experiments revealed identical transmission characteristics between BSE and vCJD.[30,32]

The Gerstmann Sträussler Scheinker syndrome (GSS) is a familial disease. The heredity is autosomal dominant and clinical signs emerge within an age of 30 to 40 years. Mutations of the *Prnp* gene (cp. 1.6, p. 27 *et seqq.*) are regarded to be the triggers of the disease. The course of GSS covers a period of up to five years. Typical symptoms are ataxia, spasms and dementia.[33,34] Like GSS the fatal familial insomnia (FFI) can be inherrited, but also sporadic cases have been reported.[35] Insomina, dysautonomia (malfunction of the autonomic nervous system), dementia as well as phobia and panic attacks characterize the course of FFI that inevitable ends with the death after 7 to 15 months.[36] Similar to GSS, spongiform abnormalities can be observed and the thalamus shows atrophies. Nevertheless, the

clinical signs are hard to distinguish from CJD. Thus, it is difficult to reach a definitive diagnosis.[37]

Contrary to CJD, GSS and FFI, kuru has been well-described for a couple of hundred people in a district of Papua New Guinea. Dementia is a typical symptom of CJD. However, although symptoms like ataxia, uncoordinated movements, blackouts, general weakness and decreasing cortical capacity have been associated with kuru, dementia has not been observed. A characteristic of kuru are pathologic bursts of laughter. Thus, the name "The laughing death" has become established. C. Gajdusek revealed an oral human-to-human transmission of the kuru-agent in the wake of cannibalism.[38,39] By ritual eating of their death the local natives were exposed to high-amounts of infectious material. It was thus hardly surprising that the symptoms also affected children which indicated that the incubation periods are significant shorter than it was known from the sporadic or familial forms of CJD.

TSEs are widespread under mammalian species, for instance they were described in sheep, goats, minks, mule deer, feline species and ungulates. Apart from the bovine spongiform encephalopathy the most extensive studies have been made on scrapie and the chronic wasting disease (CWD). Scrapie is known to affect goats and sheep and first records of its existence date back to the 18th century.[40] Strong itching sensation, leading affected animals to scrape off their wool or hair, is followed by ataxia, excitability and lack of interest. Histological investigations of brains from scrapie affected animals showed strong similarities to CJD. By coincidence, the transmissibility of TSEs was first shown in the wake of the administration of vaccines to Scottish sheep[41], but also transmissibility across species was observed, for example in mice[42], rats[43] and hamsters[44]. The chronic wasting disease of mule deer[45] is an expanding problem in north America, spreading from Colorado to further states. While the origin of CWD is still unknown the disorder shows substantial impact on mule deer populations.

The risk of CJD transmission due to surgical intervention or medical treatment is believed to be relatively low. Sporadic CJD seems to be limited to CNS tissue.[46–48] Thus, for instance, transmissions to primates have so far only been demonstrated using CSF fluids[49,50] and peripheral nerves, tonsils, spleen, cervical lymph nodes, appendix, kidneys, liver, lung and heart muscle have been tested negative for transmissibility.[48] Furthermore, *in vivo* transmission studies have shown that peripheral nerves, intestine, bone marrow, blood, skeletal muscles, adipose tissues and also excretions seem to be non-infectious.[49] However, the situation is different with vCJD. Contrary to sporadic and familial CJD, GSS and Kuru not only CNS tissue was demonstrated to be infectious. For expample, the infectivity of lymphatic

tissues (spleen, lymph nodes, tonsils) and the gastrointestinal tract has been demonstrated uniquely for the variant form of the Creutzfeldt-Jakob disease.[46,48,51–53] This suggests a higher risk for iatrogenic CJD, but so far only three cases have been reported. Interestingly, the iatrogenic CJD of these individuals is likely to be caused by blood transfusion.[48,54,55] Regarding the low number of cases and the fact that infectivity could not be substantiated for blood plasma and buffy coat samples[51] the risk of transmission via blood transfusion can be considered as relatively low. Nevertheless, the british government assessed the risk as high for blood transfusion recipients of certain time intervals and in certain risk groups, like haemophiliacs. The vast majority of iatrogenic CJD cases resulted from an exposure to high-titer tissues, like infectious brain, dura mater and cornea or was attributable to treatments with pituitary homones and is rather caused by transmissions of sporadic CJD.[19,56] However, the appearance of the variant form was discussed heavily within the scope of a diet-related transmission, but up till August 2012 not more than 173 vCJD cases have been reported in the United Kingdom.[24] After the BSE crisis, the outbreak of vCJD was an often discussed scenario, but fortunately it did not become reality and over the years predicted numbers were corrected downwards.

It was argued that a genetic predisposition might influence the progression of the disease because the majority of the vCJD patients was homozygous for methionine 129 in the human *Prnp* gene on chromosome 20. In addition, the *Prnp* codon 129 genotype frequencies show different distributions for sCJD, vCJD and the normal population. Furthermore, the genotypes seem to be correlated to the transmission pathway. Patients which have been transmitted directly showed to be homozygous for methionine. A peripheral transmission (e.g. by hormone therapy) causes a longer incubation time in the heterozygous case. Interestingly, the polymorphism has no effect on the incubation time of transplant recipients. In view of the fact that TSE incubation periods can last several years and clinical symptoms can be attenuated, the susceptibility of heterzygous genotypes (Met/Val), but also for Val/Val might not be zero.[18,57–61] Thus, it is hard to define the risk of iatrogenic transmission, especially for variant CJD.

Without doubts effective and safe decontamination is of prime importance to prevent human-to-human transmssions via surgical instruments. TSE agents show a high resistance to heat, UV-radiation and enzymatic degradation. Especially their high binding affinity to steel surfaces poses problems[20,56] and necessitates specific decontamination procedures. Treatments that are considered appropriate for decontamination include the use of sodium hydroxide or hypochlorite, but also the decontamination effects of alkaline detergents, phenolic agents and different autoclaving procedures have been surveyed. Even the effect of gas plasma was

tested.[20,62–67] The World Health Organisation (WHO) for example, recommends an hour-long treatment of heat-resistant instruments, wastes and materials which were directly exposed to high or low-infective tissues with 1N NaOH or hypochlorite (20,000 ppm) followed by autoclaving at 121 or 134°C. For disposable materials an incineration is proposed while heat-sensitive instruments should be treated with 2 N NaOH or undiluted hypochlorite for 1 hour.[68] A summary of efficient decontamination methods is given in Table 1.2.

Table 1.2: Typicial prion decontamination protocols with a log reduction larger than five[56,62]

Method	Parameters
Chemical	20,000 ppm NaOCl at 20°C for 1 h 1N NaOH at 20°C for 1 h
Alkali	Hamo 100 Prion inactivation detergent (Steris) 1.6% (v/v) at 43°C for 15 min
Phenolic	Environ LpH 5% (Steris) at 20°C for 15 min
Autoclaving	Autoclaving at 134°C for 18 min, immersed in water
Enzymatic	Kienzyme (Steris, 1.4 mg/ml at 25°C for 3 h) and vaporized hydrogen peroxide (0.8% (v/v) at 43°C for 5 min)

1.2 The protein only hypothesis

The transmissibility of TSEs was discovered by pure chance in 1937 (cp. 1.1) and was initially attributed to viral infection.[41,69–71] It was Alper who showed that the molecular weight of the infectious agent deceeds the characteristics of a virus.[72] Furthermore, a high resistance against radiation and digests with DNAse and RNAse substantiated the absence of a nucleic acid in the TSE agent.[73–75] Initially declared as a ‘slow virus disease’ the facts were more and more shaking existing dogmas and a proteinaceous cause was dicussed controversially. A cascade of facts suggested that the infectious agent is mainly consisting of protein. For instance, the infectivity could be decreased using protein inactivation methods. Moreover, the aggregation behavior and its major localization in cell membranes indicated that the infectious agent mainly consists of protein.[76–82] Nevertheless, the ‘protein only hypothesis’, which tried to explain the results of Alper[83], was not completely accepted. For example, it was argued that nucleic acids are still involved, but are covered by compact and resistant protein coats.[84,85] Finally, it was shown that the prion protein (PrP) forms the majority of TSE agent enriched samples. Today it is widely accepted that the disease associated, pathological form of the prion protein, PrP^{Sc}, is the main if not only part of a ‘proteinaceous infectious particle’ or

'prion'.[86,87,88,89,90] *In vivo*-studies revealed that the infectious titer is directly correlated to the PrP^{Sc} concentration. Furthermore, anti-PrP antibodies could reduce the infectivity of the TSE agent. In its altered state, PrP^{Sc} binds and converts its benign cellular isoform (PrP^{C}) into likeness of itself (cp. 1.4, p. 19 *et seqq.*). Both forms are encoded by a single gene.[91] However, chemical differences between these isoforms could not be shown using mass spectrometry and amino acid sequencing.[92] Nevertheless, PrP^{Sc} is enriched in β-sheet secondary structure, less soluble than its cellular form and able to form larger-order aggregates.[93–95] Its precipitability by NaPTA (sodium phosphotungstic acid) or the exposure to certain epitopes allow to make further case distinctions. PrP^{Sc} shows a partial resistance to protease K digests ($rPrP^{Sc}$), but also a susceptible form is known ($sPrP^{Sc}$).[96–100] The protease resistant core of PrP^{Sc}, has an apparent molecular mass of 27-30 kDa ($PrP^{27\text{-}30}$).[3] However, protease resistance is not necessarily accompanied by infectivity, which caused the designation PrP^{res} (Figure 1.1).

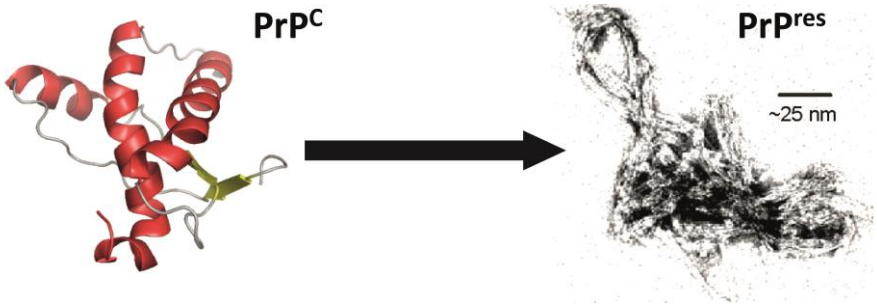

Figure 1.1: ***Conversion of the cellular prion protein to its abnormal isoform***
The cellular prion protein (PrP^{C}, simplified depiction of murine PrP without posttranslational modifications) can undergo a conversion to an aggregated, β-sheet-rich isoform which can show partial protease K resistance (PrP^{res}).

The discussion on wether proteins can be infectious in the absence of nucleic acids continued to be controversial. Many studies supported the protein only hypothesis. An evident finding, for instance, was a TSE resistance in mice lacking the PrP gene. Additionally, it was shown that the susceptibility can be reconstituted by inserting a PrP transgene.[101] It was also demonstrated that several PrP gene mutations are associated to familal TSEs.[3,15,102] Still there was criticism: PrP overexpressing mice with GSS related mutations were shown to develop TSE similar symptoms including transmissibility[103,104], but the experiment could not be reproduced[105]. Furthermore, *in vivo*-studies were formerly performed using transgene mouse models. In consequence PrP was overexpressed. Dwindling acceptance due to the possible toxic character of high PrP concentrations cast doubt on presented results.[106] That the TSE agent might lack any nucleic acids was one of the central arguments of the 'protein only hypothesis'. Nevertheless, there were uncertainties about the agent[3,107,108]: On the one hand it was demonstrated that RNA interacts

with the prion protein[109–111] and promotes its conversion *in vitro*[112], on the other hand infectious prions could be generated in the absence of any mamallian cofactors.[90]

1.3 Prion strains and transmission barriers

Generally, interspecies transmissions of TSEs are less efficient compared to intra-species transmissions.[113] This ‘species barrier’ is particularly reflected by prolonged incubation times and incomplete attack rates. Amino acid sequence deviations between donor and recipient species were the base of first attempts of explanation. The primary structure of PrP is highly conserved.[114,115] Between hamster and mouse for example, the proteinase K resistant core of PrP^{Sc} exhibits only eight amino acid differences. However, hamster prions have no effect on wild-type mice, whereas transgenic mice, which express hamster PrP, are susceptible.[116] Nevertheless, the barrier could be circumvented using transgenic mice which expressed a chimeric PrP (MH2M). These animals could be successfully transmitted with either hamster or mouse prions.[117] Furthermore, prions which were generated in the chimeric mouse line transmitted disease to wild-type hamsters and mice. In another experiment transmission of classical CJD prions into wild-type mice failed, while a transmission into humanized animals was successful.[29,118] Thus, the species barrier is attributable to the primary structure of the prion protein.

It was hypothesized that resembling PrP sequences of donor (PrP^{Sc}) and recipient (PrP^{C}) might be a pressuposition for an efficient prion propagtion *in vivo* and polymorphism effects in sporadic and acquired CJD might be used as an argument: individuals, which are homozygous at residue 129 of PrP present the majority in vCJD case statistics.[18,57–61] Thus, the term ‘sequence barrier’ might also be appropriate.[119] Then again, experiments with human prions also indicated that cellular factors might play a role for successful transmission (cp. 1.4, p. 19 *et seqq.*). Nevertheless, prion infectivity can also vary if the amino acid sequence of host and donor is the same.[120] For example, a ‘transmission barrier’[121] was observed if humanized mice were inoculated with vCJD prions, while sCJD prions showed to be highly infectious.[29]

In addition to the variations of the prion inter-species transmissibility described above, several phenotypic TSE variants were discovered in genitically identical mouse models.[122,123] These prion strains show consistent characteristics if they are inoculated into distinct hosts, such as incubation times and brain lesion profiles (Figure 1.2 A). Moreover, the intrinsic properties of prions strain were also

maintained after subpassages in other species (Figure 1.2 B).[124] Nevertheless, changes of the PrP primary structure could not be shown in this context.[125]

A possible clarification of the question how proteins can lead to different disease phenotypes was given by proteinase cleavage experiments with hamster prion strains. After proteolytic digestion of the prion strain isolates hyper (HY) and drowsy (DY) peptide fragments of different size were detected, which indicated conformational differences.[126–128]. Indeed, several prion strains could be identified and characterized using conformation-dependent immunoassays, digestion kinetics, denaturation experiments, metal binding analysis or IR spectroscopy.[98,129–131] Electrophoretic size separation of prion samples after protease K digestions showed different PrP^{Sc} glycoform ratios (un-, mono- and diglycosylated) and animal transmission experiments revealed that they are a consistent characteristic of prion strains. (Figure 1.2 A and B).[25,132] Indeed, experiments with monoclonal PrP^{Sc}- and gycosylation-specific antibodies have shown that glycoforms are physically associated to native PrP^{Sc} in strain-specific ratios.[133] Hence, different disease phenotypes and variations of the prion inter-species transmissibility were attributed to the existence of polymorphic prion strains: assuming that a prion strain comprises multiple PrP^{Sc} conformations, the particular compatibilty of one or some conformations to the amino acid sequence of the host might trigger inter-species transmission, while less compatibility causes a species barrier or dramatically increases the incubation periods. Thus, the largest selective advantage determines the disease phenotype.[121] Furthermore, the number of PrP^{Sc} conformations or strains might be limited by their thermodynamic stability and their replication kinetics which have to show a faster build-up than counteracting cell protein degradation processes.[121] Indeed, multiple PrP^{Sc} types have been detected in CJD brains[134,135] and mouse adaption of hamster prion strains by multiple passaging (Figure 1.2 C) provides further evidence for this theory.

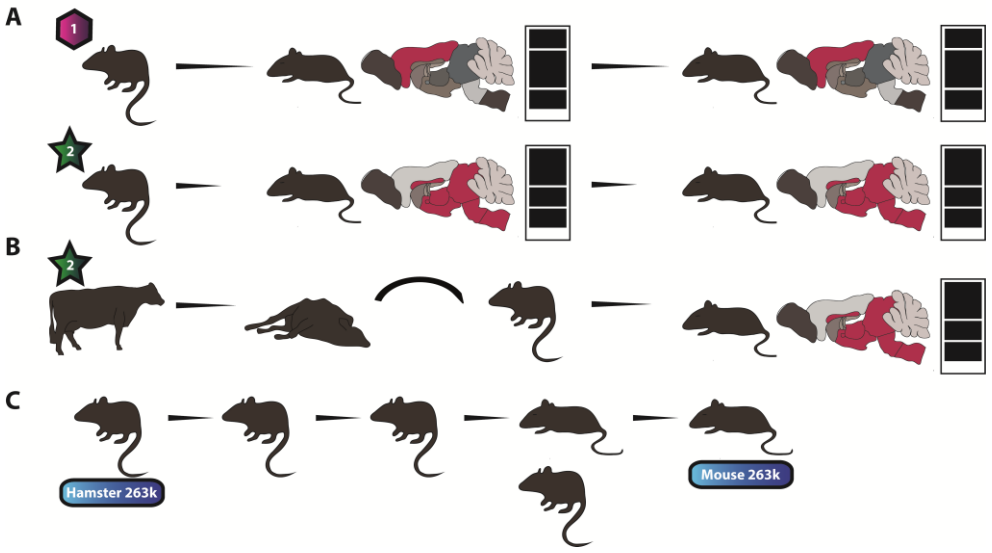

Figure 1.2: ***Prion strains, interspecies transmissibility and strain adaption***

(A) *Prion strains (designated here as 1 and 2) differ in incubation periods (length of black arrows), neuropathology (affected brain areas indicated in red) and glycosylation pattern (black boxes, simplified illustration of a western blot). These strain characteristics are maintained over serial passages.* ***(B)*** *The strain properties may also retain after multiple passages in an intermediate species with a distinct PrP^C sequence.* ***(C)*** *Strain adaption: Mice were inoculated with hamster prions (here strain 263K) Over several passages the species barrier prevents effective transmission or at least clinical signs. During transmission an adaption of the prion strain can occur, but the properties of the strain might change.(modified from[121])*

Additionally, distinct cattle prion isolates showed phenotypic characteristics similar to BSE if they were inoculated into transgene mice which overexpressed bovine PrP. In contrast, transmission into transgenic ovinized mice leaded to a different pathology.[136] Thus, an abrogation of the species barrier seems to be associated with strain switching and therfore different phenotypes and prion strains may occur. Remarkably, the pathological and biochemical properties of vCJD could only be retained in humanized mice, which expressed PrP with a methionine a position 129, while a different phenotype was observed if methionine was substituted by valine. Moreover, after multiple passaging the transmission of BSE prions was inefficient.[137] That genetic differences of the host species are not required for the occurrence of strain ‘mutations’ has also been shown.[138,139] These experiments also clearly demonstrated that intra-species strain mutation might occur if the primary sequence of the host differs from that of the inoculated prion agent. Nevertheless, strain adaption *in vivo* necessitates two or more subpassages, presumably because several rounds of replication and conformational selection are necessary.[119,140]

Then again, it was suggested that environmental influences might change prion strain properties. For example, it is likely that the thermostability of BSE prions is

caused by the selectional processes of offal recycling and its processing to carcass meal respectively.[121,141] Evidence to support this notion comes from different thermodynamic stabilities of PrP^{Sc} sub-populations in thermostable TSE agents.[142]

Additionally, prion strains were described as ‘quasi species’ which comprise readily interconverting conformers. This would imply that the adaption to exogenous constraints or the host environment is due to slightly changes of the PrP^{Sc} conformation. In a particular environment this would lead to a coexistence of a major conformation and several variants (sub-strains, cp. Figure 1.3, p. 20).[119] The theory is based on characteristic transmission properties of 22L prions under selective constraints in cell culture. PK1 cells were treated with mouse 22L prions in the presence of swainsonine. Swainsonine (swa) is a Golgi α-mannosidase II inhibitor which is capable to inhibit > 99% infection of PK1 cells by RML and 79A, but interestingly not by 22L prions. In contrast to brain-derived 22L prions, the replicated PK1[22L] prion samples failed to infect R33 cells. Moreover, the derived PK1[22L] prions became susceptibil for swa after several doublings. The inhibitor sensitivity increased over time up to a value of 30 to 40% per culture. However, the swa-sensitivity took a gradual course and was not observed directly after the first prion replication round. Hence, an influence of brain- or cell-components was excluded. The inhibitor resistance and the R33-competence could be recovered using low concentrations of the agent as a selective pressure. Once the inhibitor was omitted, resistance was lost again. Contrary to swa-sensitivity the build-up of swa-resistance was faster. It was argued that the selective advantage of swa-sensitive prions in the absence of a selective pressure is relatively small compared to swa-resistant prions, but is still high enough to enable this conformation to become dominant. If they were backpassaged into mouse brains all prion strains that were replicated in cell-culture regained the original 22L cell tropism. Indeed, similar osbservations were made before.[143,144] The heterogenity of the 22L prion strain was also observed if cell cultures were biologically cloned by end-point dilution over several passages in the absence of swa. In order to explain the observations, evolutionary processes in prion propagation were proposed. It is noteworthy in this context, however, that real conformational differences between swa-resistant and swa-sensitive prions could not be shown.[140] Nevertheless, strain shifts were also observed after cloning *in vivo*. When a non-cloned mouse strain was passaged into mice with slightly different *Prnp* sequences a new strain was derived while a cloned strain maintained its characteristics.[145] But cloning does not consequently exclude the emergence of new transmission properties, as demonstrated with the prion strain 139A.[146]

1.4 Protein misfolding

Many neurodegenerative disorders, as, for instance prion diseases, Alzheimers disease or Parkinsons disease are associated with protein misfolding. In a self-templated process which resembles seeded crystallization pathologic protein aggregates bind and structurally corrupt benign protein monomers.[2] Thus, the terms 'protheopathy' or 'conformational disease' might also be appropriate. The presumably self-perpetuating mechanism leads to seed amplification as the pathogenic aggregates sequester more and more monomers over time. Protein misfolding was firstly described for prion diseases and today it is widely accepted that the disease associated, pathological form of the prion protein, PrP^{Sc}, is the main if not only part of a 'proteinaceous infectious particle' or 'prion'.[86,87,88,89,90] (cp. 1.2, p. 13 *et seqq.*) Thus, PrP^{Sc} can bee seen as the seed in mammalian prion diseases. There are clear indications that fibril formation is an intrinsic feature of polypeptides[147–150]: amyloids show a cross-β structure with β-strands perpendicular to the long axis of the fibril.[147,151,152] Interestingly, precursor proteins, such as Aβ (Alzheimer), α-synuclein (Parkinson), Amlyin (diabetes type II), Insulin (diabetes type II) or β_2-microglobulin (dialysis-related amyloidosis) have no sequence similarity and show structural diversity. Nevertheless, the structure of proteopathic seeds is not completely dertermined by the amino acid sequence. Thus, for instance, different amino acid side chain packing is possible in amyloid-like protein fibrils.[149,150] Moreover, different Aβ-fibril morphologies were observed if fibril growth conditions were changed[153] and different PrP^{Sc} conformations were shown to modulate the phenotypic characteristics of prion strains[132]. It was assumed for a long time that amlyoid formation is based on a mechanism in which primary (homogenous) nucleation is the rate-limiting factor.[154–161] Primary nucleation is dependent on the concentration of monomeric peptides, but recent research in this field showed that amyloid formation seems not to fit in simple nucleated polymerization models.[162–167] Thus, fibril formation has been attributed to the existence of secondary nucleation pathways, in which already formed fibrils catalyze the formation of new fibrils.[168–170] Using the growth of actin as a model Wegner described the role of fragmentation in the context of secondary nucleation.[171,172] Recent studies clearly demonstrated that spontaneous fragmentation plays a role in fibrillar growth, albeit the spontaneous generation of nuclei is slow. Regarding the elongation of fibrils, at least for the amyloidogenic yeast prion protein, it could be shown that growth occurs by monomer addition.[173] If fragmentation is used as a driving force growth curves show a sigmoidal shape and there is clear evidence that primary nucleation is negligible. In such a system the maximal growth rate is independent from the number of initial nuclei or the primary

nucleation rate which is contrary to the prevailing view in literature where growth rate and lag-phase are dependent of primary nucleation.[154,174] Recent research not only addressed the influence of fibril fragmentation in amlyoid assembly, but also in cytotoxicity. Fragmented to different extent shorter amyloid β_2m (β_2-microglobulin) fibrils, for example, showed higher seeding efficiency and higher ability for membrane disruption, while keeping the same structural properties as their longer counterparts.[175,176] Lower infectivity and converting activity was also found for large native prion protein fibrils, whereas particels of 17-27 nm (300-600 kDa) showed substantially higher values. Interestingly, in both cases (PrP and β_2m) oligomers showed no or only low effect. This stands in contradiction to lots of findings which indicate that prefibrillar oligomers represent the toxic species in amyloid diseases.[177–181] There is plausible reason to assume that specific molecular structures of proteopathic seeds and their stability have crucial influence on their propagation *in vivo* and only a limited number of specific seed conformations might go along with infectivity. For instance, prion replication *in vivo* does not consequently lead to the occurance of clinical signs[182–184] and seeding effictivity of synthetic Aβ fibrils *in vitro* is not automatically accompanied with seeding activity *in vivo*.[185,186] The folding of a polypeptide towards its native structure is often described by sequence-specific energy landscapes where local energy minima represent one or more thermodynamically stable protein conformations (Figure 1.3).[147,187] As announced earlier (1.3, p. 15 *et seqq.*), it was proposed that prion strains comprise seed populations of interconverting conformations (‘quasi species’).[119] Hence, the structural interconversion of prion strains and ‘sub-strains’ was explained by relatively low activation energy barriers (Figure 1.3).[119,121]

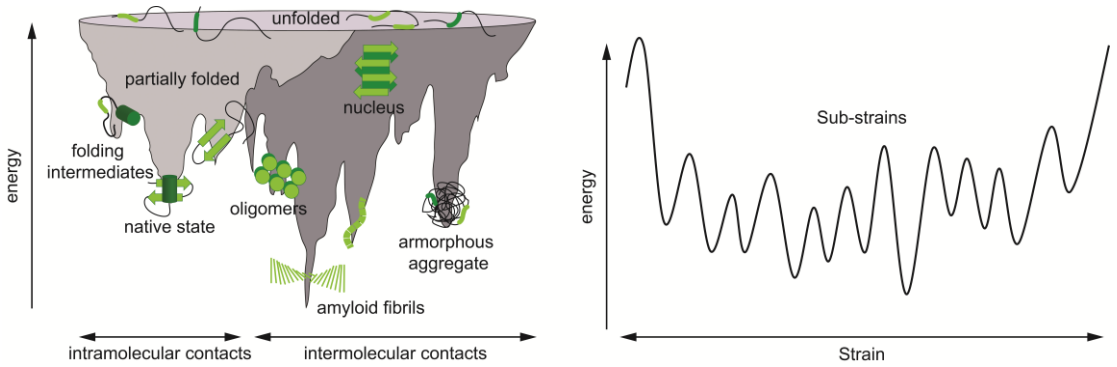

Figure 1.3: ***Schematic energy landscape***

(Left) *The sequence specific energy landscape can be regarded as a three-dimensional funnel where the surface represents the large number of potential conformations which change to reach local energy minima. Intra- and intermolecular contacts determine the outcome of the process. (modified from* [147]*)*
(Right) *Suggested energy landscape for prion strains and ‘sub-strais’: Strains are delimited by relatively high energy barriers, while sub-strains are represented by interconvertible confomers. Energy barriers between sub-strains can be overcome by selective pressure. (modified from*[119,140]*)*

Amyloid formation *in vitro* is often realized under slightly denaturant or destabilizing conditions like low pH, high temperature or amino acid substitutions. For example the conversion of recombinant PrP in the QuIC (Quaking-induced conversion) assay (cp. 1.5, p. 23 *et seqq.*) takes place in the presence of SDS (sodium dodecyl sulfate). It is likely, that partial unfolding of the native state is favored and therefore, potentially, the conversion to an amyloidogenic state.[147,188] However, till date the exact structure of PrP^{Sc} as well as the underlying conversion mechanisms have not been solved. Nevertheless, three hypothesis can be usually found in the literature (Figure 1.4 A-C). In the template assisted (heterodimer) model the pathological isoform of PrP (PrP^{Sc}) shows a high thermodynamic stability, but in the kinetic point of view its conversion is hard to accomplish.[94,189] The heterodimer model assumes the formation of an instable intermediate (PrP*). The equilibrium lies on the side of PrP^{C}, but with support of a chaperone, for example, PrP* can form a heterodimer with PrP^{Sc}. A spontaneous conversion of the heterodimer and a subsequent dissociation leads to two new templates and therefore exponential growth. It was argued that the the catalytic properties of PrP^{Sc} must be extremely high to generate full blown TSE symptoms within a lifespan.[190] Indeed, there is a low incidence rate of spontaneous TSEs.[191] Hence, Prusiner suggested a cooperative autocatalytic model (cooperative Prusiner model) in which a higher number of PrP^{Sc} molecules supports the conversion of PrP, while the catalytic effect of a single PrP^{Sc} molecule is kept low. It was also suggested that the critical step of the conversion reaction is the formation of an instable nucleus.[192,193] In the so-called nucleation-polymerization model the equilibrium lies on the PrP^{C} site of the reaction until the unstable PrP^{Sc} oligomers form an aggregate with a decaying rate slower than the forming.[194,195] These PrP^{Sc} aggregates bind to PrP^{C} and change the equilibrium. The assisted-nucleation model on the other hand suggested that PrP^{Sc} cannot exist as a monomer. In this case, a cofactor might promote the binding and conversion of new PrP^{C} monomers, while fragmentation of the growing PrP^{Sc} aggregates forms new nuclei.[190]

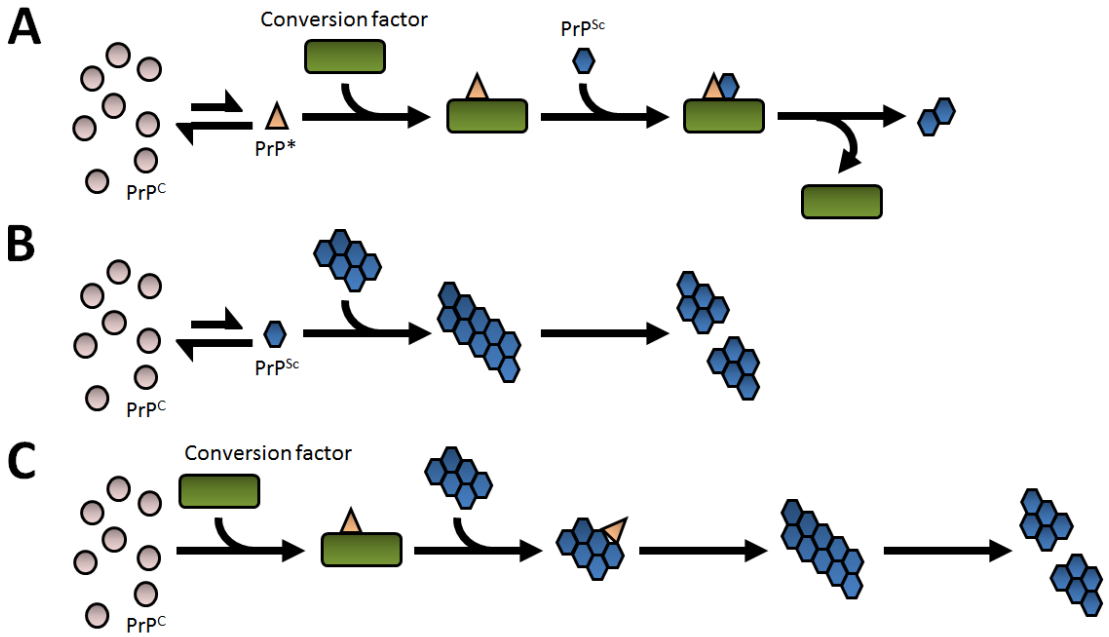

Figure 1.4: ***Molecular mechanism models for the conversion of PrP^C to PrP^{Sc}***
(A) *Template assisted (heterodimer) model;* ***(B)*** *Nucleation-polymerization model;* ***(C)*** *Assisted-nucleation model; (modified from*[190]*)*

It was argued that the structural conversion of PrP^C to its pathological conformer might be promoted by a cofactor (‘factor X’) or a chaperone (‘protein X’). The idea arose from transmission studies of human prions in mice: Transmission from human CJD prions to transgenic mice expressing human and mouse PrP failed. In contrast, the inoculation of chimeric mice leaded to disease symptoms. A subsequential transmission of human prions into humanized mice only successed if the mice were crossed into a PrPnull background. The observations were attributed to a mouse protein X, which interacts with murine PrP (mPrP), but does not bind to human PrP (hPrP).[196] Moreover, the regions which were supposed to bind to protein X were mapped.[197] The theory found support in cell-free conversion experiments. While highly purified PrP^C could not be converted in the presence of PrP^{res}, an addition of cell proteins reconstituted the conversion ability.[198] But not only proteins were discussed as potential partners in the misfolding process of PrP. Sequence-specific DNA binding to mPrP and the interaction between PrP^C and polyionic ligands, such as sulfated glycosaminoglycans, or anions in general have been shown early on.[199,200] *In vitro* conversion experiments also indicated a key role of synthetic polyanions and RNA. Moreover, nucleic acid-promoted *in vitro* amplification seems to be strain-specific, especially if synthetic polyanions are used.[201] However, attempts to structurally convert recombinant expressed PrP have already indicated that host cell proteins and cofactors might play a role, but are not obligatory.[202–205] Finally, latest investigations have proven that neither cofactors nor additional

proteins are necessary to replicate infectious prions *in vitro*.[90] The mechanisms *in vivo*, however, stay unclear.

1.5 *In vitro* conversion of the prion protein

In order to reveal the underlying mechanisms of prion diseases it is of prime importance to investigate the conversion process of host PrP^{C} to its abnormal, unsoluble and partially protease resistant isoform PrP^{Sc}. First attempts to propagate prions *in vitro* started in the lab of Stanley Prusiner. But neither simple mixing of chimeric cell lysates from mouse/syrian hamster (MHM2) PrP and purified $PrP^{27\text{-}30}$ nor the incubation of metabolically radiolabeled $mPrP^{C}$ in prion infected cell cultures leaded to an *in vitro* or *de novo* formation of protease resistant PrP in detectable amounts. Furthermore, it was tried to structurally convert PrP^{C} which was synthesized in the presence of microsomal membranes from PrP^{Sc} infected sources, unfortunately without success.[206] The first successful experiment of this type was performed in 1994[199] In the presence of guanidinium as a denaturing component a conversion rate of 10-20% could be accomplished. Nevertheless, infectivity could not be shown[199] and further experiments with cell-lysates followed.[198] A main problem of these methods was the large excess of $PrP^{27\text{-}30}$ which had to be used for a successful amplification of PrP^{res}. However, the spontaneous conversion of PrP was believed to be relatively slow and the non-satisfiying amplification yields necessitated a new method.[199] In 2001, Saborio and coworkes used an ultrasonic approach to generate significant amounts of highly protease-resistant PrP^{Sc}-like protein (PrP^{res}) with a relative molecular mass of 27,000-30,000 in its N-terminally truncated form (similar to $PrP^{27\text{-}30}$).[5] The method of *in vitro* replication of seed conformation was dedicated Protein Misfolding Cyclic Amplification (PMCA). It is based on periodic cycles of ultrasonic treatment which are believed to cause fribril fragmentation. The surface augment which attends this process is believed to apply more growth sites and therefore an increasing number of converting units (Figure 1.5).[5]

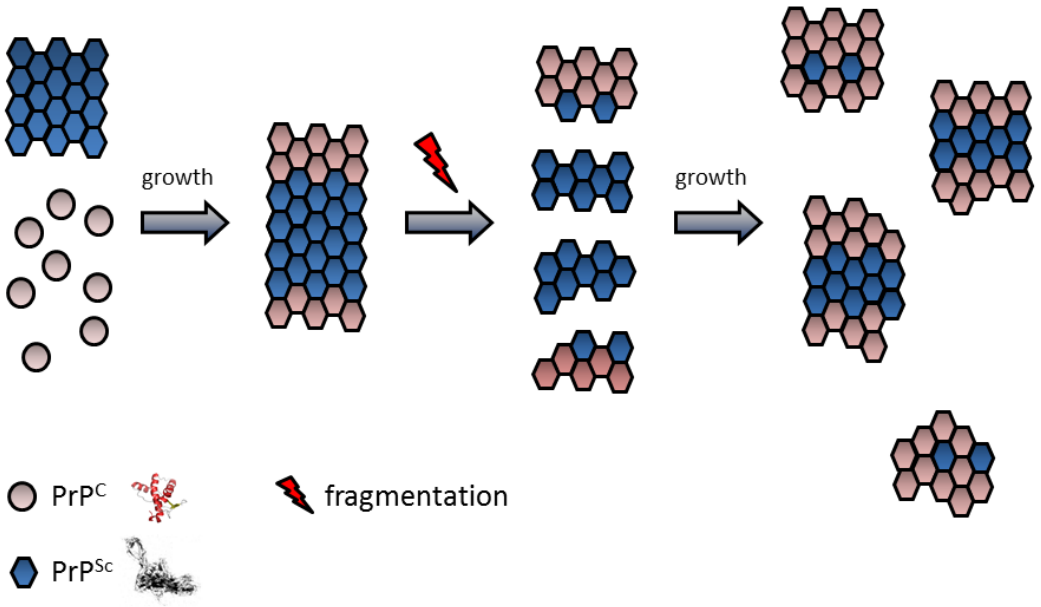

Figure 1.5: **In vitro *conversion of prion particels in PMCA***

Prions consist mostly if not completely of PrP^{Sc}. PrP^{Sc} can act as a conformational template which structurally corrupts benign PrP^{C} monomers. Seed amplification in PMCA is based on alternating cycles of incubation and sonication in the presence of excess PrP^{C}. Fibril fragmentation is believed to generate more growth sites and might therfore promote seed amplification. (adapted from[5])

In PMCA minor amounts of infectious tissue homogenate are mixed with a large excess of healthy brain homogenate[5,207,208] or purified recombinant PrP[202] (Figure 1.6). Cellular PrP that was purified from brain homogenate can also be used.[209]

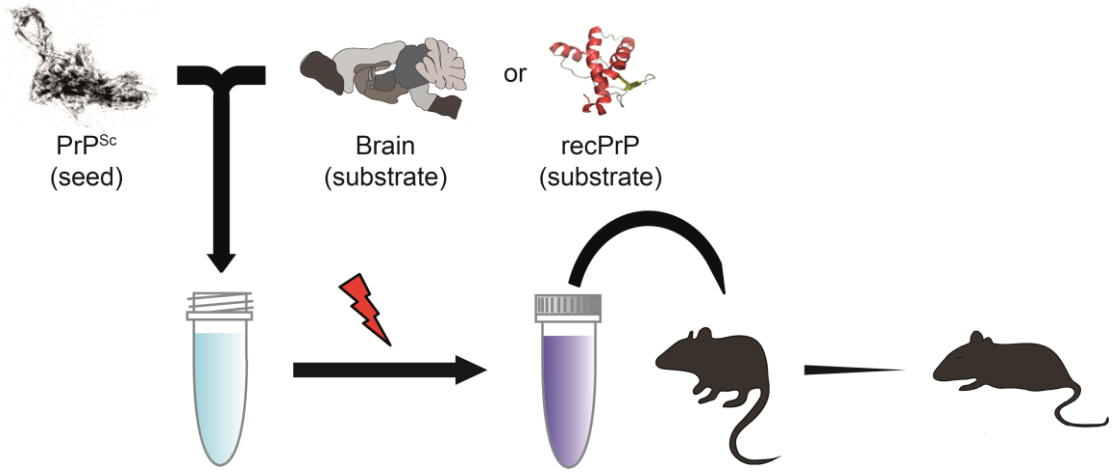

Figure 1.6: ***Cell-free* in vitro *conversion assays for prions***

The prion amplification in vitro *is usally based on a mixture of proteopathic seeds (e.g. scrapie brain homogenate or purified PrP^{Sc}) and native PrP (e.g. brain tissue homogenate of healthy animals, purified PrP^{C} or recombinant PrP (recPrP)). In Protein Misfolding Cyclic Amplification (PMCA) seed amplification is predicated upon alternating cycles of ultrasonic bursts and incubation (indicated by the red flash). Besides replication of PrP^{Sc} PMCA was shown to amplify prion infectivity.*[207]

Protease resistant PrP (PrP^{res}) that was generated with PMCA was shown to further propagate protein misfolding (serial PMCA).[210] By serial dilution of the original seed it could be demonstrated that PMCA is not only capable of amplifying PrP^{Sc}, but also prion infectivity (Figure 1.6).[207] Further development and automatization of the PMCA leaded to high effeciency, making the *in vitro* conversion much more senstive than the bioassay.[4,5,207–209,211–213] Even though low amplification of PrP^{Sc} can also be observed without sonication[5,112,214], PMCA provides and efficient way for amplification of proteopathic seeds, especially when it is compared to cell-culture based assays. For several years the PMCA has been used as a robust system for qualitatively analysis of prion containing samples of different origin, such as blood, brain or liver tissue.[212,215] Various approaches were tried to optimize the yield and reproducibility of PMCA experiments. As stated before the binding of PrP^{C} to polyanions has been observed (cp. p. 22).[199,200] Thus, nucleic acids have been tried to improve PMCA. Purified RNA, for instance, promotes the seed amplification in hamster tissue homogenates.[216] Using native PrP^{C} and copurified lipids it was demonstrated that polyanions seem to be necessary to generate infectious prion particles.[203] But also reduced pyridine nucleotides, such as NADPH (Nicotinamide adenine dinucleotide phosphate) seem to enhance the propagation of hamster-adapted PrP^{Sc}.[217] Aside from nucleic acids, synthetic polyanions like Poly(A) are also believed to interact with PrP[218] and stimulate the amplification of PrP^{Sc}.[219] Apart from charged molecules also several detergents have been tested to increase the PrP^{Sc} amplification yield. For example, CHAPS (3-[(3-Cholamido-propyl)dimethyl-ammonio]-1-propanesulfonate), CHAPSO (3-[(3-Cholamidopro-pyl)dimethylammonio]-2-hydroxy-1-propanesulfonate), n-Decyl β-D-tiomaltoside and n-Undecyl β-D-tiomaltoside as well as NOG (N-oxalylglycine) were testet in PMCA. And in fact, the additon of NOG was found to be the most suitable to increase the reaction yield.[220]

Nevertheless, the use of special additives often causes just minor effects which are not seldom controversy: dextransulfates, especially potassium dextran sulfate, increase the reaction outcome in PMCA using bovine brain homogenates.[221] In contrast, dextransulfate does not work out if RML is used as a seed.[216] Thus, cofactors might be seed specific. Supporting evidence for this notion comes from the species-dependent effect of RNA in PMCA reactions.[216] However, the role of nucleic acids in the misfolding mechanism of PrP has not been clarified yet. Literature indicates a promoting effect of RNA and poly(rA)[112,203,205], but generation of infectious prions seems also to be possible in the absence of any cofactors[90].

Except for additives, the PrP^{C} concentration, as well as its constitution seem to influence the amplification reaction. While the replication of RML prions

necessitates unglycosylated PrP^C molecules, the diglycosylated form seems to be essential for the propagation of certain hamster prions (Sc237).[222] Moreover, in substoichiometric levels unglycosylated hamster PrP^C, but also certain PrP deletion variants can inhibit the conversion.[218,222] Furthermore, a higher PrP^C content in the tissue homogenate enhances the conversion reaction[223], but also PrP fragments have been shown to modulate the reaction outcome. Especially C-terminal and core region peptides increase the PrP^{Sc} amplification yield.[224]

Due to the metal-binding capacity of PrP[225] the effect of transition-metals was investigated in PMCA. In contrast to Cu or Fe the addition of manganese leads to different PrP^{Sc} glycosylation patterns. This is especially interesting, because increased manganese concentrations were found during scrapie transmission in hamsters.[226]

Only a few attempts were focused on physical parameters like the influence of sonication times. The results indicated different optima for mouse adapted BSE and scrapie strains.[227] Furthermore it was demonstrated that the PrP^{Sc} amplification yield is directly correlated with the amount of cycles in a PMCA experiment.[5,228,229] Technical improvements, however, have never been tested with one exception: the usage of Teflon™ beads seemed to increase the otherwise relatively low conversion rate in PMCA (PMCAb). Unfortunately, the phenomenon could not be explained in detail and better amplification yields were said to be caused by a better fragmentation. It was further argued that the method could also increase the accessibility of PrP^C or potential cofactors. Additionally, a cavitation mitigating effect was assumed if beads are used, leading to more specific conversion and less unspecific aggregation of PrP^C.[230]

Despite the yearslong utilization of PMCA in many laboratories the *in vitro* replication of uncharacterized prion seeds is often based on trial and error.[231] There is also the fact that the generated samples were often not tested *in vivo*. Therefore, no statemant can be given wether or not the tested additives have a substantial effect on infectivity and ‘strain-ness’. Indeed, that is to that extent important, since *in vitro* generated prions are 10 to 100 times less infectious than native prions.[207]

PMCA was also used to convert recombinant full-length hamster PrP and the generated PrP^{res} was shown to be different from spontaneous formed fibrils as well as native prions with respect to the IR spectra and the proteolytic sensitivity. Recombinant PMCA generates seed-specific particles of 11, 12, 13 and 17 kDa (after PK digest). Additionally, a spontaneous formation of PrP^{res} was observed. Interestingly, recPrP-PMCA necessitates the presence of SDS.[202] The QuIC assay (quaking induced conversion) uses buffer conditions similar to those of

recPrP-PMCA. Instead of sonication – the driving force in PMCA – alternating cycles of shaking and incubation are taken out in a programmable laboratory shaker. In contrast to PMCA the QuIC assay shows higher sensitivity. Even femtogram amounts of PrP^{res}, a concentration which lies below the lethal intracerebral dose, are detectable.[204] Recent efforts leaded to high-throughput methods for estimating the relative amount of prions in samples of different origins.[232] The quantification of prion samples is taken out by a thioflavin T based bioassay - the real-time QuIC (RT-QuIC). Its sensitivity is comparable to end-point quantification assays in animals, but less time consuming. Latest improvements made it possible to detect even ~2 ag/ml of proteinase K resistant particles.[233,234] Nevertheless, the QuIC assay was not shown to amplify infectivity.

Despite strong supporting evidence for the prion only hypothesis[126,132,199,203,207,235,236] (cp. 1.2, p. 13 *et seqq.*), the generation of a recombinant prion with bacterially expressed PrP would clearly dispel the last doubts. Indeed, PMCA could be used to amplify recombinant mammalian prions and their incidental infectivity in the presence of minor amounts of PrP^{Sc}. Moreover, the absence of any additives seemed to invalidate the long discussed involvement of mammalian cofactors.[90] Besides seeded amplification of infectious prions, also *de novo* generation of recombinant prions was demonstrated using PMCA.[205]

1.6 The cellular isoform of the prion protein (PrP^{C})

The prion protein (PrP) is a ubiquitously expressed 253 (in some species 252) amino acid long glycoprotein which is divided in two domains. It is encoded by a single-copy gene, designated *Prnp* in mice. Between mammalian species the amino acid sequence is highly conserved.[114,115] It consists of a signal peptide (22 amino acids) for co-translational secreting into the endoplasmic reticulum (ER), five N-terminal copper-binding octapeptids and two glycosylation sites (cp. Figure 1.7).

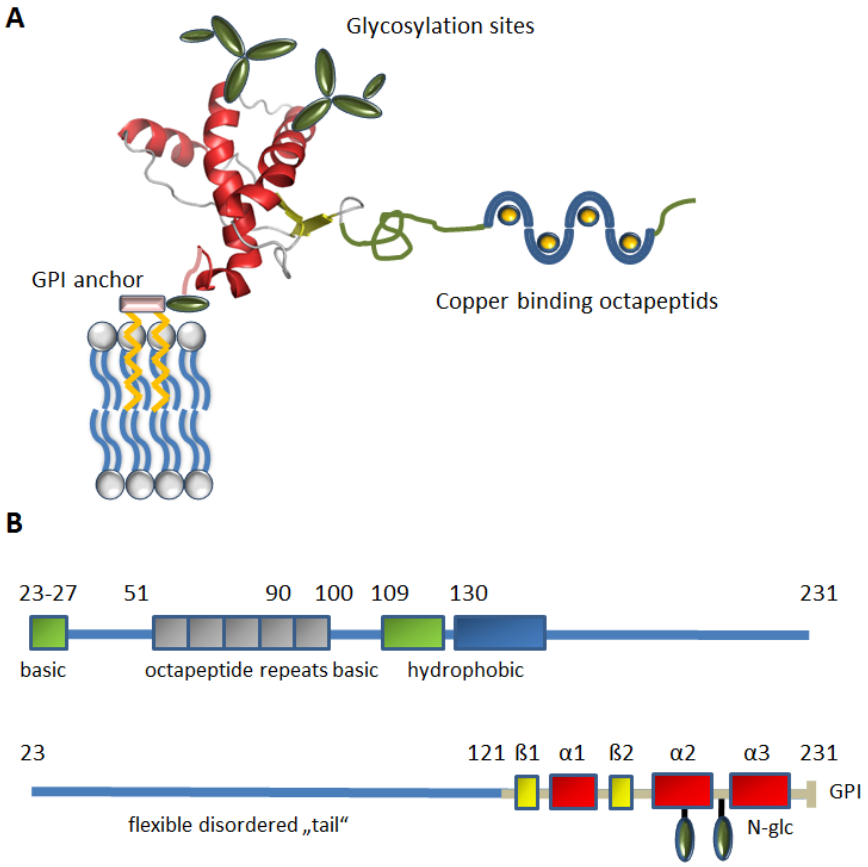

Figure 1.7: The prion protein

(A) *Illustration of the structure of the* Mus musculus *prion protein mPrP(121-230); The copper binding octapeptide repeats, glycosylation sites and the GPI-anchor are illustrated.* ***(B)*** *Sequence of mPrP(23-231) and mapping of secondary structure; (Top) Two basic stretches are shown in green, one hydrophobic stretch is shown in blue and the octapeptide repeats are indicated by grey boxes. (Bottom) The flexible disordered tail of mPrP is shown as a blue line while the globular domain is represented by a grey line. Sequence motifs are shown by colored boxes, α-helices are shown in red (α1, α2, α3), β-strands are symbolized by yellow boxes (β1, β2, β3). Specific sequence positions are indicated by numbers.(modified from*[237,238]*)*

Furthermore, one disulfide bridge can be found.[239] PrP is located in lipid rafts – sphingolipid- and cholesterol-rich microdomains on the outer cell membrane.[240–242] Lipid rafts are detergent resistant and often contain cellular receptors, tyrosine kinases and GPI-anchored proteins.[243,244] Indeed, PrP shows a 23 amino acid long C-terminal glycosylphosphatidylinositol (GPI) sequence. C- and N-terminal signal sequences get cut off in the ER and the Golgi apparatus during post translational modification. Species and strain dependent, three forms of PrP exist – mono-, di- and unglycosylated PrP.[245,246] The oligosaccharides are from the high mannose-type, endoglycosidase H sensitive and undergo a postmodification in the Golgi apparatus. While the N-terminal tail is structurally undefined, the C-terminal part is mainly globular and characterized by secondary structure elements. PrP^{C} is a soluble, mainly alpha-helical and a monomeric protein.[93,237,247] Until now, the

structures of recombinant PrP have been solved for many species including human PrP (hPrP)[248], mouse PrP (mPrP)[237,238], syrian hamster PrP (shPrP)[249], bovine PrP (bPrP)[250], as well as chicken, turtle and frog[251].

1.6.1 The function of PrP^C

The prion protein is mainly expressed in neural tissue, but can also be found in other mammalian organs.[252] In spite of the efforts made, the physiological function of the prion protein still remains elusive: several studies revealed that PrP-deficient mice show no specific or lethal phenotype and no neural problems. Nevertheless, electrophysiological and circadian rhythm effects[101,253,254], increased oxidative stress markers and higher sensitivity to neurological damage could be observed[255]. However, the symptomatology is strongly correlated with the type of the knock-out strategy. If the flanking regions like the splice acceptor site of the third exon are involved, ataxia and Purkinje cell loss can occur.[256] It could be shown that cell degeneration and demyelisation of peripheral nerves lead to ataxia.[256–258] Among other things exon skipping leads to an involvement of *Prnd*, which lies 16kb downstream of *Prnp* and encodes for Doppel (Dpl). Doppel gets overexpressed under control of the *Prnp* promotor[258,259] and the onset of clinical signs is inversely correlated to the measured level of Doppel in the brain[258]. Doppel is similar to PrP, but lacks the N-terminal tail. Interestingly, the same effects could be reproduced in transgenic mice if PrP fragments were expressed which lacked the same sequence part as Dpl.[260] Moreover, the negavie effect of a higher Dpl expression could be antogonized by an insertion of *Prnp*. Therefore, the cell loss can be attributed to the altered transcription of a neighboring gene and different models have been published to delineate the function of PrP as a neuroprotective antagonist to Doppel.[190,260] The concentration of Doppel itself has no effect, neither on the TSE incubation time, spongiform degeneration nor PrP^{Sc} deposits.[261] Interestingly, homozygous PrP-knockout mice are resistant to scrapie. They show no clinical signs for two years and neither propagation of prions in brain or spleen nor scrapie-specific pathology within 57 weeks after inoculation could be detected.[235] Nevertheless, low levels of infectivity can be made out in PrP knock-out mice brains directly after intracerebral inoculation.[262,263] However, a genotype with a single *Prnp* allele leaded to almost doubled incubation times, but similar levels of infectivity.[264]

The octapeptide of PrP is able to bind copper ions (cp. Figure 1.7 A, p. 28).[265,266] Thus, PrP might act as a recycling receptor for the copper assimilation of the cell. Indeed, copper chelating agents can induce TSE-like pathology[267], while an overexpression of PrP also leads to increased copper assimilation and superoxide-

dismutase (SOD) activity. SODs prevent cells from superoxide toxicity.[268] In addition, the slightly dismutase activity of PrP is inhibited in the presence of PrP^{Sc} or shorter PrP fragments. This might explain, at least in part, the neural damage caused by prion diseases.[269] Usually PrP plies between plasma membrane and endocytotic compartiments.[270,271] However, the internalization of PrP^{C} can be reversible stimulated by copper ions.[272] Reduced copper concentration in brain tissue of PrP-knockout were observed, while increased copper levels were detected in serum samples.[265] Unfortunately, these results could not be confirmed.[273] Nevertheless, a change in copper concentration, lower PrP-copper binding as well as a decreased antioxidant activity were observed in scrapie infected mice.[274,275] Similar observations were made for sCJD. The copper level in brain tissue of sCJD patients was found to be 50% less compared to healthy brain tissue samples.[276] Furthermore, copper increases the stability of β-sheets and promotes the shift from an alpha-helical to a β-sheet-rich isoform (PrP^{res}).[277]

It was also argued that PrP plays a role in signal transduction. For example, PrP^{C} binds to Fyn – a member of the Src-family of tyrosine kinases.[278] PrP also interacts with the prion interactor protein Pint1.[279] Physiological relevance or effects, however, could not be shown. Because of its property to bind to Bcl-2 or BH2, the role of PrP in programmed cell death was also discussed. If it is overexpressed, Bcl-2 is able to decrease the susceptibility for apotosis of $PrP^{-/-}$ neurons.[280] Similar to PrP, the sequence of BH2 (Bcl-2-homologe domain of Bcl-2-family) shows octarepeats. It binds to the proapoptotic protein Bax and inhibits apoptosis. Additionally, PrP^{C} itself inhibits Bax induced apoptosis.[281]

2 Objectives

The molecular structures of protepathic seeds, such as PrP^{Sc}, and the underlying mechanisms of neurodegenerative disorders are still elusive. However, it is likely that specific seed conformations are not an exclusive feature of prion diseases. A better knowledge of the formation and stability of proteopathic seeds would provide a more accurate picture of the underlying principles in self-templated protein misfolding and could help to find new therapeutic approaches against neurodegenerative disorders. Unfortunately, neither seed populations, nor their hypothetical conformational interconversion have been observed directly. Nevertheless, it was demonstrated that amyloids share similar features. For instance, amyloid fibrils show a cross-β structure with β-strands perpendicular to their long axis.[147,151,152] They are stabilized by hydrogen bonding and steric zippers. Interestingly, variable side-chain interactions of the constitutive protein monomers modulate the mechanical properties of the protein fibril.[282–287]

Based on the assumption that differentially structured proteopathic seeds are selectable because of their specific fragmentability, we were thus looking for a new concept for the *in vitro* selection of individual seed populations from mixed starting populations.

3 Materials and methods

3.1 Materials

3.1.1 Chemicals

If not indicated otherwise the chemicals used in this PhD thesis were ordered from one of the following companys: Aldrich, Difco, Emerald Biostructures, Fluka, Gerbu, GIBCO BRL, Hampton Research, Merck, Millipore, Pharmacia, QIAGEN, Riedel-de Haën, Roche, Roth, Sigma und Stratagene.

If not stated otherwise, all chemicals used were of ‘pro analysis’ (p.a.) grade.

Water was deonized using a Milli-Q Plus Water Purification System (Millipore).

Molecular-biological methods used in this work are adapted from standard collections of methods and protocols.[288–290] These methods will not be explained in detail. Only variations of standard protocols have therefore been described below.

3.1.2 Enzymes

For the digestion of prion samples proteinase K (PK) from Merck was used.

3.1.3 Size standards

All SDS gels were performed using the SeeBlue® Plus2 Pre-Stained Standard from Invitrogen (3-188 kDa for the use with Invitrogen NuPAGE® MES gels).

3.1.4 Additional agents and materials

Specific agents are scheduled in Table 3-1.

Table 3-1: Specifc agents

Purpose	Name	Manufacturer
Antibodies	mAb 6H4 (primary) A4a (secondary)	Prionics
Protease inhibitor mix for SSA buffer	Complete tablet EDTA-free	Roche

Purpose	Name	Manufacturer
SDS-PAGE	20 x running buffer	Invitrogen
	4 x LDS (Lithium dodecyl sulfate) sample buffer	
	NuPAGE® Novex 4-12% Bis-Tris Midi Gel	
SSA additive	Dihexanoylphosphatidyl-choline (DHPC)	Avanti Polar Lipids
	Dimyristoylphosphatidylserine (DMPS)	
Western blot	SuperSignal West Pico stable peroxide solution	Thermo Scientific
	SuperSignal West Pico luminol enhancer solution	Thermo Scientific
	Immobilon-P transfer membrane (PVDF 0.45 µm)	Millipore
	Nitrocellulose transfer membrane	Millipore

3.1.5 Bicellar mixtures

Bicellar mixtures were used to optimize PMCA reactions (cp. 3.6.1, p. 46 *et seqq.*). Bicelles are bilayered micelles and have originally been thought to be used in solid-state NRM-studies. Used in an aqueous solution the edges of bilayer fragments are stabilized by certain detergents (Figure 3.1). Typical mixtures of dimyristoyl-phosphatidylcholine (DMPC) with mild detergents like dihexanoylphosphatidyl-choline (DHPC) or 3-(choalmi-dopropyl)-diemthylammonio-2-hydroxy-1-propane-sulfonate (CHAPSO) are known to form bicelles. Thus, liquid crystalline like bilayer properties can be achieved with different detergent:lipid ratios (~1:2-1:5). The wide range of possible pH values and temperatures (~30-50°C) provides good accessibility for biochemical approaches. The capability to vary detergent concentrations without significant changes in bicelle properties makes this model system interesting for structural NMR-studies. By this means, observations can be verified using different detergent:lipid ratios and made observations can be ruled out to be due to detergent concentration. Additionally, bicelles can be aligned in magnetic fields and therefore present a good source for structural information. Several studies support the capability of DHPC-DMPC bicelles to mimic membrane bilayers and functional reconstitution of water-soluble protein activity.[291–298]

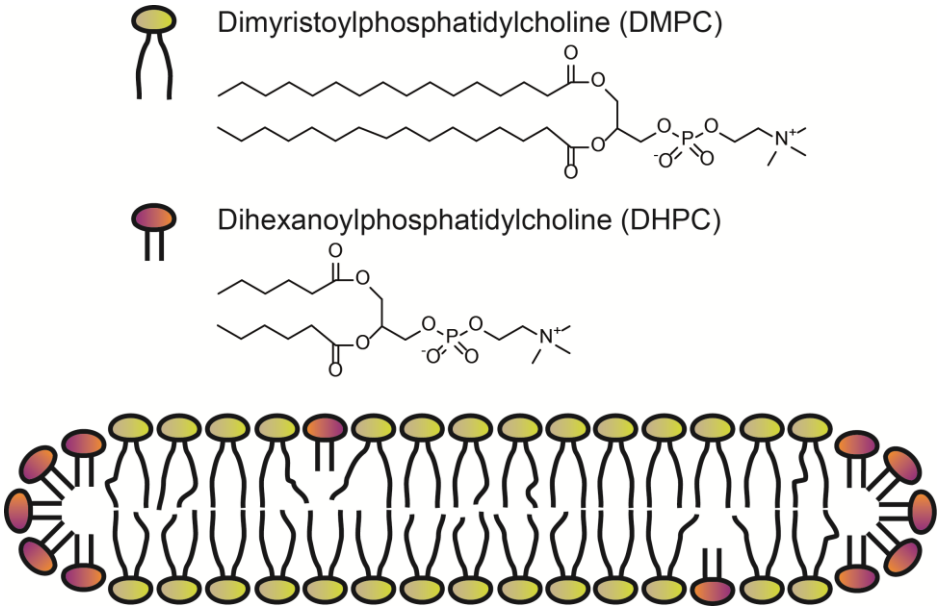

Figure 3.1: ***Model of a DHPC-DMPC bicelle***
Molecules of dimyristoylphosphatidylcholine (DMPC) form distinct bilayers. The edges are stabilized by the detergent dihexanoylphosphatidylcholine (DHPC).

Previous studies give support for the application of bicellar solution in PrP conversion experiments. So, cellular prion protein could be converted to a β-sheet-rich form using equimolar mixtures of DHPC and dimyristoyl-phospholipids. Regarding the positively charge of PrP a small percentage of negatively charged dimyristoylphosphatidylserine (DMPS) was added to the solutions. However, *de novo* generated PrP^{β} and $PrP^{\beta f}$ (PrP^{β} after detergent removal) failed to show infectivity in transgenic mice, which might be due to non-compatible conformational properties, the non-physiological pH-value of 5.0 during conversion or the lack of putative cofactors.[11,299]

The bilayer thickness can be approximately calculated.[300] The data needed for calculations, e.g. CMC (critical micelle concentration) and free DHPC content in bicelles has already been published.[301–303] Specific volumes for calculations are taken from publications of Tanford and Tausk.[304,305] With given specific volumes of 0.865 (DHPC) and 0.961 $cm^3\ g^{-1}$ (DMPC) and an estimated value of 0.961 $cm^3\ g^{-1}$ for DMPS a 250 mM stock solution (10 x) was prepared. For bicelle mixtures a DMPC:DHPC ratio of 1 was used ($q = [DMPC]/[DHPC] = 1$; $q^{eff,\ 37°C} = 1.25$). The calculated bilayer thickness was 5.49 nm.

The composition for 1 ml DMPC/DHPC resp. DMPC/DHPC/DMPS bicelle solutions is given below (Table 3.2). An appropriate intermixture of DHPC and bicelle solutions has been ensured by repeated freezing and thawing of the completed solutions.

Table 3.2: Composition of bicellar compounds for PMCA or QuIC

DHPC stock 40% (w/v)						
DHPC	1	g	0.865	cm³		
ddH_2O			1.635	cm³		
			2.5	cm³		

Bicelle stock (w/o DMPS)						
DMPC	250	mM	169.5	mg	162.8	µl (solid)
DHPC	250	mM	113.4	mg	283.5	µl stock
			282.9	mg	446.3	µl
					553.7	µl buffer
					1,000	µl

Bicell stock (with DMPS)						
DMPC	250	mM	169.5	mg	162.8	µl (solid)
DHPC	250	mM	113.4	mg	283.5	µl stock
% DMPS	10		17.5	mg	16.9	µl (solid)
			283.5	mg	446.8	µl
					553.2	µl buffer
					1,000	µl

3.1.6 Instruments

A list of all instruments used during this thesis can be found in Table 3.3.

Table 3.3: Instruments

Purpose	Name	Manufacturer
Autoclave	HAST 4-5-6	Zirbus
Blot cell	Trans blot® cell	Bio-Rad
Electrophoresis chamber (SDS-PAGE)	XCell4 SurelockTM Midi-Cell	Invtitrogen
Gel documentation	Electrophoresis Documentation	Kodak
Shear-generators (shear-generators for mechanical SSA)	Silent crusher S (tool 3 F)	Heidolph
Incubator	FunctionLine	Heraeus
pH-Meter	MP 230	Mettler-Toledo
Photometer	Ultraspec 3,000	Pharmacia Biotech
Mechanical SSA array	Prototype (cp. 3.6, p. 46 *et seqq.*)	Self-made Patent number EP2489427A1 and WO2012110570A1[306,307]
Thermoshaker	Thermomixer comfort with attachments for 1.5 ml reaction tubes or microtiter plates (MTP)	Eppendorf
Ultra sonic devices (PMCA)	Misonix 4,000 with Cup Horn for PMCA	Misonix
PMCA setup	Standard setup, as delivered by manufacturer (cp. 3.6.1, p. 46 *et seqq.*)	Misonix
	Modified water supply and drain of standard setup as well as rotating sample holder and sample holder with Chladni-figure-matched positions (cp. 3.6.1, p. 46 *et seqq.*)	Self-made
Acoustic SSA	Prototype (cp. 3.7.1, p. 52 *et seqq.*)	Self-made Patent number EP2489427A1 and WO2012110570A1[306,307]

Purpose	Name	Manufacturer
Deionized water supplies	Milli-Q Advantage A10	Millipore
	Milli-Q Plus	
Centrifuges	4K15C	Sigma
	5417	Eppendorf
Centrifuge rotors	Aerosol-tight rotor for Eppendorf 5417	Eppendorf
Centrifuge rotors	Swing-out rotor for Sigma 4K15C for 50 ml, 15 ml reaction tubes and microtiter plates	Sigma
Dry bath	FB15103	Fisher Scientific
Luminometer	LAS 3000	FujiFilm

3.1.7 Prion strains

Prion strains which have been used to seed *in vitro* PMCA and SSA reactions are listed below (Table 3.4). *In vivo* propagation (3.4, p. 42 *et seqq.*) in Syrian golden hamsters has been used for strain maintenance.

Table 3.4: Prion strains

Prion strain	Description	Source of supply
Sc237	Hamster PrP^{Sc}	Dr. Eckhard Flechsig and Prof. Dr. Michael Klein (Institute of Virology, University of Würzburg)
263K	Hamster PrP^{Sc}	Bruce W. Chesebro, M.D. (National Institutes of Allergy and Infectious Diseases, Hamilton)

3.1.8 Buffer solutions

Buffer solutions used in this thesis are listed below (Table 3-5).

Table 3-5: Buffer solutions

Application	Buffer	Ingredients/manufacturer
SDS gel electrophoresis	NuPAGE® MES SDS Running Buffer 20 x	Invitrogen

Application	Buffer	Ingredients/manufacturer		
	LDS sample buffer 4 x	Invitrogen		
Proteolytic digest of prion samples	PK Digestion buffer 2 x	2% (w/v) N-Lauroylsarcosin (Sarkosyl)/1 x PBS or 1 x PBS w/o Sarkosyl		
	PK solution	100 µg/ml proteinase K in 2 x PK Digestion buffer		
	PMSF (phenylmethyl-sulfonyl fluoride) solution	20 mM PMSF in isopropanol		
General	PBS 10 x	$Na_2HPO_4*2H_2O$	100	mM
		$NaH_2PO_4*H_2O$	100	mM
		NaCl	1,300	mM
Brain homogenate	Perfusion buffer	EDTA	5	mM
		KCl	2.68	mM
		$KH_2PO_4*H_2O$	1.76	mM
		$Na_2HPO_4*2H_2O$	8.09	mM
		NaCl	137	mM
		pH 7.4 with HCl		
		Filter with 0.2 µm pore size.		
		* added from a 100 mM stock solution		
PMCA or Acoustic/ Mechanical SSA	PBS-EDTA 1 x	NaCl	137	mM
		KCl	2.68	mM
		$Na_2HPO_4*2H_2O$	8.09	mM
		$KH_2PO_4*H_2O$	1.76	mM
		EDTA*	1	mM
		pH 7.4 with HCl		
		Filter with 0.2 µm pore size.		
		* added from a 100 mM stock solution		
	Conversion buffer	PBS-EDTA 1 x	19.2	ml
		5 M NaCl*	600	µl
		Triton X-100*	200	µl
		Add one Complete protease inhibitor pill.		
		* Add fresh before use.		
Western blot	TBST 20 x	Tris base	500	mM
		KCl	60	mM
		NaCl	2,800	mM
		Tween 20	1	% (v/v)
	Transfer buffer 10 x	Tris base	200	mM
		Glycine	1,500	mM
		10% (w/v) SDS	1	ml/l
		Methanol	20	% (v/v)
	Blocking solution in 1 x TBST	Milk powder	5	% (w/v)
		Goat Serum	1	% (v/v)
	Washing solution in 1 x TBST	Milk powder	1	% (w/v)
	Rinsing solution	1 x TBST		

Application	Buffer	Ingredients/manufacturer
	Primary antibody	mAb 6H4 1:5,000 in washing solution
	Secondary antibody	A4a 1:2,000 in washing solution

3.2 Protein analytical methods

3.2.1 SDS-Polyacrylamid-gel electrophoresis (SDS-PAGE)

SDS gels of digested prion and recombinant PrP samples were performed using the NuPAGE® SDS-PAGE Gel System (XCell4 Surelock^{TM} Midi-Cell, Invitrogen) and NuPAGE® Novex 4-12% Bis-Tris Midi Gels. All gel runs were carried out using 1 x LDS (Lithium dodecyl sulfate) sample buffer (working concentration 1 x, Invitrogen) and 1 x running buffer (from a 20 x stock solution , Invitrogen). For electrophoretic separation 200 V for 45 min were applied. Completed gels were used for subsequential western blot analysis (cp. 3.2.2).

3.2.2 Prion sample proteinase K digest and western blotting

Frozen prion samples were thawed up and short spun at 4°C. By pipetting the pellet was resuspended and 20 or 30 µl were transferred in a 1.5 ml screw cap reaction tube and stored on ice. After finishing the aliquots, step-by-step, the same volume of ice cold PK solution was added to the prion samples, to give a final concentration of 50 µg per ml. Once the PK was added, the mixture was vortexed immediately for three seconds and digested on a Thermoshaker (37°C, 750 rpm). Following a short spin for five seconds and an additional vortex step all samples were digested for one hour.

To stop the digest, exactly after one hour, 1/3 volume of 4 x LDL sample buffer was added to the digestion mixture. The sample was vortexed and immediately incubated at 96°C (750 rpm) for more than 10 min. After boiling, the samples were centrifuged for ten seconds at 25,000 *x g* (4°C).

Thereafter, samples were used for SDS-PAGE analysis (cp. 3.2.1). On the brink of transferring to the gel, samples were shortly mixed. Subsequently, a western blot using a nitrocellulose or PVDF membrane (activated with methanol) was performed using the Bio-Rad Trans blot® cell system at 65 V for 1.5 hours. The protocol for blot development is given below (Table 3-6).

In an alternative protocol higher numbers of prion samples were digested using 96-well PCR plates and compatible Eppendorf Thermoshaker attachments. This method was especially applied for numerous samples of SSA reactions (3.6, p. 46 *et seqq.*):

Shock-frozen samples of SSA reactions were thawed for 10 min at 22°C using Thermoshakers with a rotation speed of 1,000 rpm. Kept at 4°C and after short mixing with a 1,000 µl pipette volumes of 10 µl were successively transferred to a pre-cooled microtiter plate. The plate was sealed with translucent adhesive foil and centrifuged for one minute at 500 *x g*. Using an eight-channel pipette 20 µl of PK solution were added and samples were mixed by pipetting. Again the microtiter plate was covered with foil. To ensure sealing of the foil and to avoid aerosol leakage during the digest a strong pressing on is highly recommended. The plate was transferred to a prewarmed Thermoshaker and samples were digested for one hour at 37°C and 1,000 rpm. Directly after five minutes the incubation was interrupted for a short centrifugation step (500 *x g* for 1 min at RT) followed by a continuation of the digest for the remaining 55 minutes. Following this, the plate was stored on ice for 5 min.

Under usage of a multichannel pipette 1 µl of PMSF (phenylmethylsulfonyl fluoride) stock solution was added to each well to inhibit protease acitvitiy. The protease inhibitor was intermixed with the digestion mix by stirring at 1,400 rpm for 1 min using the Thermoshaker (precooled to RT). Once again the plate was incubated on ice for 5 min, followed by the addition of 4 x LDS sample buffer (7 µl per well) with aid of the multichannel pipette. For the boiling step that followed (96°C ≥ 10 min in a dry bath) the plate had to be sealed with PCR lid stripes instead of adhesive foil, which showed up not to be heat resistant. Before boiling the plate was thoroughly shaken to ensure good intermixture (Thermoshaker, 1,400 rpm for 1 min at RT). Boiled samples were stored on ice until further use for SDS-PAGE (cp. 3.2.1, p. 39). Completed gels were transferred to PVDF (activated by methanol) or nitrocellulose membranes using a methanolic transfer buffer and the Trans blot® cell system (Bio-Rad). For transfer 65 V for 1.5 hours were applied. Development of the blot followed the steps which are given in Table 3-6.

Table 3-6: Blot development

Step	Time [min]	Temp. [°C]	Solution	Vol. [ml]
Blocking	45 (or o/n)	RT (4°C)	Blocking solution	40
Rinse	0.5	RT	Rinsing solution	~40
Washing	3 x 10	RT	Washing solution	40
1st antibody	45	RT	mAb 6H4 goat-anti-mouse PrP, 1:5,000	10
Rinse	0.5	RT	Rinsing solution	~40
Washing	3 x 10	RT	Washing solution	40
2nd antibody	45-60	RT	A4a, 1:2,000	10
Rinse	0.5	RT	Rinsing solution	40
Washing	3 x 10	RT	Washing solution	40
Rinse	0.5	RT	Rinsing solution	40
Detection		RT	ECL Western Pico	2 + 2[1]

3.2.3 Quantification of prion samples by western blotting

Developed western blots were submerged with ECL Western Pico solution (2 ml peroxide solution + 2 ml enhancer for a standard blot size corresponding to a 26 lane the NuPAGE® MES Bis-Tris Midi-gel) and analyzed using the LAS 3,000 system (FujiFilm). Sensitivity was set to "super" and plate position 2 was chosen. Shots were successively taken after exposure times of $^1/_8$; ¼; ½; 1; 2; 4; 8; 10; 30; 60; 120 and 240 seconds. Quantification was performed using the Aida Image Analyzer software (Raytest).

3.3 Safety precautions for work with scrapie prions

The performed work was agreeable to the order 603 of the Health and Safety Executive (Federal institute of industrial safety and industrial medicine; Ger.: Bundesanstalt für Arbeitssicherheit und Arbeitsmedizin). All decontamination and disinfection protocols have been adapted from several publications[20,62,64,66,67,308] and are listed in Table 3.7.

[1] A standard blot made from a 26 lane the NuPAGE® MES Bis-Tris Midi-gel was developed using 2 ml peroxide solution + 2 ml enhancer solution per membrane

Table 3.7: Decontamination protocols

Type of object	Decontamination
Surface (e.g. lab furnitures), Plastic ware (e.g. dishes, beakers)	1 M NaOH (≥ 1 h), general cleaning with 1% (v/v) LpH^{TM}se
Solid waste (e.g. gloves, tissue paper) and animal cages	autoclaved at 134°C (2 bar) for one hour or at 143°C for 30 minutes
Body parts of prion inoculated animals	incubated in 1 M NaOH/0.5% (w/v) SDS (≥ 1 h) and autoclaved at 121°C for one hour in this solution
Metal-objects and glassware	Due to higher resistance of prions on metal surfaces and glassware[309] objects were treated with 1 M NaOH/0.5% (w/v) SDS (≥ 1 h), rinsed with water, followed by a decontamination in 5 M GITC (≥ 1 h).
Shear-generators (dispersion tools)	Disassembling and decontamination in 1 M NaOH/0.5% (w/v) SDS (submerged, ≥ 1 h) PTFE (polytetrafluoroethylene) bearings and O-rings were discarded, rest was thoroughly washed with deionized water decontamination in 5 M GITC (≥ 1 h) all parts were thoroughly washed with deionized water, only metal parts were autoclaved at 121°C for 30 min in 1 M NaOH/0.5% (w/v) SDS parts were again rinsed with water and incubated in high concentrated formic acid (≥ 1 h)

3.4 *In vivo* prion propagation

Strain maintenance of prion strains and the provision of sufficient amounts of prion isolates for *in vitro* experiments were ensured by *in vivo* passaging.

For that purpose six to eight weeks old, male, healthy wild-type Syrian golden hamsters (*Mesocricetus auratus*; Harlan or Charles River) were anesthetized and injected intracranially into the right hemisphere with 30 µl of 1% (w/v) inoculum in filter sterilized PBS (prion strains 263K or Sc237). After strain-specific latency periods of 90-100 days the animals started to show clinical signs like ataxia, disinterest and drowsy behavior. If adequate and sufficient dietary intake could not

be ensured anymore due to illness, badly affected animals were sacrificed for brain removal (cp. 3.5, p. 44 *et seqq.*).

The animals were anesthetized using subcutaneous injection of Ketamin and Medetomindin. Antagonization was performed using Atipamezol. Concentrations and dosage are listed in Table 3.8. Intracerebral injection was performed with help of Dr. Verena Haist (University of Veterinary Medicine Hannover, Institute of pathology). A tuberculin syringe was used. Injection depth and the necessary cannula size to drill through the skull plate had been investigated by tests with dead animals. Reproducibility of injection depth was ensured by usage of self-made spacers (built from the cannula cap). After injection of the homogenate the needle was not directly removed to avoid unwanted reflux and therefore spread of contaminated liquid. To stabilize the cardiovascular system, inoculated hamsters were bedded on warmed gel pads.

Table 3.8: Anesthetization and antagonization of Syrian golden hamsters

Anesthetization working solution				
			Final concentration	
Ketamin (10%, WDT, Garbsen, Germany)	0.6	ml	12	mg/ml
Medetomindin (Domitor, Pfizer, Karlsruhe, Germany)	0.1	ml	0.02	mg/ml
Physiological saline solution	4.3	ml		
Total	5	ml		

Dosage
0.8 ml working solution /100 g body weight s.c.

Equal to dosage			
Ketamin	96	mg/kg	body weight
Medetomindin	0.16	mg/kg	body weight

Depending on the animal behaviour it can be necessary to inject additional 0.1-0.2 ml of the working solution after 20-30 min.

Antagonization working solution		
Atipamezol (Antisedan, Pfizer, Karlsruhe, Germany)	0.1	ml
Physiological saline solution	4.9	ml
Total	5	ml

Dosage
Use 1/3 to 1/2 of the initial anesthesia injection volume s.c. approx. 1-1.5 hours after anesthesia.

Equal to dosage			
Atipamezol	0.3-0.4	mg/kg	body weight

3.5 Brain tissue homogenate

Brains of healthy, six to eight weeks old, male Syrian Golden hamsters (*Mesocricetus auratus*; Harlan or Charles River) were used to prepare normal brain homogenate (NBH). Since the concentration of PrP^C is relatively high in neural tissue[252,310,311], NBH was used as a substrate for *in vitro* PrP conversion experiments (cp. 1.5, p. 23 *et seqq.*), such as PMCA and SSA.

Euthanasia, perfusion of the circulation system as well as the organ harvesting of healthy hamster brains and the later tissue homogenization were performed on a prion free workbench. The animals were asphyxiated with carbon dioxide. The abdominal wall was opened with a small incission, the conjunctive tissue was disjointed using surgical scissors. Following three cuts were performed: two lateral relief cuts and one ventral cut from the xiphoid of the sternum up to the throat. Two additional relief cuts towards the paws were performed after dissecting the conjunctive tissue of the thorax. The hepatic lobes were set aside. In the next step the diaphragm was cut semicircular, following the curvature of the thorax. With lateral cuts the costal arches were severed and the thorax was opened.

Then, a 20 ml-disposable syringe was filled with perfusion buffer (RT). A 21 G-cannula was used for horizontal injection into the left ventricle. Once the cannula had been injected, the right atrium was cut in. The perfusion was performed using two times 20 ml with a constant flow rate of approximately 10 ml/min. After

refilling the syringe, the same injection point was used again to avoid buffer leakage.

A successful perfusion of the brain is indicated by a rapid discoloration of the liver and the fine intestine blood vessels.

Afterwards, the animal was decapitated between the skull base and the first cervical. Hampering muscle tissue was removed. With small scissors a horizontal cut below the brain to the ears was done on both sides. A last vertical cut was done along the cranial suture.

Ideally, the skull plate opens up by itself. The perfused brain is of yellowish white color and shows no reddish discoloration.

Nasal nerves and stem brain were removed and the brain was washed with about ten milliliters of perfusion buffer. Rinsed brains were flash frozen in liquid nitrogen and stored at -80°C until later use. The time period between the animal's death and the shock freezing of the brain averaged out to 20 min.

Brain tissue homogenate of scrapie affected hamsters was used to seed *in vitro* PrP conversion reactions. When pronounced clinical signs of prion disease became evident in the hamsters, the brains were harvested (cp. 3.4, p. 42). Contrary to healthy animals, the procedure was carried out on a prion working bench under certain biological safety aspects: Instead of protective goggles a safety ventail was used and the arms were covered with protective sleeves. Furthermore, the procedure was performed in a plastic dish. Additionally, the surrounding surfaces were covered with aluminium foil.

Contrary to the preparation of substrate (NBH) for *in vitro* prion amplification and the preparation of seed (scrapie brain homogenate, ScBH) does not necessarily require perfused brains. Anyway, the absence of blood might positively influence the reaction.

Materials and body parts were decontaminated as stated in Table 3.7 (p. 42).

For the preparation of brain homogenate frozen hamster brains were taken out of the storage freezer and immediately covered with ice. The brains were covered with the necessary volume of freshly prepared ice cold conversion buffer to finally create a 10% (w/v) brain homogenate. Filled into the glass tube of a pre-cooled dounce homogenizer, the organs were squashed by rotation of the pistil at the bottom. Followed by twenty strokes the tissue was finally crushed. Bubble formation was avoided. Afterwards, aliquots of about four milliliter were centrifuged in pre-cooled

15 ml-reaction tubes for 2 min, 2,000 *x g* at 4°C. The supernatants were pooled. In contrast to NBH the homogenization procedure of scrapie prion brains was performed using sterile 10 ml-disposable syringes (18 G and 21 G-cannula, ten strokes).

After the homogenization procedure the NBH should have a yellowish white color. A reddish color indicates residual blood in the tissue. In this case, the homogenate was discarded. Freshly prepared NBH was stored on ice and used within one hour. Scrapie brain homogenate was aliquoted, flash frozen and stored at –80°C until further use.

3.6 PrP^{Sc} amplification by ultrasonic processing

3.6.1 Protein Misfolding Cyclic Amplification (PMCA)

As stated earlier the PMCA represents a powerful method for generating significant amounts of infectious prions *in vitro* (cp. 1.5, p. 23 *et seqq.*). Optimiziation strategies to amplify uncharacterized prion isolates, however, are based on a trial and error.[231] Prior to acoustic SSA we tested the standard PMCA approach (cp. 3.7.1, p. 52 *et seqq.*). Observations that were made on the overall amplification efficiency directly leaded to improvements of the standard PMCA setup[207] as well as the development of the acoustic SSA (cp. 3.7.1, p. 52 *et seqq.*). The standard ultrasonication setup – as purchased from Misonix (Misonix 4,000) consists of a control device, an ultrasonic generator and a corresponding Cup Horn sonotrode with an attachable water bath. The standard sample holder is a floating plate that can be used for prion amplification reactions in thin-walled PCR tubes (Figure 3.3 A). An output frequency of 20 kHz is stated for the device. Regarding the propagation velocity of sonic waves in water the wave length is calculated as follows:

$$\lambda = \frac{c}{f} = \frac{1{,}45\ km/s}{20{,}000\ Hz} = \frac{1{,}45\ km/s}{20{,}000} \cdot \frac{1}{s} = 7{,}25\ cm \qquad (3.1)$$

λ represents the wavelenght.

c is the propagation velocity of sonic waves in a particular elastic medium.

f is the frequency.

Water inlet and outlet of the system were connected to a customary temperature-controlled water bath with an implemented pump. To guarantee a constant water fill level in the Cup Horn water bath the tube lengths and dimensions as well as the

height differences between pump and Cup Horn were never changed. Bacteria growth was avoided by regularly renewel of the water. Thus, also metal particles that were detached from the sonotrode surface by cavitational damage (cp. Figure 3.2) were removed. The wear and tear of the sound emitter, which mainly consists of aluminium (AlMgSi, > 99% aluminium), necessitates a frequent exchange. On that purpose, sonotrode replicas were ordered from a local milling company.

The standard stetup from Misonix was used for initial experiments using the hamster prion strain Sc237. Different starting seed dilutions were tested. Therefore, a 10% (w/v) ScBH was diluted 1:10, 1:20, 1:50, 1:100, 1:200 and 1:400 into a 10% (w/v) NBH. Aliquots of 100 µl were processed at a power level of 90% for 40 seconds every 60 minutes (24 cycles, 37°C). Additionally, the seeding capability of the generated reactions product was tested in serial PMCA. On that purpose, the processed reaction mixture was diluted 1:10 into new NBH and again processed for 40 seconds every 60 minutes (24 cycles). In a second experiment the influence of sample positioning was surveyed. A 10% (w/v) Sc237BH was diluted 1:20 into a 10% (w/v) NBH. Aliquots of 100 µl were processed at a power level of 90% for 40 seconds every 60 minutes (24 cycles, 37°C, sonotrode replica I).

Bicellar mixtures are known to show substantial effect on the conversion of recombinant PrP to a β-sheet-rich isoform.[11,299] As announced earlier DHPC-DMPC bicelles showed the potential to act as membrane bilayers (3.1.5, p. 33).[291–298] The prion protein is GPI-anchored. Thus, it is likely that the *in vivo* conversion of PrP^{C} takes place at certain membrane sites with or without support of other membrane-associated molecules. The C-terminal domain of PrP^{C} is largely positively charged. Therfore, negatively charged bicelles (charged by addition of phosphoserine) were thought to show the strongest effects. Thus, the effect of lipid and bicelle addition was surveyed in PMCA. Therefore, a 10% (w/v) Sc237BH was diluted 1:20 into a 10% (w/v) NBH. The reaction mixture contained DHPC/DMPC bicelles (final concentration 25 mM (0.5 or 10% Phosphoserine), cp. 3.1.5, p. 33) or DHPC alone (12.5, 25 or 50 mM). Aliquots of 200 µl were processed at a power level of 90% for 40 seconds every 60 minutes (24 cycles, 37°C, sonotrode replica I).

In order to further investigate if the PrP^{res} amplification is better near to the center of the sonotrode or at the rim, a centered sample holder with a helical positioning of the samples was used. Floating on the water surface this device could rotate around an axis perpendicular to the middle of the sonotrode and was driven by the water flow of the system (Figure 3.3 B). A 10% (w/v) Sc237BH was diluted 1:20 into a 10% (w/v) NBH. The amplification of PrP^{res} was surveyed in the presence and absence of DHPC/DMPC bicelles (final concentration 25 mM (no Phosphoserine),

cp. 3.1.5, p. 33). Aliquots of 100 µl were processed at a power level of 90% for 40 seconds every 60 minutes (48 cycles, 37°C, sonotrode replica I).

To investigate the soundwave emission of the sonotrode, we took a closer look at the shape of the cavitation damage pattern on the Cup Horn surface (Figure 3.2). Three recreated Cup Horns showed individual patterns of irregular shape (Figure 3.5, p. 54) which resemble the geometry of the underlying harmonic surface oscillation function.

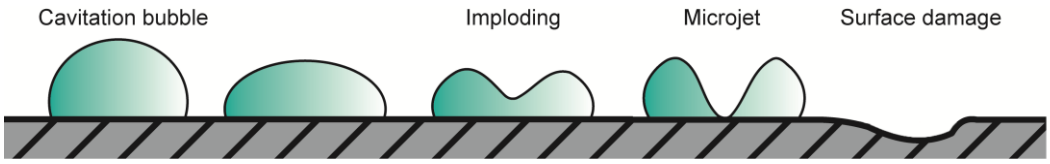

Figure 3.2: ***Cavitation effect in local pressure minima due to oscillation of the sonotrode***

Following the law of Bernoulli the static pressure of a liquid gets lower with its increasing velocity. If the static pressure deceeds the vapor pressure of a liquid, steam bubbles can occur. Moved by the flowing liquid these bubbles reach areas of higher pressure. The rapidly increasing static pressure leads to a sudden condensation at the bubble walls. Implosively water streams back and an extreme temperature and pressure boost is the consequence. Cavitation bubbles are relatively big (up to 150 µm) and occuring pressure and temperature gradients can reach up to 500 bar and 5200 K. Sticked to a surface, these cavitation bubbles form a microjet which leads to known damages on pump parts, ship's propellers and also sonotrodes. Cavitation effects occur in a low frequency range from 20 to 100 kHz.

With the purpose to understand the influence of the oscillation behavior on the amplification of PrP^{res} we considered to use fixed sample positions. Thus, a new sample holder was developed. The position of the reaction vials were matched to the estimated anti-nodes of replica I (Figure 3.3 C and Figure 3.4). Additionally, the water bath was modified to ensure a better water circulation and therefore a better temperature control (cp. Figure 3.4). This was achieved by four flexible tubes attached to four T-piece adapters, which were fixed at the outer plastic ring of the Cup Horn water bath. All tubes were connected to the water inlet of the pump and rendered the existing outlet tube unnecessary. This, in turn, from then on worked as a second water inlet. By usage of T-piece adapters the newly connected tubes were upwardly opened and trapped air bubbles were avoided. The height difference of pump and Cup Horn water bath, flow rate, as well as tube lengths and arrangements were checked prior to each experiment to allow a constant water level above the Cup Horn and therefore a reproducible oscillation behavior of the sonotrode. The sample holder was always completely submerged.

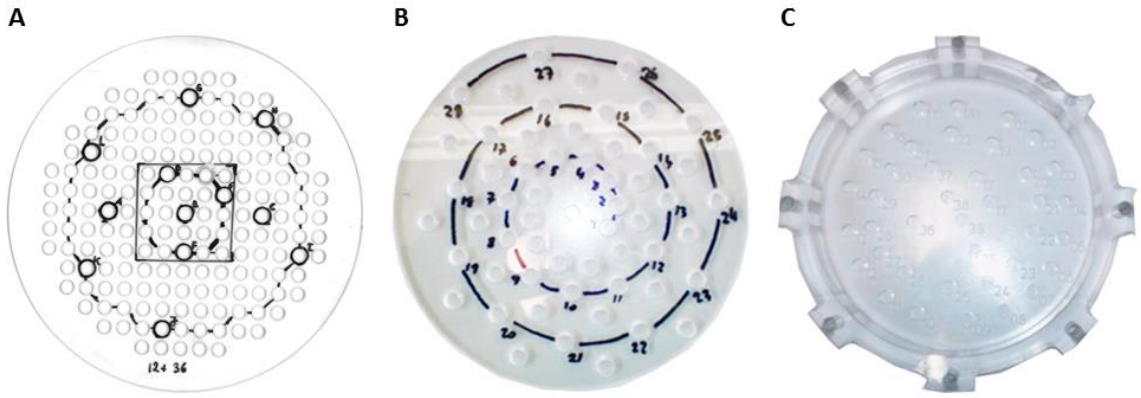

Figure 3.3: ***Different sample holders for PMCA***

(A) *Standard floating sample holder (Misonix 4,000 PMCA setup);* ***(B)*** *Centered sample holder to analyse the radius dependence of sonotrode in PMCA reactions; The device could rotate around an axis perpendicular to the middle of the sonotrode. It was propelled by the water circulation.* ***(C)*** *Fixed sample positions; The positions of the reaction vials were matched to the observed vibrational pattern of replica I. Eight screws at the rim of the sample holder could be used to adjust the height. The screws were standing on the plastic rim of the water bath with no direct contact to the sonotrode.*

The amplification of the hamster prion isolates 263K and Sc237 was determined at multiple heights (0.5, 3, 5, 7 and 9 mm) above the sonotrode surface. A 10% (w/v) ScBH was diluted 1:20 into a 10% (w/v) NBH. Aliquots of 200 µl were processed at a power level of 90% for 60 seconds every 10 minutes (24 cycles, 37°C, sonotrode replica I).

Reaction mix and preparation steps for PMCA

Frozen scrapie brain homogenate was thawed and mixed with freshly prepared NBH (cp. 3.5, p. 44 *et seqq.*) by pipetting. If not mentioned otherwise a 5% (v/v) mixture of 10% (w/v) ScBH in 10% (w/v) NBH was used for conversion reactions. Long storage as well as freezing of the homogenates before usage was avoided.

Thin-wall PCR-tubes were filled with the reaction mix and were flash frozen in liquid nitrogen for later use. Reaction volumes varied and are given for the particular experiments (cp. Table A**.1**, p. 91). Before using frozen samples were thawed at 37°C for 10 min. If necessary, sample tubes were mildly spinned to avoid deposition of droplets in the lids. However, pellet forming was avoided.

Another fact which has to be stated is that freshly produced brain homogenate is viscous. Included SDS and Triton X-100 act as frothing agents. Thus, to exclude later differences in amplifcation due to different processing, trapped air bubbles and froth were strictly avoided. Reaction tubes with droplets in the cap, spurted from the homogenate at the bottom, were also not rarity in standard reactions. Of course this

effect entailed incomplete processing and could be avoided if reaction tubes were mounted as described in Figure 3.7 A. Prior to each experiment the samples were exposed to one sonic burst (power level and length were set as the process steps for the particular experiment) to redissolve settled material.

A list of all performed PMCA experiments is given in Table A.1 (p. 91)

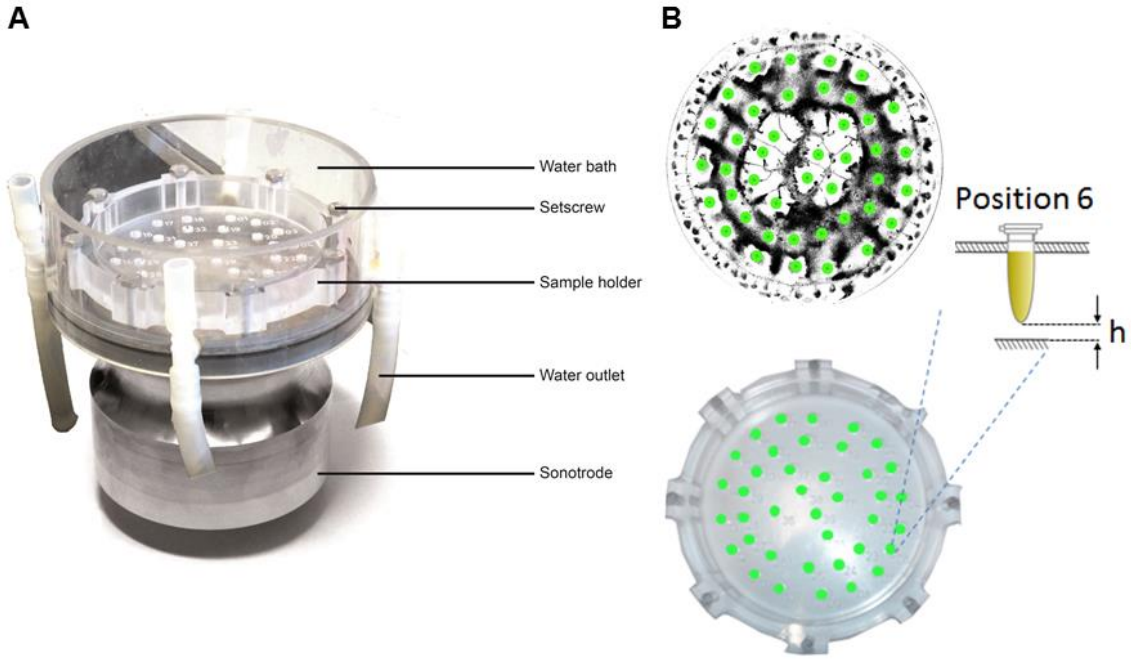

Figure 3.4: ***Fixed sample positions in PMCA***

(A) *Water bath modification in PMCA. Four flexible tubes were attached to four T-piece adapters, which were fixed at the outer plastic ring of the Cup Horn water bath (Misonix). All tubes were connected to the water inlet of the pump and rendered the existing outlet tube unnecessary. This, in turn, from then on worked as a second water inlet. By usage of T-piece adapters the newly connected tubes were upwardly opened and trapped air bubbles were avoided. The modifications of the water drainage avoided unnecessary sample heating. Additionally, a Cup Horn specific sample holder was built. The positions were matched to the observed vibrational pattern of a recreated sonotrode. While the reaction vial position could be exactly reproduced in the horizontal plane, eight screws also allwed to control the height. Vertical postioning was accurate to half a millimeter.* ***(B)*** *Wrong color image of a recreated sonotrode (replica I, cp. Figure 3.5, p. 54); Vibration nodes are black (top). The corresponding sample holder is shown in top view (bottom). Estimated optimal positions are indicated in green (top and bottom). A cross-sectional view is exemplary shown for position six. All technical modifications of the sonotrode setup were planned and realized by Dr. Thorsten Lührs (HZI). The system is registered under the patent number EP2489427A1 and WO2012110570A1.*[306,307]

3.7 Selective Shearing Amplification (SSA)

Today it is widely accepted that phenotypically distinguishable prion strains are largely determined by prion seed conformations (cp. 1.3, p. 15 *et seqq.*).[312] Nevertheless, the molecular properties of self-propagating proteopathic seeds still remain unclear. It is, however, well known that the specific seeding activities of protein seeds depend on the particle size.[177] Thus, fibril fragmentation influences fibril formation processes.[174,313] Indeed, these facts were supported by experiments of Silveira and coworkers which demonstrated that the specific infectivity of the hamster prion strain 263K strongly depends on the size of the prion particles.[177] It is possible that a uniform seed population might comprise a distribution of size-separable particles of the same conformation, which differ in their activity. Although the molecular structures of protein seeds are unclear, it was demonstrated that amyloids share similar features. For instance, amyloid fibrils show a cross-β structure with β-strands perpendicular to their long axis.[147,151,152] They are stabilized by hydrogen bonding and steric zippers. Interestingly, variable side-chain interactions of the constitutive protein monomers modulate the mechanical properties of the protein fibril.[282–287] We therefore expected that differentially structured proteopathic seeds are selectable because of their specific fragmentability. Kinetic models provided by Knowles and coworkers indicated that the number of initial nuclei resp. the primary nuclation rate do not influence the maximum growth rate (V_{max}) in polymerization (cp. 1.4, p. 19 *et seqq.*). Moreover, fragmentation clearly promotes *in vitro* polymerization of fibrils and toggles growth rate and lag time. In the particular case of seeded growth primary nucleation processes can be neglected.[174,314] Thus, fibrillar growth is determined by seed elongation, monomer dissociation and seed fragmentation. In the case of induced fragmentation, spontenaous fragmentation processes can also be neglected.

We developed a new concept for the *in vitro* selection of individual seed populations which is based on shear stress induced seed fragmentation. Shear forces act parallel to particle cross-sections and critical shear leads to log-normal particle size distributions[315] which evince an explicit similarity to equlibrium fibril length distributions.[313] With a given shear stress the mean particle size can be calculated using equation (3.2).[315] If a constant shear-stress is assumed, the median particle size increases proportionally to the stabilizing forces between the monomers. Alternating periods of seed growth and selective shearing would kinetically select seed population which are optimally fragmented. The amplification of seed populations that show a distinct mechanic fragmentability, however, would be

suppressed. Therefore, Selective Shearing Amplification (SSA) provides a concept for the *in vitro* selection of uniform seed populations from putative mixtures.

$$\langle n \rangle = e_{ij}\, \tau^{-q} \tag{3.2}$$

$\langle n \rangle$ is the asymptotic mean particle size

τ ist the shear stress (cp. Figure 3.8)

e_{ij} is a seed particle specific constant that ist proportional to the binding strength of the monomers, while q has been found to be ~0.74 ± 0.02.[315]

3.7.1 Acoustic SSA

The concept of selective shearing had to be proven experimentally. On that purpose the *in vitro* amplification of hamster scrapie prions was surveyed in healthy brain tissue homogenates using an ultrasonic approach. It is known that PMCA reactions are cappable to amplify infinite amounts of infectious prions.[207] Unfortunately, former approaches using a modified PMCA setup (cp. chapter 3.6.1, p. 47 *et seqq.*) revealed its inefficiency regarding a selective ultrasonic fragmentation (cp. 4.1, p. 65 *et seqq.*): We could demonstrate the feasibility of seeded conversion using the hamster prion strain Sc237. However, we also revealed technical drawbacks of the technique with respect to the total yield in PrP^{Sc} and the experiment reproducibility Although the experimental data indicated a promoting effect of bicelles we were not able to circumverent the observed variabilities in the reaction outcome. These problems could be attributed to the irregular oscillation behavior of the Cup Horn sonotrode, which represents a superficial source of sound. Contrary to PMCA, we used a sonotrode with a symmetric pattern for acoustic SSA. These patterns are also referred to as Chladni-figures (Ernst Florenz Friedrich Chladni, 1787). Chladni demonstrated that fixed metal plates can be excited to harmonic vibrations. The physical effect can be visualized if sand is sprinkeled on a vibration plane. The sand grains are repulsed from anti-nodes and are collected in nodes. The used sonotrodes mainly consists of relatively soft aluminum (AlMgSi, > 99% aluminium) and a Chladni-like pattern becomes visible by cavitational damage. Cavitation bubbles occur in areas of strongest amplitudes and implode on the sonotrode surface (Figure 3.2, p. 48). Resulting surface damage generates a Chladni-like pattern, the ‘fingerprint’ of a standing wave, which represents a non-homogeneous sound power density distribution. In other words, the Chladni figure reflects the geometry of the harmonic surface oscillation function.

For acoustic SSA we used a sonotrode replica which showed a clear five-fold symmetry in the Chladni-pattern (Chladni I, Figure 3.5). The Cup Horn was pro-

duced by a local milling company. Shear forces are highly position dependent in the horizontal plane. Correct sample positioning, thus, is recommended for optimal PrP^{res} amplification yields.[316] Consequently, a new ultrasonic setup was designed. And the sample positions were exactly matched to the anti-nodes of the Cup Horn (Figure 3.6). Ultrasound waves can be considered as alternating pressure amplitudes and solvent velocity amplitudes. Occurring velocity gradients, *w*hether spatial or temporal, induce the fragmentation of contained particles by corresponding shear forces. As mentioned before, shear acts parallel to the cross-sections of a certain particle. Reaching a critical value it leads to the breakage at the weakest point. The shear stress, τ, is the product of the solvent viscosity, η, and the local velocity gradient, ∇v (3.3). The local velocity gradient is also known as shear rate, G. A multiplication of the particle velocity $\boldsymbol{v}(t)$ with the acoustic pressure, $p(t)$, gives the sound intensity, $\boldsymbol{I}$ (3.4).

$$\tau = \eta \times \nabla v = \eta \times G \tag{3.3}$$

$$\boldsymbol{I} = \boldsymbol{v}(t) \times p(t) \tag{3.4}$$

Conclusively, the maximal pressure gradients are proportional to the magnitude of the maximal particle velocity gradients, ∇v_{max}, if a constant mean sound intensity is assumed. Furthermore, the maximal shear stress is correlated with the pressure gradients (3.5). The effective acoustic pressure decreases inversely proportional to the distance of the sound source.[316]

$$\tau \propto \nabla p \tag{3.5}$$

Thus, relative shear forces can be controlled by the sample height above the Cup Horn surface. Therefore, the sample mounting in acoustic SSA was planned to be height-adjustable (Figure 3.6).

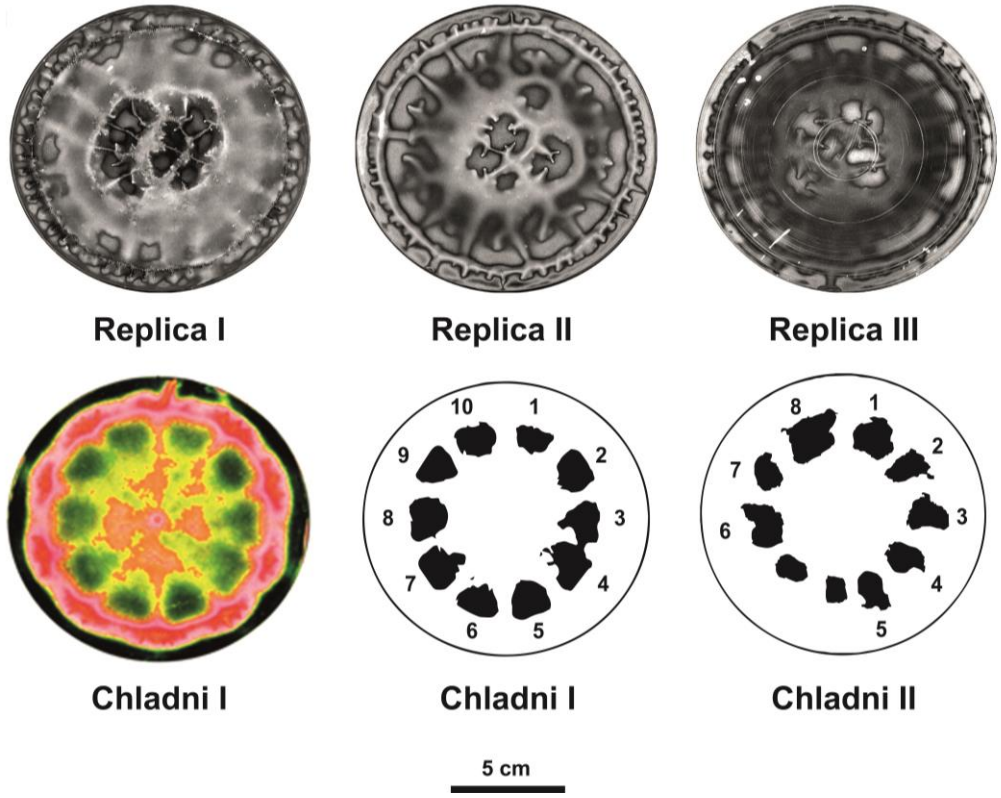

Figure 3.5: ***Cavitation damage patterns of customized harmonic sonotrodes***

Replicas of the original Misonix M4,000 Cup Horn were analyzed with respect to their oscillation behavior. The images visualize the location of vibrational nodes. For that purpose new sonotrodes were covered with 1 cm of water and operated for 20 min at 37°C. Afterwards the surface was scanned as color image using a customary scanner. Every sonotrode showed a specific and unique pattern. The original Misonix Cup Horn (not shown) displayed a pattern similar to replica I-III. PMCA experiments which were performed using the height-adjustable sample holder, as described in Figure 3.3 C and Figure 3.4 (p. 49 and 50), were performed with replica I. A five-fold axial symmetry is evident for Chladni I and II, which were used in acoustic SSA (Figure 3.6). Contrast enhancement and further digital image processing accentuated the spatial distribution of the cavitation damage (Chladni I, bright colors, image provided by Dr. Thorsten Lührs, HZI), which coincides with the location of vibration nodes. In the interest of easier comparibility Chladni I and V are also shown as monochrome images which demonstrate the location of anti-nodes (black).

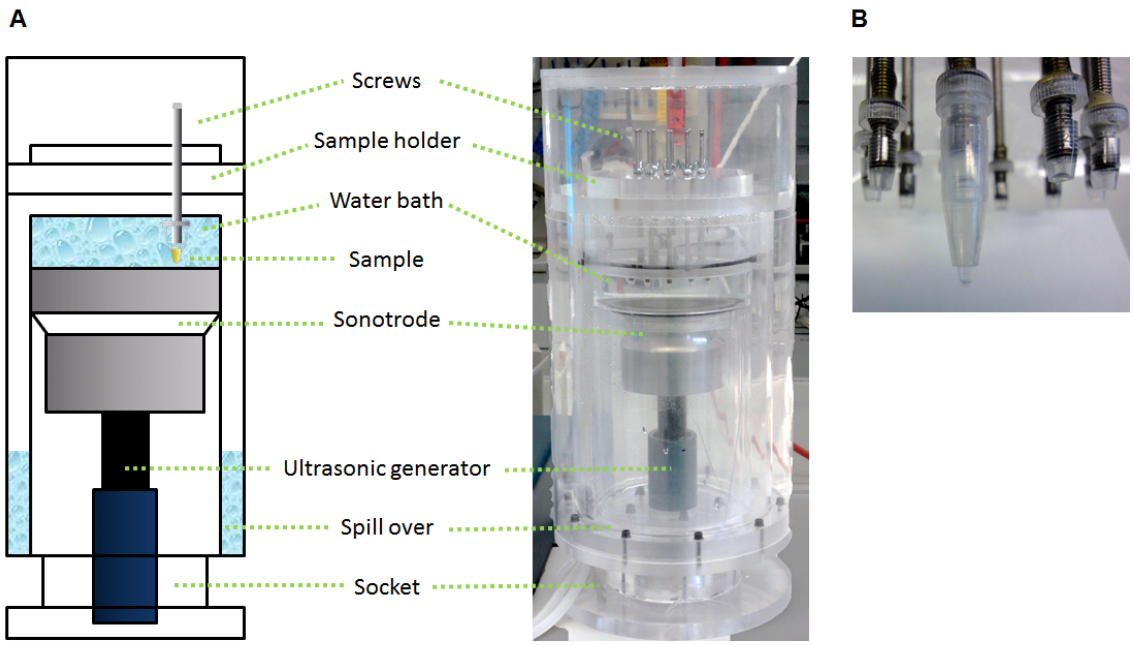

Figure 3.6: ***Acoustic Selective Shearing Amplification (SSA)***

(A) *Cross-sectional view of the designed setup for prion seed amplification by acoustic SSA. The ultrasonic generator (Misonix) can be lowered onto a secure stationary base. The sonotrode is fixed inside a water bath. Overflowing water (indicated in light blue) is collected and pumped out at the base of the device. The water is exchanged at a rate of six litres per minute. In our experiments water inlet and outlet were connected to a customary temperature-controlled water bath with an implemented pump. Height differences between pump and Cup Horn as well as tube lengths and dimensions were kept constant to guarantee a consistent water fill level. By this means the oscillation behavior of the sonotrode was kept reproducible. The water was renewed regularly. Bacteria growth was avoided, but more importantly detached metal particles were removed thereby. Ten independent drop rods end in aerosol tight screw cap tubes, which act as containers for the reaction vials. The sample positions were matched to the Chladni-figure of Chladni I (Figure 3.5).The positional reproducibility was better than ± 0.2 in the vertical direction and ± 0.5 mm in the plane direction.* ***(B)*** *Detailed view of a reaction vial in the water bath; The PCR tubes that are filled with the reaction mix are fixed inside of the sample containers (cp. Figure 3.7 B, p. 57). The Height can be adjusted using the drop rods at the top. The acoustic SSA was designed by Dr. Thorsten Lührs (HZI). The system is registered under the patent number EP2489427A1 and WO2012110570A1.*[306,307]

3.7.2 Test of the Acoustic SSA device

To investigate the effect of different relative shear forces on the PrP^{res} amplification yield, acoustic SSA experiments with different sample heights were performed. Frozen scrapie brain homogenate was thawed and mixed with freshly prepared NBH (cp. 3.5, p. 44 *et seqq.*) by pipetting. If not mentioned otherwise a 2% (v/v) mixture of 10% (w/v) ScBH in 10% (w/v) NBH was used. The used normal brain homogenate, resp. the prepared reaction mix are cell suspensions. Even though complete protease inhibitor was added freshly and temperature was maintained at

4°C, aging, enzymatic degradation and of course precipitation processes cannot be excluded. Thus, long storage of the homogenates before usage was avoided. Aliquots of 125 µl (in thin-walled PCR-tubes) were flash frozen in liquid nitrogen for later use. Before using frozen aliquots were thawed at 22°C for 10 min under gentle agitation (Eppendorf Thermoshaker comfort, 750 rpm). The sample tubes were mildly spinned to avoid deposition of droplets in the lids. However, pellet forming was avoided. Tubes were mounted in the positioning ring as described in Figure 3.7 B. Then, the assembly was inserted into the ultrasonication waterbath. Care was taken to match the orientation of the Chladni figure (Figure 3.5). All drop rods were screwed down so that the samples slightly touched the surface of the sonotrode. Subsequently, the height was adjusted using a defined number of turns (1 turn of the height control screw is equivalent to 1 mm). All samples were adjusted to the same height within a particular experiment. Otherwise acoustic SSA provides inconsistent data sets. This effect could be attributed to potential interferrences in the sound field expansion. If experiments with less than ten samples were peformed, water-filled PCR-tubes were mounted in the empty positions of the positioning ring. The reaction samples were processed at 240 W (corresponding to 85% set power at the Misonix 4,000) for three seconds every five minutes (264 cycles, 37°C) at heights of 0.5; 1; 1.5; 2; 3; 4; 5; 6; 8; 10; 12; 14; 16 and 18 mm (Chladni I, positions 1-10) and 0.5-12 mm (Chladni II, positions 1-8). Prior to each experiment the mounted reaction vials were exposed to one sonic burst (240 W for five seconds) to redissolve settled material. Trapped air bubbles and froth were strictly avoided.

A list of all performed acoustic SSA experiments and the corresponding reaction parameters is given in Table A.3 (p. 92).

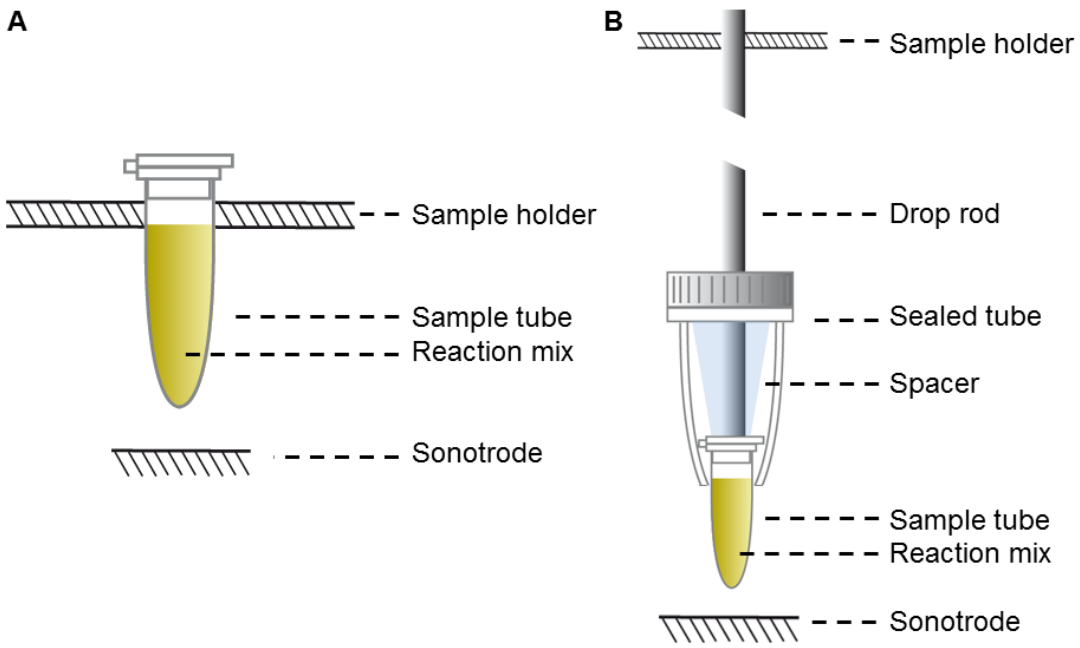

Figure 3.7: ***Positioning of reaction vials in PMCA and acoustic SSA***

(A) *PMCA: Positioning of tubes in Misonix 4,000 standard sample holder, the rotating sample holder as well as the height controlled sample holder (Figure 3.3, p. 49); The upper edge of the reaction mix ended with the lower edge of the sample holder, but no air filled gap was left. Thus, unwanted cavitation effects and therefore spurting into the lid of the PCR tube was avoided.* ***(B)*** *Acoustic SSA: An aerosol tight screw cap tube was attached to a drop rod for height adjustment. The screw cap tube was cut at the bottom, so that a PCR tube fit in tightly. The protuding lug of the PCR tube cap was removed with a scalpel. A silicone spacer at the end of the drop rod kept the PCR tube in position and perpendicular to the sonotrode surface. To avoid cavitation and spurting of the reaction mix, the air filled part of the PCR tube was kept within the watertight screw cap tube.*

3.7.3 Mechanical Selective Shearing Amplification (SSA)

To validate the principle of selective shearing for the selection of seed population an alternative shearing meachanism was tested. Mechanical shear stress can be generated in the laminar flow of an incompressible viscous solvent if it is filled in the gap between two coaxial cylinders which are rotating relative to one another (Couette flow).[317] The movement provides a solvent velocity gradient between the outer and the inner cylinder and creates homogenous shear fields that are proportional to the rotation frequency. Apart from the rotor shape, the viscosity and the space between rotor and stator are directly correlated to the applied shear force.[318] Using custom-designed, induction-driven dispersion tools (Heidolph, Silent Crusher S, tool 3F; rotor radius kR = 1 mm, 0.3 mm gap width) as shear-generators, homogeneous and reproducible shear forces could be applied to arbitrary reaction volumes (Figure 3.8 B).

3.7.4 Mechanical SSA array

Mechanical SSA provides the opportunity to test different parameters (e.g. different shearing conditions, cycle times, interprocessing delay, buffer compositions, additives) using several geometrical identical shear-generators (disperion tools 3F, Silent Crusher S from Heidolph, Schwabach, Germnay) in parallel. To make this possible the SSA-array was built (Figure 3.8 A, C and D). It consists of 21 slots for shear-generators in a temperature controlled environment. Using computer controlled switching relays, every single device can be programmed separately for experiments using rotation frequencies ranging from 40 to 1,201 Hz.

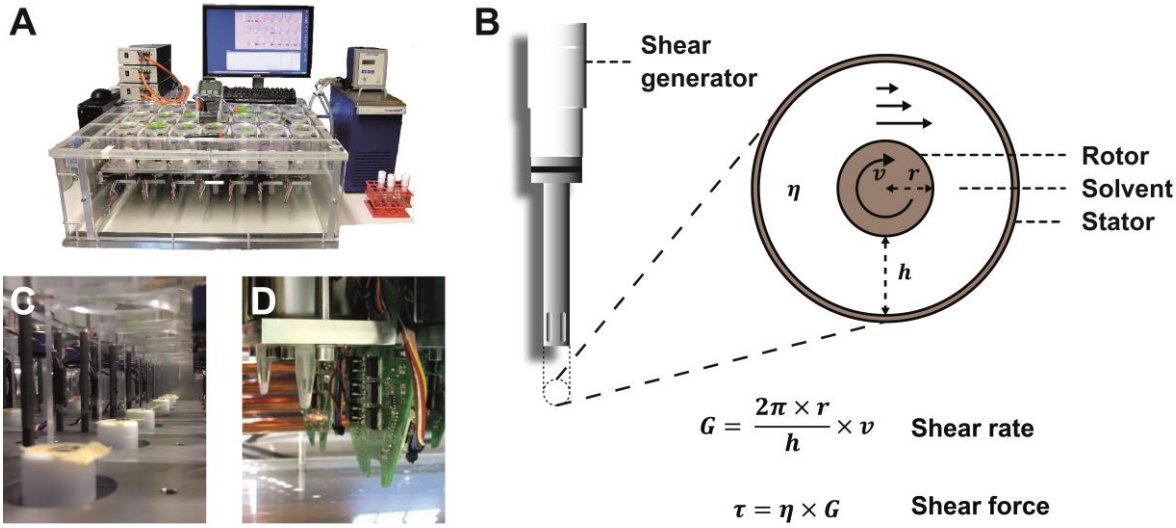

Figure 3.8: ***Mechanical Selective Shearing Amplification (SSA) array***

(A) *The SSA array is a self-built, temperature-controlled device. It can independently operate 21 identical shear generators (disperion tools 3F, Silent Crusher S from Heidolph, Schwabach, Germnay). The shear generators can be individually controlled and are located in expandable sockets. Processing time, interprocessing delay as well as total reaction time can be altered. A water pump connected to a copper coil ensures the temperature exchange. Several fans provide a homogenous temperature distribution.* ***(B)*** *Schematic illustration of a shear generator; The principle of a Couette-type shear generator is explained. The shear rate depends on the radius of the rotor r, its frequency v and the gap of height, h, between rotor and stator. The shear force is determined as a product of the shear rate and the viscosity, η, of the solvent. The shear force is proportional to the rotation frequency of the rotor.*[317] ***(C)*** *Detailed view of the SSA array; A row of seven shear generators is shown. Each device is preasembled in a laminar-flow hood and sealed aerosol tight.* ***(D)*** *Detailed view of the SSA array; In the foreground a driving unit, the corresponding mainboard with connecting cables and the reaction tube can be seen. The mechanical SSA was designed by Dr. Thorsten Lührs (HZI). The system is registered under the patent number EP2489427A1 and WO2012110570A1.*[306,307]

On that purpose the original setup of the shear-generators was modified. Removing the base only the drive unit ring and the mainboard were kept. The implemented

potentiometer was replaced by a more accurate component. Connecting the power supply line to customary relay cards, computer programmable on-/off-cycles were made possible. A second, independent power supply line was interrupted by a multi-pole plug. Read directly from the mainboard circuit, the frequency signal was looped through this plug. This construction made it possible to start individual shear-generators independently from the implemented relay card circuit and, moreover, a fine-adjustment of the frequency. The frequency range of the driving unit could be extended by fine adjustment of the onboard potentiometers. The power supply was ensured by commercially available power packs.

To guarantee reproducible reaction sequences, consistent movement of the dispersion tool rotors is inevitable. Teflon™ bearings from Heidolph served the purpose, but they showed deficiencies especially in longer runs and primarily with processing frequencies above 600 Hz. Abrasion and formation of particles often influenced the rotor movement. Related to these problems, imbalances and local heat buildups cropped up. A further problem was the reusability of the commercial bearings. Once removed from the stator the Teflon™ parts could not be reused, but disassembling of the shear-generators was strongly recommended for successful decontamination (cp. 3.3, p. 41 *et seqq.*). To solve the problem the bearings were replaced by customary Teflon™ tubes (Bola, Grünsfeld, Germany). Cut to the required size and a little shortened compared to the original parts, self-made bearings could be henceforth used as disposable parts. To ensure smooth rotor movement the edges were scrupulously burred using a scalpel. Due to production the wall size of Teflon™ tubes can vary. Therefore self-made bearings were often squeezed to a rectangular shape. Thus, the rotor was girded more tightly and wobbling was reduced. Prior to each experiment all shear-generators were tested (cp. 3.7.11, p. 62 *et seqq.*). The procedure avoided rotor dropouts, but also polished new bearings and removed barely visible imperfections. To guarantee a better intermixture of the reaction mix holes were drilled in the stators of all shear-generators.

3.7.5 Proof of principle

To test the feasibiltiy of shear promoted selective prion amplification a single non-modified shearing device was tested to amplify hamster prions of different prion isolates (Sc237 and 263K). A 10% (w/v) ScBH was diluted 1:10 into a 10% (w/v) NBH and processed for 60 seconds every nine minutes (144 cycles). Processing was performed at 0; 15,000; 30,000; 45,000 and 75,000 rpm. The whole shearing device was incubated in an incubator at 37°C. Alternating processing and incubation steps were realized by a customary switching relay.

3.7.6 Test of the SSA array

The comparison of the hamster prion strains Sc237 and 263K was repeated using the SSA array. Beside parallel processing the new hardware allowed a higher maximal processing frequency as well as a finer adjustment of the processing frequencies. Thus, a logarithmic scale increment of 35% per interval was selected. A 10 % (w/v) ScBH was diluted 1:10 into a 10% (w/v) NBH and processed for 60 seconds every 60 minutes (24 cycles, 37°C). Processing was performed at 40; 54; 72; 96; 129; 173; 232; 311; 417; 559; 749 and 1,004 Hz. For non-seeded control reactions a 10% (w/v) NBH was processed for 60 seconds every 60 minutes (24 cycles, 37°C, 900 µl per reaction). Processing was performed at 54; 173 and 417 Hz.

3.7.7 The kinetic buildup of PrP^{res}

To analyze the kinetic buildup of PrP^{res} in subsequent mechanical SSA experiments samples of ~20 µl were taken at different time points. On that purpose the reactions vials were modified. The thread of a customary HPLC vial with screw cap and septum was cut and welded on the reaction vial using a gas jet. Tuberculin syringes could be used for sampling. Considering the volume decrease with each taken sample a higher reaction volume (1,150 µl instead of 900 µl) was chosen. To avoid over-processing of the homogenate not more than eight samples (~160-200 µl) were taken from running reactions. Furthermore, the edges of the rotor blade wer rounded down by manual grinding to minimize vibrations of the shear-generators.

To investigate the influence of the cycle time on the amplification of Sc237 prions the kinetic buildup was surveyed. A 10 % (w/v) ScBH was diluted 1:50 into a 10% (w/v) NBH and processed for five seconds every 5/15/30/60 or 90 minutes (480/160/80/40 or 27 cycles, 37°C). Processing was performed at 1,000 Hz.

Subsequently a comparison of the kinetic buildup of PrP^{res} was performed for the prion strains Sc237 and 263K. A logarithmic scale increment of 35% per interval was selected. Based on the results of the prior experiment a 10 % (w/v) ScBH was diluted 1:50 into a 10% (w/v) NBH and processed for 5 seconds every five minutes (264 cycles, 37°C). Processing was performed at 96; 119; 150; 189; 238; 300; 476; 600; 756; 953 and 1,201 Hz.

Interprocessing delay

Without affecting the processing the influence of a contious cycle time increase on the amplfication of Sc237 prions was investigated. A logarithmic scale increment of

35% per interval was selected. A 10 % (w/v) ScBH was diluted 1:50 into a 10% (w/v) NBH and used as a reaction mixture. The increase of the cycle time is defined by equation (3.6). Processing was performed at 96; 119; 150; 189; 238; 300; 476; 600; 756; 953 and 1,201 Hz.

$$C(t) = C1 + (C2 - C1)\left(1 - \exp\left(-\frac{1}{Ck * t}\right)\right) \qquad (3.6)$$

$$C1 < C2$$

$C1$ represents the start cycle time (5 min, t=0).
$C2$ is the final cycle time (10 min).
Ck determines the initial slope (=18).

3.7.8 Non-processed reactions

Non-processed control reactions were performed to investigate the influence of processing in mechanical SSA using the prion strains Sc237 and 263K as seeds. A 10 % (w/v) ScBH was diluted 1:50 into a 10% (w/v) NBH and incubated in the SSA array at 37°C for 24 h.

3.7.9 Effect of seed and homogenate treatment

Different Sc237 seed dilutions were tested in mechanical SSA. Therefore, a 10 % (w/v) ScBH was diluted 1:25, 1:50, 1:75, 1:100, 1:125, 1:150, 1:75, 1:200 and 1:225 into a 10% (w/v) NBH and processed five seconds every five minutes (288 cycles, 37°C). Processing was performed at 600 Hz.

Furthermore, the influence of a reaction mixture (NBH + Sc237BH) pretreatment was tested. Therefore, a 10 % (w/v) ScBH was diluted 1:50 into a 10% (w/v) NBH and span at 2,000; 5,000; 10,000; 15,000 and 25,000 *x g* for 10 min at 4°C. The supernatant was processed five seconds every five minutes (576 cycles, 37°C). Processing was performed at 1,000 Hz.

Additionally, the effect of a NBH pretreatment was surveyed. A suspension of freshly prepared 10% (w/v) healthy hamster brain in conversion buffer was span at 25,000 *x g* for 10 min at 4°C. The supernatant was used to create 1:50 dilution of 10% (w/v) Sc237BH, which was processed five seconds every five minutes (576 cycles, 37°C). Processing was performed at 96; 119; 150; 189; 238; 300; 476; 600; 756; 953 and 1,201 Hz.

3.7.10 Effect of SDS

To investigate the effect of denaturing agents in selective shearing amplification reactions SDS was added to the reaction mixture. Therefore, 10 % (w/v) NBH was prepared using conversion buffer which already contained SDS (to reach final concentrations of 1; 2 or 5 mM SDS in the reaction mixture). A 10 % (w/v) ScBH was diluted 1:50 into the NBH and processed five seconds every five minutes (576 cycles, 37°C). Processing was performed at 150 and 1,201 Hz.

3.7.11 Reaction mix and preparation steps for mechanical SSA

Frozen scrapie brain homogenate was thawed and mixed with freshly prepared NBH (cp. 3.5, p. 44 *et seqq.*) by pipetting. If not mentioned otherwise a 2% (v/v) mixture of 10% (w/v) ScBH in 10% (w/v) NBH was used. The used normal brain homogenate, resp. the prepared reaction mix are cell suspensions. Even though complete protease inhibitor was added freshly and temperature was maintained at 4°C, aging, enzymatic degradation and of course precipitation processes cannot be excluded. Thus, long storage of the homogenates before usage was avoided. In the normal case, buffer completion, preparation of homogenate and reaction mixture, sample aliquotation as well as the final shear-generator assembly were done in one go. In order to minimize the time between homogenate preparation and the reaction start, experiments were always prepared by two persons.

On that account experiment preparations followed the following steps:

1. Pre-heating of the mechanical SSA array; if necessary water refill

   The SSA array needs at least 2 hours to heat up from room temperature to 37°C. Especially for reactions, which are planned to run longer than 24 hours, the water level should be checked from time to time.

2. Shear-generator decontamination, washing, drying, assembly

   Shear-generators were decontaminated like described in chapter 3.3 (p. 41 *et seqq.*). After drying the stators were carefully equipped with new self-made Teflon™ bearings. The length of the bearings was taken over from the original part size (Heidolph, Schwabach, Germany), but they protuded the stator by not more than 0.5 mm. These Teflon™ parts were simply cut from a tubing (Bola, Grünsfeld, Germany) with aid of a brass tube template, which fitted the inner diameter. Edges were cut with a straight scalpel grind, leaving

as few as possible slanted burrs. Thereafter, the edges were smoothed with one circular movement of the hand using a curved scalpel grind.

3. Test run of the shear-generators, followed by a centrifugal drying

   For a successful run of the shear-generators, especially at frequencies higher than 600 Hz, the bearings should fit tightly. To avoid squeezing of the bearing only the first millimeters were pressed into the stator using the bare hands. Using the rotor the rest of the tubing was stuffed into the stator. Normally a little frictional resistance should be perceptible while carefully pressing the rotor down. Drawing out the rotor, the bearing should remain within the stator. Less friction often leaded to wobbling effects and therefore an inaccurate processing frequency of the particular shear-generator. Inappropriate edges often caused particles during the test run, leading to clanking noise of the tools. Disassembling the shear-generators and rinsing with deionized water fixed the problem in most of the times. Anyway, an exchange of the bearing was often mandatory.

   All assembled shear-generators were tested at 1,000 Hz with 900 µl deionized water in a 1.5 ml reaction tube. On that account tools were run for ~30 seconds to check for vibrations. Trapped air bubbles could cause unwanted wobbling and noise in the first seconds, but long-lasting problems during the run were always an indication for grit and/or the necessity for a bearing exchange. In contrast to lower frequencies, shear-generators, which were supposed to run with more than 1,000 Hz, were tested at 1,201 Hz.

   After testing each array position was set to the wanted frequency using the particular tool.

   Afterwards the water was removed from the attached 1.5 ml-reaction tubes. Reassembled with the empty tubes the shear-generators were transferred into 50 ml-reaction tubes and centrifuged two times for two minutes at 500 *x g* (higher speeds can cause non-reparable damage of rotor and stator).

4. Preparation of ice bath; pre-cooling of buffer, reaction tubes and dounce homogenizer

5. Preparation of NBH and reaction mixture (cp. 3.5, p. 44 *et seqq.*)

6. Assembly of shear-generators and incubation

   As not indicated otherwise 900 µl aliquots were filled into decontaminated reaction tubes (1,150 µl if kinetic experiments were performed). The lid of the tubes was removed beforehand. One by one, each 3F dispersion tool was assembled and incubated for 20 min at 37°C. To avoid leakage of contaminated liquids/aerosols and/or loosening of the reaction vial or the remove retainer one layer of parafilm was wrenched around the dispersion tool. During incubation the parameters for the run (duration, cycle time (on/off-time), interprocessing delay) were set.

7. Reaction start

A list of all performed mechanic SSA experiments and their reaction parameters is given in Table A.4 (p. 94).

4 Results

4.1 PrP^{Sc} amplification by ultrasonic processing

4.1.1 Protein Misfolding Cyclic Amplification (PMCA)

Using the hamster prion seed Sc237 the experiments provided expected results: Protease digests and subsequent SDS-PAGE and western blot analysis showed product sizes of 37 kDa and high protease resistance of converted PrP^{C} in all PMCA experiments. The reaction products of the initial round were sucessfully used to seed fresh NBH in a subsequent conversion reaction (serial PMCA). Decreased seed concentrations provided less amplification yield, as shown in Figure 4.1 A. However, the the the total yield of PrP^{res} showed significant variability if samples were variously positioned on the standard sample holder (Figure 4.1 B). Centerpiece of the Misonix device is the circular surface of a 20 kHz sonotrode, which is clamped in a sealing plastic ring – the base of the overlying water bath. Experiments with the centered sample holder indicated a higher conversion efficiency near to the center of the sonotrode, but the reaction outcome still turned out to be strongly variable with respect to the yield of PrP^{res} (Figure 4.1 D).

Bicelles clearly showed positive effects in PMCA reactions. To avoid different processing tubes with different biochemical compositions were placed in direct neighborhood. Interestingly, bicelles without charge (no phosphoserine was added) provided the highest yield of PrP^{res}. Compared to standard reactions also DHPC alone, at concentrations of 25 and 50 mM, caused a higher reaction outcome in one of the experiments (Figure 4.1 C). The positive effect of bicelles became even more manifest if amplification was tested on the centered sample holder (Figure 4.1 D).

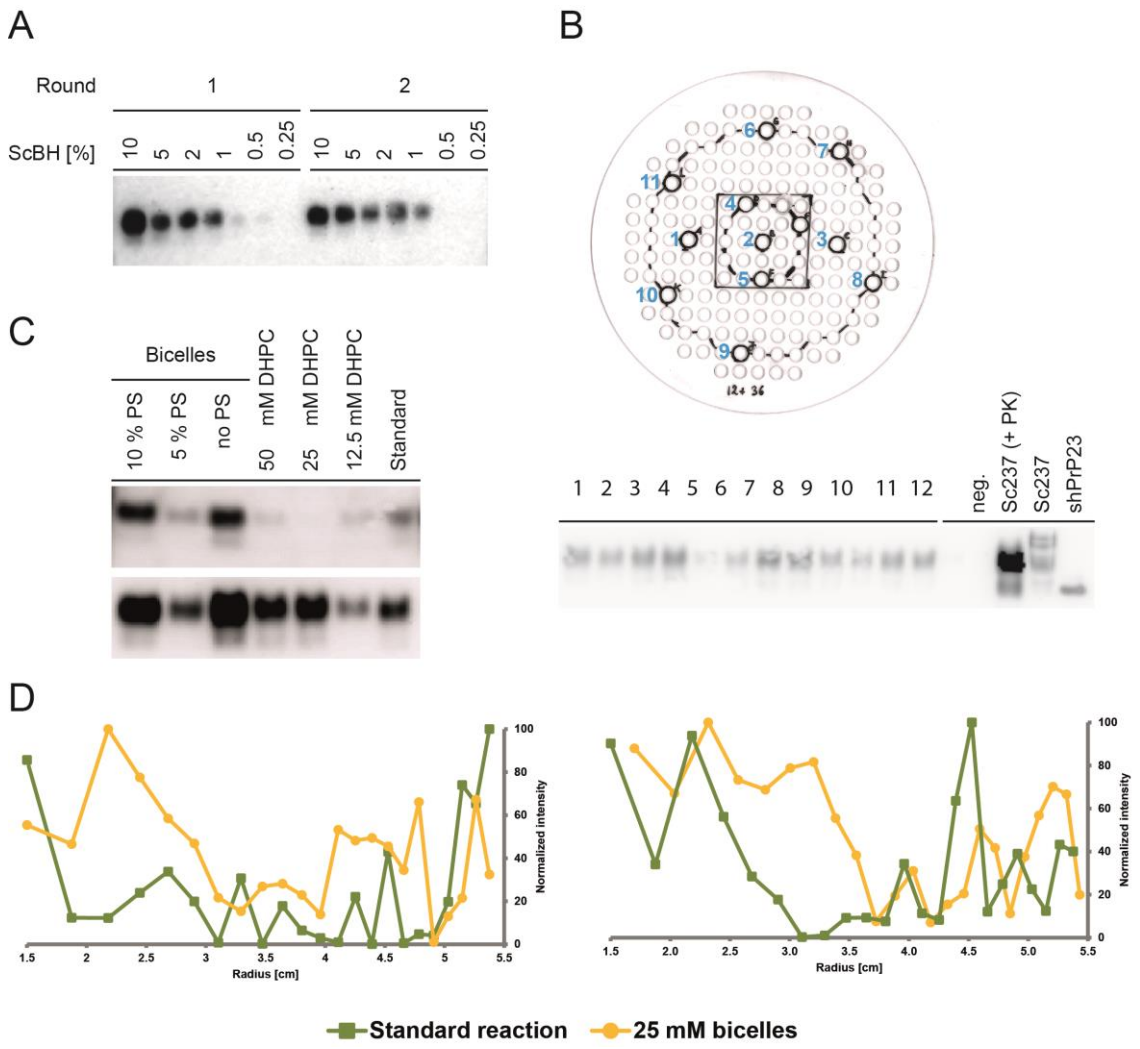

Figure 4.1: ***PMCA experiments***

(A) *Seed dependence of Sc237-seeded PMCA; Different dilutions of ScBH in NBH were tried for conversion reactions. Particular samples (10% v/v) were used to seed a further reaction round (serial PMCA).* ***(B)*** *Position effects in PMCA; Comparison of simultaneously performed PMCA reactions on different postions (1-12) of the original sample holder (Misonix).* ***(C)*** *Effect of bicellar mixtures in PMCA****;*** *Different negatively charged bicellar mixtures were added to PMCA reactions (25 mM final concentration). Beside this the influence of DHPC was tested.* ***(D)*** *Radius dependence in PMCA****;*** *The oscillation behavior of the sonotrode (replica I) was analyzed using a centered rotating sample holder. Plots of two separate experiments are shown. Samples with and without bicelles (25 mM, w/o PS) were alternately mounted on the sample holder. Experiment results are therefore illustrated as two graphs. For all experiments(except (A)) 5% (v/v) ScBH (Sc237) in NBH was used as reaction mix. Reactions were performed in 100 or 200 µl aliquots with a power level of 90%, 40 s processing, 59.67 min incubation and 24 or 48 h duration. The original Misoinix 4,000 setup was used (sonotrode replica I, standard sample holder resp. a rotating sample holder). Samples were digested witch 50 µg/ml proteinase K (PK) at 37°C for 1 h and analyzed by western blotting (using the PrP-specific 6H4 antibody) and 1D densitometry.*

By comparing the cavitation damage profiles on the surface of the recreated Cup Horns individual patterns of irregular shape could be observed (Figure 3.5, p. 54)

which resemble the geometry of the underlying harmonic surface oscillation function. The irregular shape of the cavitation damage pattern gave rise to the assumption that the soundwaves are not emitted evenly across the surface of the Cup Horn. With the purpose to understand the influence of the oscillation behavior on the amplification of PrP^{res} we considered to use fixed sample positions. Thus, a new sample holder was developed. The position of the reaction vials were matched to the estimated anti-nodes of replica I (Figure 3.3 C and Figure 3.4). Nevertheless, the determination of the PrP^{res} amplification yields of the hamster prion isolates 263K and Sc237 at multiple heights still revealed high variability and limitied position comparability (Figure 4.2).

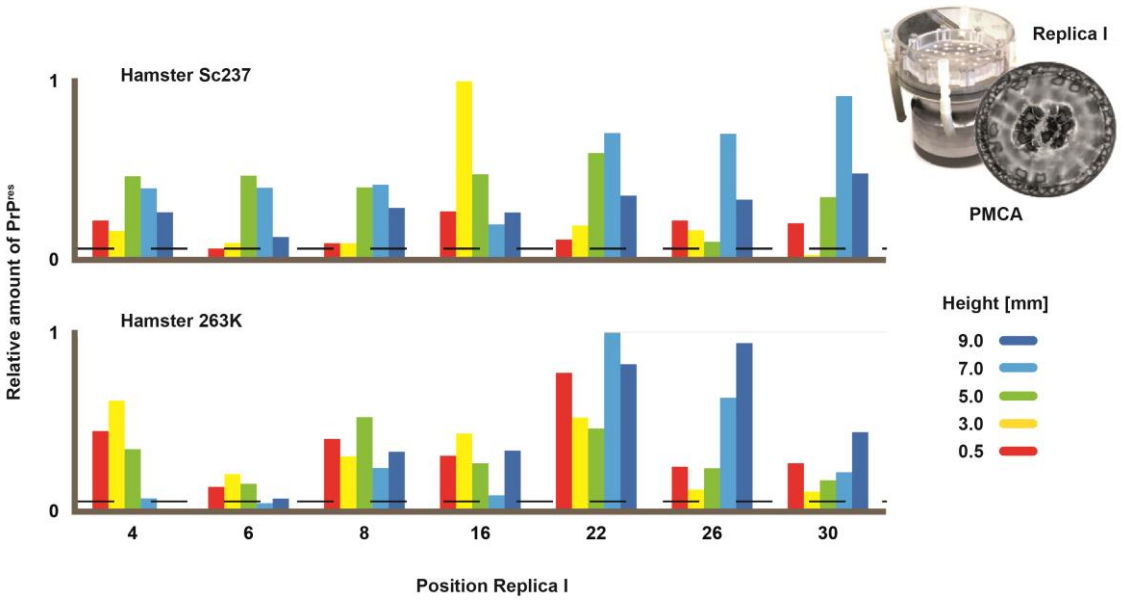

Figure 4.2: ***Height profiles of Sc237 and 263K hamster prion seeded PMCA reactions***
Height-dependent amplification of PrP^{res} was analyzed using a height-adjustable sample holder with fixed positioning (sonotrode replica I). 5% (v/v) ScBH (Sc237) in NBH was used as reaction mix. Reactions were performed on separate days in 100 µl aliquots with a power level of 90%, 60 s processing, 9 min incubation and 24 h duration. Afterwards, samples were digested with 50 µg/ml proteinase K (PK) at 37°C for 1 h and analyzed by western blotting (using the PrP-specific 6H4 antibody) and 1D densitometry. The dashed line indicates the amount of seed used for these reactions.

Conclusions

PMCA was successfully established using the hamster prion strain Sc237. Nevertheless, despite the fact that non-charged bicelles positively influenced the amplification of PrP^{res}, the reaction yield still was subject to strong fluctuations which can be attributed to the acoustic behavior of the Cup Horn sonotrode. Each sonotrode replica yields a specific and unique pattern which can readily explain the

position effects in standard PMCA reactions. Thus, the acoustic SSA concept was developed which uses a sonotrode with a defined oscillation behavior.

4.2 Acoustic SSA

Contour plots of acoustic SSA experiments using the hamster prion strains Sc237 and 263K as seeds are shown in Figure 4.3 (Chladni I). The normalized PrP^{res} amplification yield is plotted against the sonotrode position and height above the surface. Both strains amplified well at multiple positions near the Chladni-horn surface. Carried out with the hamster 263K strain, the yield decreased with increasing heights. In contrast, significant amplification of PrP^{res} was also observed at heights of 3 mm and 8 mm using the Sc237 strain. In a second experiment we tested a new sonotrode (Chladni II), which showed a less symmetric Chladni pattern. Although it is still evident that both prion strains are distinctive reagarding their amplification behavior, the height optima clearly differ from the experiments with Chladni I. While siginificant amplification was observed at 0.5 mm and 2 mm in samples seeded with 263K, the height optimum for Sc237 was observed between 4 mm and 6 mm.

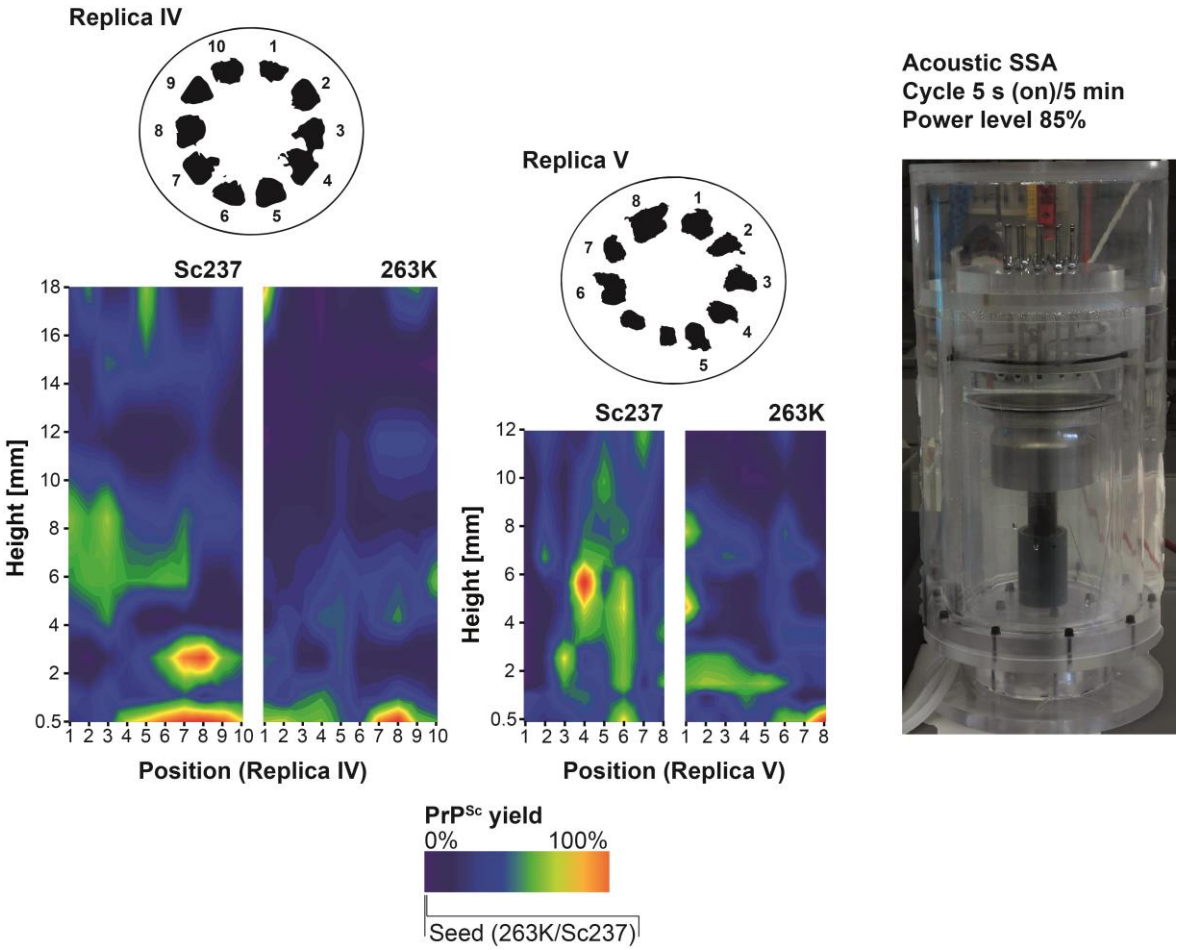

Figure 4.3: ***Height profiles of Sc237- and 263K-seeded conversion reactions in ultrasonic SSA***

Intensity contour plots are displayed. Reactions were arranged in heights of 0.5, 1, 1.5, 2, 3, 4, 5, 6, 8, 10 and 12 mm above the sontrode surface of Chladni II. Additional heights of 14, 16 and 18 mm were tested for Chladni I. Cycles were set to 5 min with 5 s processing at 85%. 5% (v/v) ScBH (Sc237) in NBH was used as reaction mix. Reactions were performed in 120 µl aliquots with a duration of 22 h. Samples were digested with 50 µg/ml proteinase K (PK) at 37°C for 1 h and analyzed by western blotting (using the PrP-specific 6H4 antibody) and 1D densitometry.

Conclusions

As mentioned before we anticipated that different structured proteopathic seeds might be selectable based on their specific fragmentability (cp. 3.7, p. 51 *et seqq.*). Indeed, the distance to the sound source influences the acoustic pressure, which in turn is correlated with the relative shear force (cp. 3.7.1, p. 52 *et seqq.*, equations (3.3)-(3.5)). The experimental data clearly showed that the PrP^{res} amplification yield is dependent from the sample height above the sonotrode surface, but also revealed that there is a clear distinction between both prion strains. The results also outlined that the vibrational pattern can dramatically influence the reaction outcome (Figure 4.3, p. 69). To validate the observed strain differences the concept of SSA was also tested using mechanical generated shear stress.

4.3 Mechanical SSA

4.3.1 Proof of principle

The feasibiltiy of shear promoted selective prion amplification was initially tested using a single shearing device. The amplification of the hamster prion strains Sc237 and 263K was surveyed at 0, 15, 30, 45, 60 and 75 krpm. Processing was performed for 60 s every nine minutes using a single and non-modified shear-generator. PrP^{res} molecules which were amplified by mechanical SSA showed similar electrophoretic behavior and resistance to protease digest compared to conversion products generated via PMCA. Furthermore, the results revealed differences between 263K- and Sc237-seeded amplification reactions with respect to the processing frequency. Seeded with brain tissue homogenate from Sc237 hamsters the highest PrP^{res} amplification yield was achieved using a speed of rotation of 30,000 rpm. In contrast, 263K seeds caused a single amplification optimum at 45,000 rpm. Moreover, the ampfliciation yield tended to zero at 60,000 rpm and 75,000 rpm. (Figure 4.4) Nevertheless, the amplfication factors did not exceed a value of five.

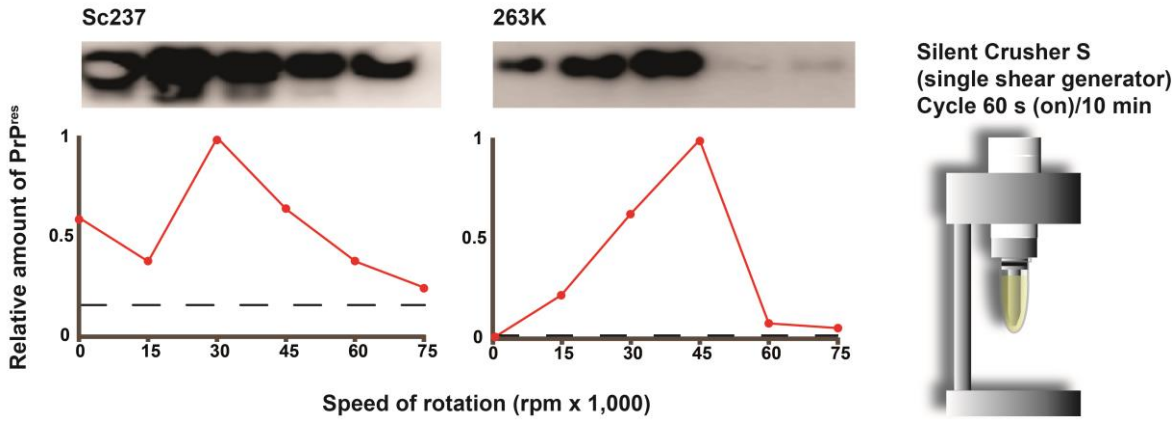

Figure 4.4: Initial proof of principle with mechanical SSA reactions

Amplification of PrP^{res} was tried out using a single customary dispersion tool. These mechanical SSA reactions were either seeded with Sc237 or 263K hamster prions. The amount of amplfied PrP^{res} is shown as a function of rotational speed. A mixture of 5% (v/v) scrapie brain homogenate in normal brain homogenate was used for conversion reactions. Processing speeds of 0, 15,000, 30,000, 45,000, 60,000 and 75,000 rpm were roughly set with the integrated potentiometer of the magnetic drive. The reaction was performed in an incubator at 37°C for 22 hours with a cycle setting of one minute processing and nine minutes incubation. Automatic switching between processing and incubation steps was achieved with a customary switching relay. Samples were digested witch 50 µg/ml proteinase K (PK) at 37°C for 1 h and analyzed by western blotting using the PrP-specific 6H4 antibody and 1D densitometry.

Conclusions

Apart from the ultrasonic approach (cp. 4.1, p. 65 *et seqq.*) the applicability of shear promoted selective prion seed amplification was successfully tested using mechanical shear. As observed in acoustic SSA the prion strains 263K and Sc237 showed clear differences with respect to the applied shear forces. In order to achieve a better comparability, further experiments were performed by parallel processing at different shear forces. For that purpose an array of shear generators was used. Beside parallel processing the new hardware allowed a higher maximal shear rate as well as a finer adjustment of the processing frequencies (cp. 3.7.4, p. 58 *et seqq.*). It was assumed that longer incubation intervals (growth phases) might positively influence the amplification factor in the following experiments.

4.3.2 Test of the SSA array

As a starting point, parallel processing of Sc237- and 263K-seeded reactions was peformed with the SSA array. A logarithmic scale increment of 35% per interval was selected for frequencies ranging from 40 to 1,004 Hz (2,400-60,240 rpm). To avoid potential overprocessing and sample heating the reactions were processed using 22 cycles of 60 seconds processing and 59 minutes incubation. To demonstrate that the generation of protease resistant PrP^{res} is not due to non-specific PrP aggregates, non-seeded control experiments were also performed. Two distinct optima of amplification could be identified at processing frequencies of 72 Hz and 417 Hz for the hamster prion strain Sc237 (Figure 4.5 A). In contrast, only one optimum near the maximal processing frequency was obseved when the mechanical shearing amplification experiment was repeated using the 263K strain (Figure 4.5 B). PrP^{res} could only be detected in prion-seeded reactions (Figure 4.5 C).

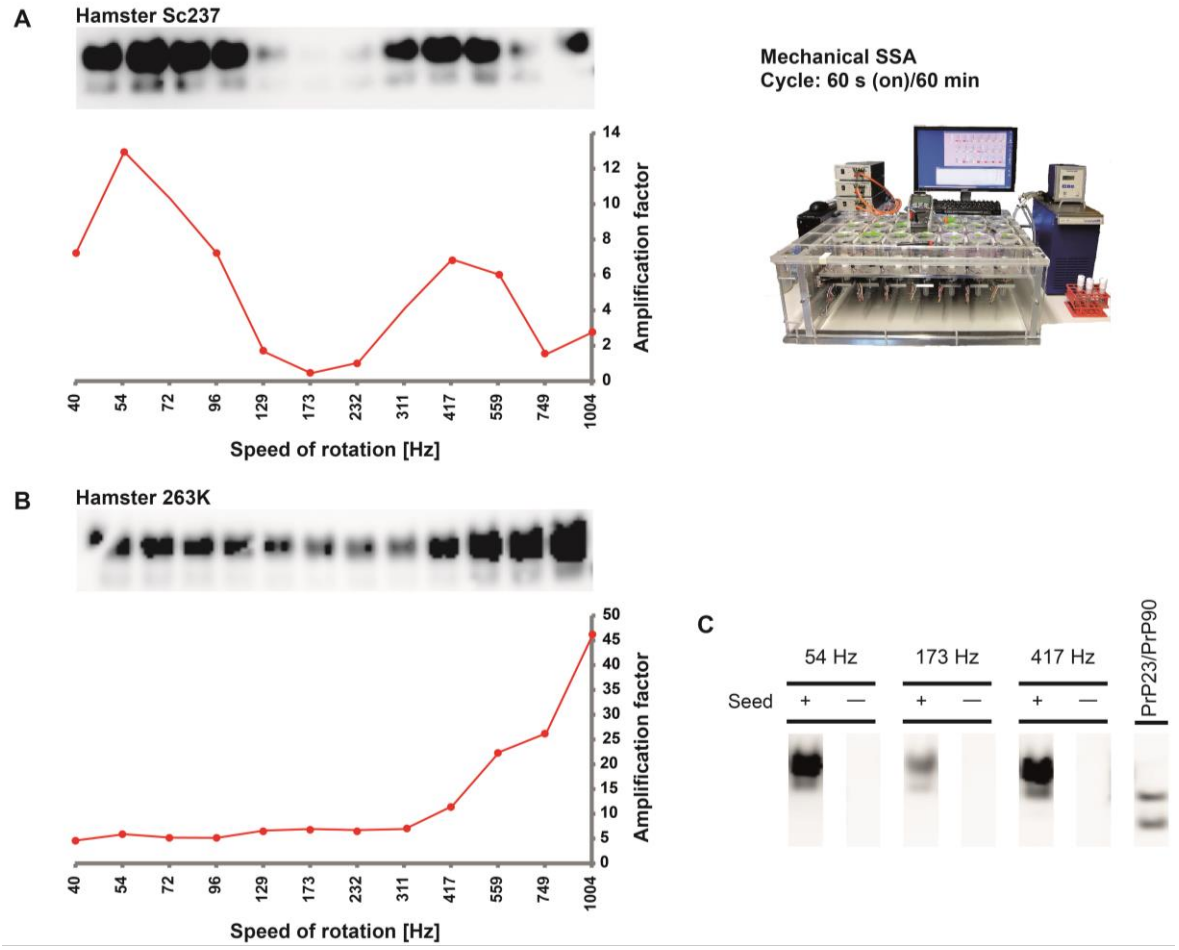

Figure 4.5: ***Influence of frequency, seed and incubation on mechanical SSA reactions***

Amplification of PrP^{res} was tried out using an array of 12 shear-generators simultaneously using a frequency range from 40-1,004 Hz. These mechanical SSA reactions were either seeded with Sc237 ***(A)*** *or 263K* ***(B)*** *hamster prions. The amount of amplfied PrP^{res} is shown as a function of rotational speed.* ***(C)*** *Non-seeded SSA reactions: Observed speed optima for the hamster prion strain Sc237 were tested without addition of infectious brain homogenate. The reactions were performed in the SSA array at 37°C for 22 h with a cycle setting of one minute processing and 59 minutes incubation. Except for non-seeded reactions a mixture of 5% (v/v) scrapie brain homogenate in normal brain homogenate was used. Samples were digested witch 50 µg/ml proteinase K (PK) at 37°C for 1 h and analyzed by western blotting using the PrP-specific 6H4 antibody, followed by 1D densitometry.*

Conclusions

The finer resolution of the processing frequencies and the changed cycle times revealed two amplification optima for the Sc237 strain, while only one clear optimum was found for 263K. In order to survey these differences which already caught our attention in acoustic SSA (cp. 4.2, p. 68), it was decided to observe the time-dependent course of the mechanical SSA reactions. In contrast the non-seeded control experiments clearly showed that the generated PK resistance resulted not only from a spontaneous aggregation of the cellular prion protein due to the applied

shear stress. Compared to the initial tests with a single shear generator (cp. 4.3.1, p. 70), longer incubation periods seemed to increase the amplification yield, which leaded to the decision to systematically test different time settings. Furthermore, we observed unwanted sample heating due to the processing. Thus, the following SSA experiments were performed using shorter processing intervals and modified rotor blades.

4.3.3 The kinetic buildup of PrP^{res}

To analyze the kinetic buildup of PrP^{res} in subsequent mechanical SSA experiments samples of ~20 µl were taken at different time points. For these experiments the edges of the rotor blade wer rounded down by manual grinding to minimize vibrations of the shear-generators (cp. 3.7.7, p. 60 *et seqq.)*. To investigate the influence of the cycle time on the amplification of Sc237 prions the kinetic buildup was surveyed at a rotor frequency of 1,000 Hz for cycle times of 5, 15, 30, 45, 60 and 90 minutes. In order to avoid heating of the reactions a processing time of five seconds was chosen. The highest amplification rate was obtained with the shortest cycle time of five minutes. Within six to twelve hours the PrP^{res} buildup reached half-maximal values. (Figure 4.6)

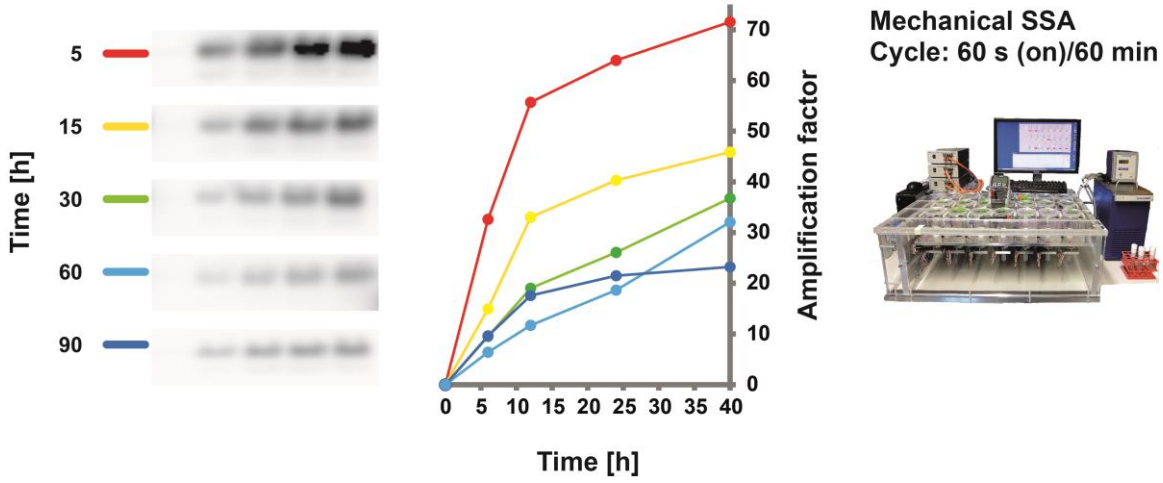

Figure 4.6: ***Mechanical Shearing Amplification (SSA) array – Influence of the cycle time***

Influence of the cycle time on the Sc237 prion seed amplification behavior. Tools were run at a rotation frequency of 1,000 Hz. A mixture of 2% (v/v) scrapie BH in NBH was used for conversion reactions (reaction volume: 1,150 µl). The reactions were performed in the SSA array at 37°C for 40 hours with a cycle setting of five seconds processing. Modified reaction tubes were used to extract ~30 µl samples at different time points. Samples were digested with 50 µg/ml PK at 37°C for 1 h and analyzed by western blotting using the PrP-specific 6H4 antibody, followed by 1D densitometry.

Maintaining a setting of five seconds processing and a cycle time of five minutes the entire accessible rotation frequency range (40-1,201 Hz) was scanned. A logarithmic scale increment of 26% per interval was selected. The experiment was also repeated using the hamster prion strain 263K to compare the kinetic PrP^{res} amplification traces of both prion isolates. The kinetic data revealed significant differences between both prion strains. The initial PrP^{res} buildup rate for Sc237 turned out to be six times faster compared to the slow initial rate of 263K, which showed a sigmoidal shape (Figure 4.7 A and D). Furhtermore, both strains again showed distinct optima of amplfication with respect to the processing frequency. Regarding the Sc237 strain three optima were identified at processing frequencies of 150, 600 and 1,201 Hz. In accordance with earlier results (cp. Figure 4.5, p. 72) only one optimum near the maximal processing frequency was observed when the conversion reaction was seeded with the 263K strain (Figure 4.7 B/C, E/F).

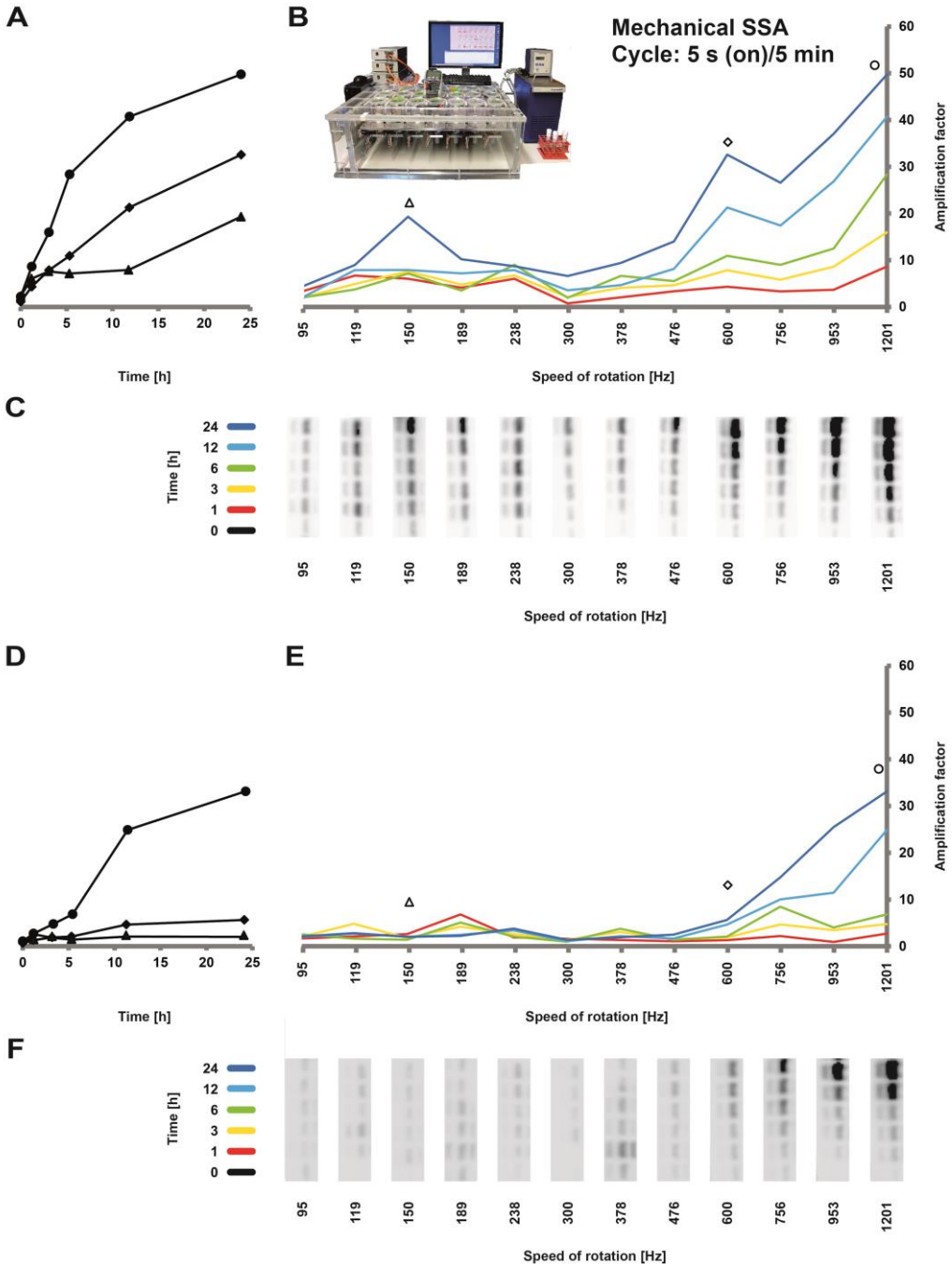

Figure 4.7: ***Mechanical Selective Shearing Amplification of hamster prion seeds***

Amplification of PrP^{res} in mechanical SSA reactions seeded with Sc237 ***(A-C)*** *or 263K* ***(D-F)*** *hamster prions. Data is shown as a function of rotation frequency and of time* ***(B and E)****. A corresponding kinetic trace of PrP^{res} amplification at the observed shearing optima of 150 Hz, 600 Hz and 1,200 Hz is also shown* ***(A and D)****. A mixture of 2% (v/v) scrapie BH (Sc237 resp. 263K) in NBH was used for conversion reactions (reaction volume: 1,150 µl). The reactions were performed in the SSA array at 37°C for 24 hours with a cycle setting of five seconds processing and four minutes and 55 seconds incubation. Modified reaction tubes were used to extract ~30 µl samples at different time points. Samples were digested with 50 µg/ml PK at 37°C for 1 h and analyzed by western blotting using the PrP-specific 6H4 antibody, followed by 1D densitometry. Corresponding western blots of the PK resistant PrP^{res} bands are shown for each time point* ***(C and F)****. The amplification factors relative to the initial seed obtained at each time point are plotted against the processing frequencies.*

Interprocessing delay

An increased cycle number did not necessary lead to a further increase of the reaction yield and often caused an abatement of already converted PrP. Above all this phenomenon became apparent in reaction samples which were processed with frequencies higher than 600 Hz. An explanation might be an over-processing of the samples. The western blot in Figure 4.9 C (> 24 h) exemplifies this effect quite explicitly. To counteract the early occurring stationary phase of the PrP^{res} buildup and to avoid potential over-processing, the former approach was reconsidered. Without affecting the processing the influence of a contious cycle time increase was investigated (Figure 4.8). Compared to an SSA experiment with a constant cycle time the amplification yield at processing frequencies of ≥ 600 Hz could be significantly increased (Figure 4.8 A and B). Two optima of amplification could be identified at processing frequencies of 600 Hz and 1,201 Hz. On the other hand, amplification at 150 Hz was comparatively low, showing similar PrP^{res} replication as in the standard experiment (cp. Figure 4.7 B). Figure 4.8 (A and C) exhibits the quantitative analysis of such an experiment.

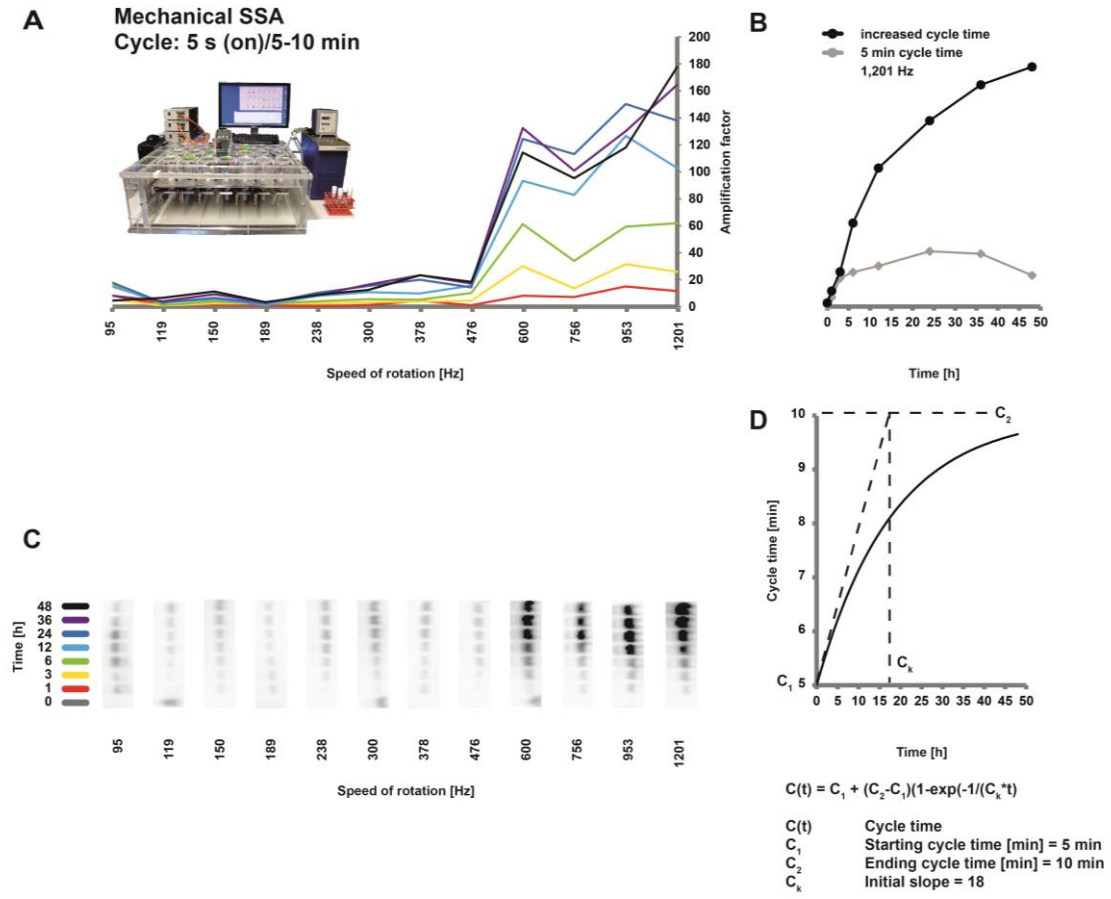

Figure 4.8: ***Extended cycle time in mechanical SSA***

The amplification of PrP^{res} in mechanical SSA reactions is shown. The cycle time was continously increased. ***(A)*** *Data is shown as a function of rotation frequency and of time.* ***(B)*** *Corresponding kinetic trace of PrP^{res} amplification at the observed shearing optima of 1,200 Hz, with and without modified cycle setting.* ***(C)*** *Corresponding western blots of the PK resistant PrP^{res} bands are shown for each time point. The amplification factors relative to the initial seed obtained at each time point are plotted against the processing frequencies.* ***(D)*** *The cycle time is plotted as a function of time. A mixture of 2% (v/v) scrapie BH (Sc237) in NBH was used for conversion reactions (reaction volume: 1,150 µl). The reactions were performed in the SSA array at 37°C for 48 hours. Modified reaction tubes were used to extract ~30 µl samples at different time points. Samples were digested with 50 µg/ml PK at 37°C for 1 h and analyzed by western blotting using the PrP-specific 6H4 antibody, followed by 1D densitometry.*

Conclusion

The kinetic buildup of PrP^{res} could be closely monitored for a timeframe of 24 hours. Compared to the previous experiments (cp. 4.3.2, p. 71 *et seqq.*) the adjustment of the processing and incubation time dramatically increased the PrP^{res} amplification yield for Sc237-seeded SSA reactions. Of course, the influences of the hardware adjustments and the different processing frequencies also have to be considered. Nevertheless, the maximum amplification factors of 263K are less high. The influence of the cycle time setting became particularly obvious if the SSA reactions were performed with an interprocessing delay. Interestingly, these settings

only positively influenced the growth rates above 600 Hz. Based on that observation, the observed amplification optima and divergent buildup rates, Sc237 and 263K might consist of conformationally different PrP^{res} populations.

4.3.4 Non-processed reactions

Despite the fact that alternating steps of processing and incubation support PrP conversion *in vitro*, it has been shown that limited amplification of PK resistant PrP is also feasible in prion seeded tissue homogenates without external ascendancies except for temperature.[198] To emphasize the influence of processing in mechanical SSA, the kinetic buildup of PrP^{res} was also investigated in non-processed control reactions. The amplification factor of control reactions seeded with the prion strain 263K did not exceed a value of five after 24 hours, while Sc237-seeded reactions did not exceed a value of 15 (Figure 4.9 B).

Conclusion

Alternating cycles of mechanical shearing and incubation dramatically increase the PrP^{res} amplification.

4.3.5 Effect of seed and homogenate treatment

As mentioned previously the addition of scrapie brain homogenate is crucial for successful conversion in brain homogenate based SSA reactions (cp. Figure 4.5 B). Therefore and to test the potential of the SSA assay, different seed dilutions were tested. All tools were run at the maximum possible processing frequency of 1,201 Hz to ensure the highest possible amplification factors. The plot in Figure **4.9** C shows the normalized time course of the PrP^{res} buildup with repsect to different prion seed dilutions. The corresponding western blot is shown in Figure 4.9 D. The experimental results revealed that dilution factors of 1:150 or higher were not sufficient to generate verifiable amounts of PK resistant PrP within 48 hours. Similar effects on the kinetic buildup of PrP^{res} could be observed if the reaction mixture (ScBH (Seed) + NBH (Substrate)) was spun down prior to a selective shearing amplification experiment. It was envisaged that a centrifugation of the seeded brain homogenate could lead to a removal of potential conversion inhibiting compounds. Although almost the same band intensity is reached after a total reaction duration of over 24 h, a flattened shape of the PrP^{res} buildup rate was observed if the reaction mixture was centrifuged at 2,000 *x g*. Especially a centrifugal acceleration of $\geq$ 10,000 *x g* resulted in almost no amplification (Figure 4.9 A).

Since good conversion results in PMCA were achieved with native PrP, which was purified from NBH[209], a pretreatment of the NBH was considered. The necessary amounts of purified native PrP for SSA reactions exceeded the limitation of the complex purification protocol. Thus, freshly prepared NBH was suspendend by centrifugation (25,000 *x g*, 10 min, 4°C). The supernatant was mixed with 10% (w/v) ScBH (2% vol/vol) and subsequently used for mechanical SSA experiments. While spinning of the reaction mix worsened the amplification results (see above) a strong centrifugation of NBH alone engendered a notable difference regarding the observed optima of amplification. Most notably was the reduced intensity of reactions which were processed at frequencies of 756 Hz and 953 Hz. Morover, optima of amplification were observed at processing frequencies of 600 Hz, 1,201 Hz, but also at 300 Hz (Figure 4.10).

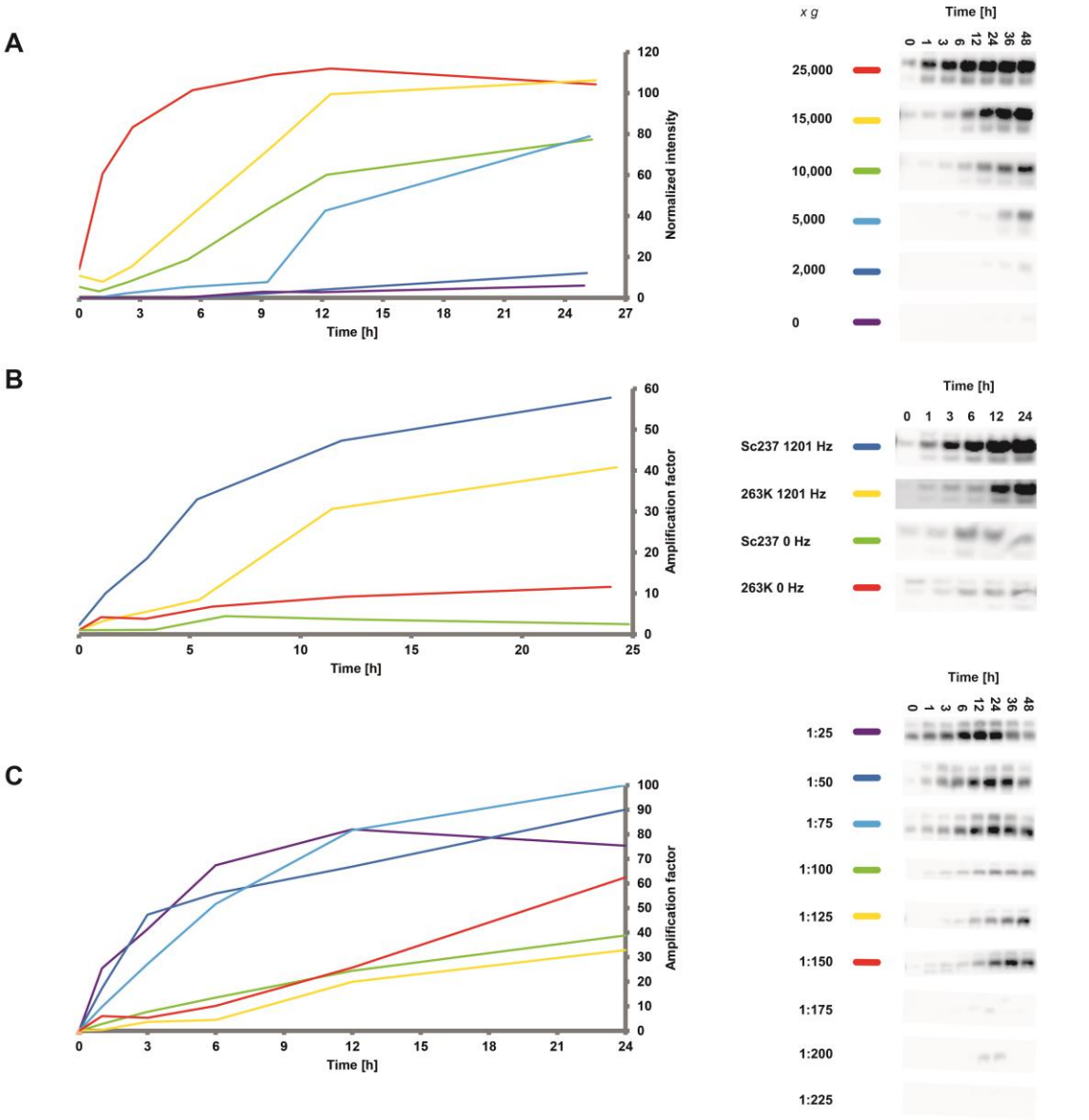

Figure 4.9: ***Influence of centrifugation treatment, seed dilution and processing in SSA experiments***

(A) *A mixture of 2% (v/v) scrapie BH in NBH was used for mechanical SSA experiments. The reaction mix was centrifuged as indicated. The supernatant was used for conversion reactions. The* PrP^{res} *amplification is shown as a function of time.* ***(B)*** *Comparison of Sc237- or 263K-seeded reactions with and without processing steps; Reactions were either carried out in shear-generators or in 15 ml reaction tubes. The* PrP^{res} *amplification is shown as a function of time.* ***(C)*** *Seed dependency over time: As indicated Sc237BH was used in different dilutions (1:50 ≙ standard). The reactions were performed in the SSA array at 37°C for ≥ 24 hours. Samples were run with a cycle setting of 5 sec processing and 5 min incubation. Modified reaction tubes were used to extract ~30 µl samples at different time points. Samples were digested witch 50 µg/ml proteinase K (PK) at 37°C for 1 h and analyzed by western blotting using the PrP-specific 6H4 antibody, followed by 1D densitometry.*

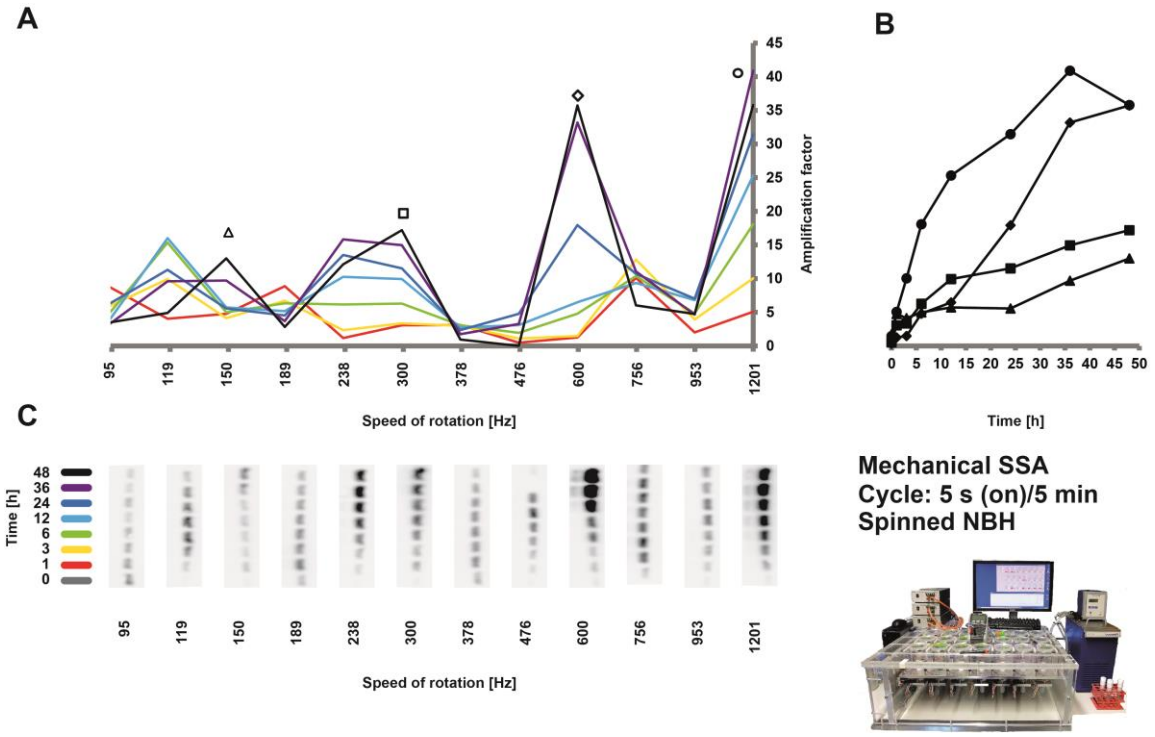

Figure 4.10: ***Influence of NBH centrifugation in SSA experiments***

(A) *Amplification of PrP^{res} in mechanical SSA reactions using the supernatant of spinned NBH. The reactions were seeded with Sc237 hamster prions. Data is shown as a function of rotation frequency and of time.* ***(B)*** *A corresponding kinetic trace of PrP^{res} amplification at the frequencies of 150 Hz, 300 Hz, 600 Hz and 1201 Hz.* ***(C)*** *Corresponding western blots of the PK resistant PrP^{res} bands are shown for each time point. Directly after preparation aliquots of 2 ml 10% (w/v) brain homogenate were spinned at 25,000* x g *for 10 min at 4°C. The supernatant was used to prepare a mixture of 5% (v/v) scrapie BH in NBH for conversion reactions. The reaction were performed in the SSA array at 37°C for 48 hours. Samples were run with a cycle setting of 5 sec processing and 5 min incubation. Modified reaction tubes were used to extract ~30 µl samples at different time points. Samples were digested witch 50 µg/ml proteinase K (PK) at 37°C for 1 h and analyzed by western blotting using the PrP-specific 6H4 anti-body, followed by 1D densitometry.*

Conclusion

Strong centrifugation of the reaction mixture potentially removed critical components for the amplification process and therefore leaded to flattened growth curves and decreased amplification factors. Similarly, if the supernatant of spun NBH is used, the disappearance of specific cell components might negatively influence the PrP^{res} buildup rates.

4.3.6 Influence of SDS

In conversion reactions of recombinant prion protein (for example in QuIC) slightly denaturant reaction conditions support the generation of PK-resistant particles.[204] Evidence for the influence of SDS on PMCA has also been given.[5] Taking account

of different models for the conversion of PrP^{C} to its resistant isoform PrP^{Sc} a denaturing effect would primarily make sense if the heterodimer model (Figure 1.4, p. 22) is assumed. If a transition state of PrP is energetically supported by changed buffer conditions the heterodimer buildup increases and the equilibrium is shifted towards PrP^{res}. Thus, the effect of a denaturing agent was surveyed in mechanical SSA reactions using 0, 1, 2.5 and 5 mM SDS at processing frequencies of 150 Hz and 1,201 Hz. While a concentration of 1 mM SDS reduced the conversion efficiency, no PrP^{res} could be detected in reactions with 5 mM SDS. (Figure 4.11)

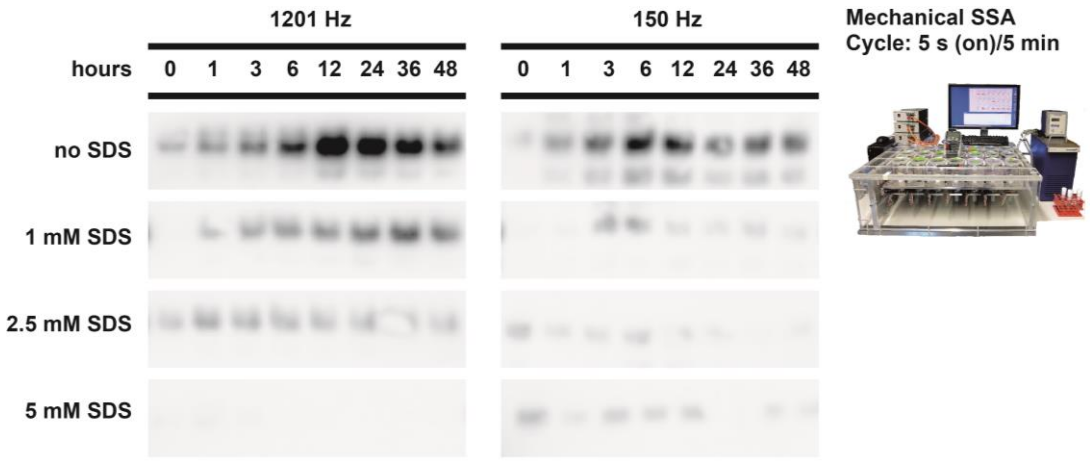

Figure 4.11: Effect of SDS on PMCA-based SSA reactions

Concentrations 0, 1, 2.5 and 5 mM SDS were tested in reactions processed with 1,201 and 150 Hz. A mixture of 5% (v/v) scrapie BH in NBH was used for conversion reactions. Reactions were carried out in 8 Heidolph 3F shear-generators with drilled outlet holes in the stator. The rotor blades were rounded down by manual grinding for smooth running behavior. The reaction were performed in the SSA array at 37°C for 48 hours with a cycle setting of 5 sec processing and 5 min incubation. Modified reaction tubes were used to extract ~30 µl samples at different time points. Samples were digested witch 50 µg/ml proteinase K (PK) at 37°C for 1 h and analyzed by western blotting using the PrP-specific 6H4 antibody, followed by 1D densitometry.

Conclusion

SDS clearly suppressed PrP^{res} amplification and is not necessary in mechanical SSA reactions.

5 Discussion

Based on the structural properties of proteopathic seeds we developed a concept for the *in vitro* selection of proteopathic seed populations from mixtures. Using the principle of a Couette-type shear generator[317] (Figure 3.8, p. 58) we were able to use precisely adjustable seed fragmentation. The selection is enabled through the different mechanic fragmentability. While alternating periods of seed growth and selective shearing kinetically select seed populations which are optimally fragmented, seed populations with distinct mechanic fragmentability are supressed. Selective shearing amplification clearly revealed that the closely related hamster prion strains Sc237 and 263K can be distinguished by the kinetic analysis of *in vitro* selected PrP^{res}. Furthermore, the data suggests the presence of multiple PrP^{res} conformations within the prion isolate Sc237. Three processing frequencies of 150 Hz, 600 Hz and 1,201 Hz were identified for optimal amplification of Sc237 prion seeds with the mechanical approach (Figure 4.7, p. 75). Importantly, the provided data of acoustic SSA showed to be in line with the optima of amplification that were detected by mechanical shearing (Figure 4.3, p. 69). Therefore, kinetic seed selection might be independent of the selected shearing mechanism. Mechanical SSA not only provides an efficient technique to amplify PrP^{res}, but also an exclusive way for kinetic seed amplification data acquisition. Thus, the kinetic PrP^{res} amplification traces were surveyed for both hamster prion strains and the experimental data provided clear evidence for characteristic differences: Contrary to Sc237, SSA reactions with 263K showed a significant lower initial buildup rate at the highest applied shear stress. Moreover, only one optimum near the maximal processing frequency was found (Figure 4.7, p. 75). Equally noteworthy is the observation that non-seeded reactions did not amplify detectable amounts of PrP^{res} and an omission of processing leaded to significant lower PrP^{res} buildup rates (Figure 4.5 C, p. 72 and Figure 4.9 B , p. 80). On the one hand this confirmed that shearing does not induce or change the conformation of the used prion seeds, on the other hand it leads to the conclusion that conformationally different major PrP^{res} populations exist. Thus, the conformation of the amplified PrP^{res} determined the time courses in these SSA experiments.

Further evidences for the conformational discriminability of the closely related hamster prion strains 263K and Sc237 can be found in previous transmission experiments which were published in the year 200: A diversification of the Sc237 hamster strain was also observed during transmission in mice. In conformity with the species barrier no clinical signs were observed within two years after

inoculation of the animals. Nevertheless, PrP^{Sc} deposits were found. In deed, the derived prions were infectious for mice and hamsters, even if it became apparent that the incubation times were relatively long.[184] However, the attack rates were 100% and the interspecies infectivity gives evidence for a heterogenity or, spoken otherwise, the evolution of a heterogeneous population of Sc237.[119] The passage history of the utilized prion strains also supports these findings. Source of all used scrapie hamster and mouse strains was the Compton "Drowsy goat" passage line which originates form first goat passages of scrapie sheep brain homogenates.[319] Interestingly, a putative *in vivo* separation of scrapie agent strains from a mixture has already been discussed in the course of observed transmission barriers.[122,123] Contrary to Sc237 the agent strain 263K is the product of limited dilution passages in hamsters. (Figure 5.1) It is likely, that the existence of a single detectable PrP^{res} population in 263K has its origin in a clonal selection of a single conformation during these *in vivo* transmission experiments. This implies that individual prion strains can be propagated *in vivo* while maintaining multiple PrP^{Sc} conformations, presumably in the absence of any obvious selective pressure.

Then again, it was hypothized that the diversification of prion strains can be attributed to the presence of readily interconverting PrP^{Sc} conformations (cp. 1.3, p. 15 *et seqq.*).[119,140] It was argued that a selective pressure promotes the amplification of minor prion populations to become the dominant species.[119,140] This assumes that certain if not all prion strains show an intrinsic conformational heterogenity. Thinking this further, serial prion replication under an selective constraint would finally dilute out the minor or less fast replicating sub-types. Interestingly, it was demonstrated that specicif prion strain characteristics, which occurred under selective conditions in cell culture were regained if the exterior constraint was restricted. However, heterogenity was also observed if the particular strain was subsequently cloned by end-point dilution. Hence, it cannot be ruled out that the Sc237 strain consits of interconverting PrP^{Sc} types. This implies, that the multiple observed shear optima are caused by a conformational adaption to the specific applied shear forces. Similarly, the single shear optimum of the 263K strain might be explained by its low propensity to undergo a spontaneous strain conformational mutation. In order to exclude this possibility, mechanical SSA should be used to serially propagate PrP^{Sc} from the Sc237 strain at a specific selective processing frequency. Subsequently, SSA might be used to test for PrP^{Sc} conformational selection: The generated reaction mixture could be split for processing across the entire accessible frequency range. A reoccurance of the three shear optima would, therefore, be indicative for the presence of 'quasi-species', while a single optimum would contradict this hypothesis. Moreover, the latter case would suggest a purification of an individual, conformational stable seed

population. Indeed, latest experiments give evidence for a successful isolation of a prion sub-population. Thus, *in vivo* selection of inherent strains is possible using kinetic seed selection.[316]

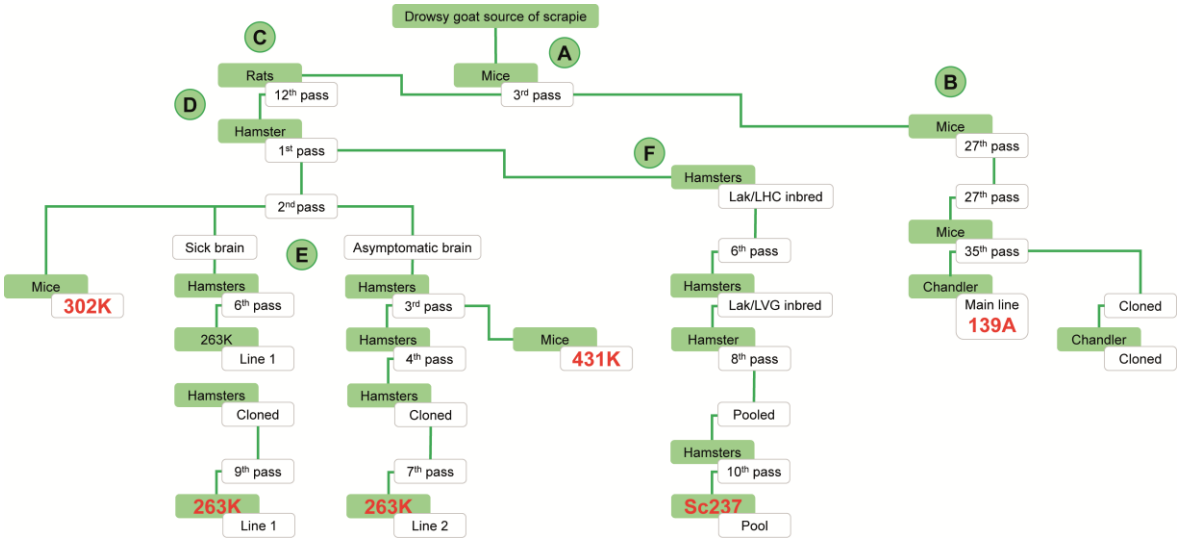

Figure 5.1: ***Passage history of prion strains Sc237 and 263K***

Source of all used scrapie hamster and mouse strains was the Compton "Drowsy goat" passage line.[319]*. Infective material was initially used for* in vivo *infection studies with mice in 1963.*[320] *After subpassages in rats*[43] *the agent was shown to produce disease in mice after five passages*[321]*. Using rat passaged (12th passage) agent, strain adaption studies in syrian golden hamsters were performed, showing long incubation times of 11 months in first passage. After a second passage mean incubation times could be dramatically reduced to 4-5 months and two pools of infectious material were used for further passages in outbred hamsters and random-bred mice.*[122,123,322] *A first passage of an isolate of the 2nd hamster passage in mice showed large species barrier (302K), while one brain of the 3rd hamster passage revealed high infectivity and low species barrier for mice (431K). Contrary to these findings no cases of scrapie developed if 6th passage scrapie agent (or later) of the hamster passage line was used for inoculation in mice. This agent was designated 263K and showed constant incubation times and hisopathology, as proven by limited dilution studies (agent was cloned). All strains, including subsequent passages in mice (302K and 421K), were found to be clearly different from the Chandler (139A) main line of mouse passaged scrapie agent. Contrary to 263K the agent strain Sc237 was originally derived from the first rat-to-hamster passage. After six passages in Lak/LHC inbred hamsters passaging was continued in Lak/LVG hamster and the agent was finally designated Sc237.*[75,122,123,323–325]*The most important difference, though, is that in these experiments no limited dilution was performed.* ***(A)*** [319] ***(B)*** [320] ***(C)*** [43] ***(D/E)*** [122,123,322] ***(F)*** [75,122,123,323–325]*; supplemented by information on the origin of the hamster prion strain Sc237 and further modified this illustration is from*[122].

Considering current techniques in prion research our findings emphasize the potential of selective shearing amplification as a relatively fast method for seed characterization. Of course, several methods exist to characterize prion strains, for instance by receiving benefit from the different prion suceptibility of certain cell lines.[326–331] The standard scrapie cell assay (SSCA), for example, helps to determine strain infectivity and the cell panel assay (CPA) showed its potential to determine

specific strain properties.[119,140,332–334] However, cell-culture-based assays remain time consuming. The same applies to the analysis of strain specific incubation times as well as a comparison of vascular lesion distributions in anatomical defined regions (‘lesion profiles’) which are accompanied by long-lasting *in vivo* transmission experiments. Thus, mechanical SSA represents a fast method that allows to select seed conformations from mixtures by finely tuned shear induced fragmentation. Optimally fragmented seeds, thus, gain a selective advantage and become the dominant population of the *in vitro* conversion reaction.

PMCA has been shown to serial replicate infectivity *in vitro.*[207] Recent research also revealed that strain-specific incubation times *in vivo* correlate with elongation rates *in vitro*.[335] It is therefore of prime interest to test the neurodegnerative potential of selectively amplified seeds *in vivo*. In addition, selectively amplified sub-populations that were sub-passaged in animals could again be screened for potential changes in their kinetic buildup rates and their shear optima. Thus, SSA could be used to reveal putative conformational changes which might occur *in vivo*. This obviously presupposes the successful isolation of single seed populations. Once purified, seed populations could be surveyed in detail, for example using different conformational stability assays.

Using PMCA it was also demonstrated that strains with fast elongation rates maintain their amplification yield irrespective of wether incubation time intervals between processing steps were varied. It was found that strain-specific elongation rates limit the overall amplification yield in a strain-dependent manner.[335] However, an interprocessing delay in mechanical shearing amplification resulted in higher PrP^{res} amplification yields and a faster buildup rate for the Sc237 strain (Figure 4.8, p. 77).

6 Outlook

A conformational selective amplification technique might promote a clearer understanding of neurodegnerative proteopathic seeds. This aspect is not merely restricted to prions. Recombinant α-synuclein seeds induce protein deposition *in vitro* as well as Parkinson-like neurodegeneration *in vivo*.[336–338] Similarly, Alzheimer peptide (Aβ) depositions could be induced in transgenic mice using brain tissue extracts of diseased Alzheimer patients and transgenic mice.[186,339] Similar to prion strains, the source of the seed as well as the genetical preconditions influence the phenotypical expression.[186] Nevertheless, there is clear evidence that specific molecular structures of proteopathic seeds have crucial influence on their propagation *in vivo*: For instance, the seeding effectivity of synthetic Aβ fibirls *in vitro* is not automatically accompanied with seeding activity *in vivo*. Sometimes in vivo transmissions showed to be directly successful and sometimes only large amounts of fibrils induce clinical signs in the animal model.[185,186] Additionally, prion replication *in vivo* does not consequently lead to the occurance of clinical signs.[182–184] Thus, only a limited number of certain conformations might go along with infectivity. Furthermore, the presence of more than one seed conformation might also be true for human neurodegenerative diseases like Alzheimer disease or Parkinson disease. Hence, the applicibility of SSA for the selective replication and structural investigation of neurodegeneration associated seeds remains to be tested. In this context a calculation of the actual shear stress values would represent a great benfit to define the structural stability of distinct seed populations. A mathematical solution is already available, but recommends a more simple tool geometry.[340] Therefore, a consistent further development of the shear-generators is reasonable. Further potential for optimization resides in the reaction composition and the reaction parameters: The total PrP^{res} amplification yield often decreased after 24 hours (cp. Figure 4.9 D, p. 80). Although this phenomenon could be prevented using cycle time variations (Figure 4.8, p. 77), a further investigation is advisable. Additionally, a pretreatment of the tissue brain homogenates showed significant influence on the conversion reactions. Centrifugation of the reaction mixture leaded to a depletion of the PrP^{res} buildup rates; the same applies to a dilution of the seed (Figure 4.9 A, C and D, p. 80). Although these experiments provide an initial insight into the sensitivity of the assay, serial amplification might dramaticaly increase the amount of detectable protease resistant PrP.[208] Interestingly, a pretreatment of NBH changed the observed shear optima. (Figure 4.10, p. 81). It was reported that the usage of purified PrP^{C} leads to better amplification results in PMCA.[209] Thus, crude tissue homogenate might comprise conversion promoting as

well as obstructive factors, which promote or suppress the amplification of specific sub-populations. However, the effect of selective shearing should be tested using a purified substrate. Slightly denaturating conditions like in the presence of SDS seem to be mandatory for *in vitro* reactions such as QuIC or recPrP-PMCA[202,204], presumably by promoting an intermediate conformation of PrP (cp. Figure 1.4, p. 22). Contrary to its effect in recombinant PrP conversion assays, SDS completely suppressed amplification of the Sc237 seed at 1,201 and 150 Hz in SSA. This might indicate that SDS has a different effect on native, glycosylated and GPI-anchored PrP^{C} than on recPrP. It is also likely that SDS disturbs the potential interaction of PrP^{C} with its proteinaceous environment. However, recent research clearly demonstrated the influence of detergents on PK-resistance. In particular, SDS was shown to weaken the PrP^{res} intensity on western blots after PK-digest.[341]

The molecular structures of mammalian prions are still elusive, and a major bottleneck for their investigation by NMR-Spectroscopy is the availability of substantial amounts of isotopically labelled recombinant prions. In recent years solid progress has been made in the generation of infectious recombinant prions using an ultrasonic approach.[90,205] Unfortunately, the PMCA technique is restricted to small reaction volumes. Thus, a further field of application of the SSA technique is the conversion of recombinant PrP. This thesis mainly focused on seeded conversion reactions, but also *de novo* generation of prions using PMCA was demonstrated[203] and most recently detailed protocols were published to achieve *de novo* formation with PMCA.[231] Interestingly, generation of infectivity was always accompanied with many serial amplification rounds. However, *de novo* generation of PK resistant PrP is likely, either by spontaneous aggregation or applied shear stress, but were not observed in mechanical SSA experiments. Of course, serial passaging of non-seeded reactions might induce spontaneous aggregation and these experiments remain to be done.

Although acoustic approach for selective shearing amplification was used several technichal drawbacks emphasize the advantages of mechanical shearing. Although cavitation bubbles within the reaction vials can be prevented if the sample positions are matched to Chladni pattern, the wear and tear of the sonotrode is anvoidable. The fast decay changes the oscillation behavior and necessitates an often exchange of the Cup Horn. Unfortunately, the oscillation pattern of each replica was unique (Figure 3.5, p. 54) and even sligthly changes in the symmetry were shown to have strong influence (Figure 4.3, p. 69). Furthermore, generated sound waves have to penetrate the wall of the reaction vials. Thus, refraction, reflection and interferrence might raise problems. Although thin-walled PCR-tubes were used, the application of other materials should be considered. The sound propagation in Teflon™

(1.52 km/sec), for example, is similar to that in water (1.47 km/sec). Thus, Teflon™ might be a better choice.

Appendix

Detailed experiment parameters for PMCA, acoustic SSA and mechanic SSA are summarized below. (p. 89 *et seqq.*)

A list of PMCA experiments and further information regarding the execution are given in Table A.1.

Table A.1: Performed PMCA experiments and reaction parameters

Experiment	Purpose	Prion strain	Cycle time On/total [sec/min]	Power level [%]	Seed [vol.%]	Volume [µl]	Duration [h]	Heights [mm]	Sonotrode replica	Sampleholder[2]	Results
1	Seed dependence (till round 2)	Sc237	40/60	90	0.25-10	100	24	-	I	O	Figure 4.1, p. 66
2	Position effects	Sc237	40/60	90	5	100	24	-	I	O	Figure 4.1, p. 66
3	Bicellar mixtures[3]	Sc237	40/60	90	5	200	24	-	I	O	Figure 4.1, p. 66
4	Radius dependence + bicelles	Sc237	40/60	90	5	100	48	-	I	R	Figure 4.1, p. 66
5	Height profile	Sc237 263K	60/10	90	5		24	0.5; 3; 5; 7; 9	I	H	Figure 4.2, p. 67

[2] O = original Misonix 4,000 setup (cp. 3.6.1, p. 44 et seqq. and Figure 3.3 A, p. 47); R = Radius dependence (centered rotating sample holder, cp. 3.6.1, p. 44 et seqq. and Figure **3.3** A, p. 47 B); H = height-adjustable sample holder (cp. 3.6.1, p. 44 et seqq. and Figure 3.3 A, p. 47 C)

[3] Composition of bicellar mixtures is given in chapter 3.1.5, p. 36. Detailed information about used bicelle concentrations are listed in Table A.**2**, p. 106.

Used bicelle concentrations for experiments 3 and 4 (Table A.1) are listed below.

Table A.2: Applied bicelle concentrations in PMCA experiments

Experiment	Bicellar mixture [mM]	DMPS [%]
3	0; 25	0; 5; 10
4	0; 25	-

A list of all performed acoustic experiments and their reaction parameters is given in Table A.3.

Table A.3: Performed acoustic SSA experiments and reaction parameters

Experiment	Purpose	Prion strain	Cycle time On/total [sec/min]	Power level [%]	Seed [vol.%]	Volume [µl]	Duration [h]	Heights [mm]	Sonotrode Chladni #	Results
1	Height profile	Sc237 263K	3/5	85	2	130	12	0.5; 1; 1.5; 2; 3; 4; 5; 6; 8; 10; 12; 14; 16; 18	I	Figure 4.3, p. 69
2	Height profile	Sc237 263K	3/5	85	2	130	12	0.5; 1; 1.5; 2; 3; 4; 5; 6; 8;	II	Figure 4.3, p. 69

Experiment	Purpose	Prion strain	Cycle time On/total [sec/min]	Power level [%]	Seed [vol.%]	Volume [µl]	Duration [h]	Heights [mm]	Sonotrode Chladni #	Results
								10; 12		

A list of all performed mechanical SSA reactions is given in Table A.4.

Table A.4: Mechanical SSA reactions and reaction parameters

Experiment	Purpose	Kinetic[4]	Prion strain	Volume [ml]	Cycle time [sec/min] On/total	Frequency [Hz]	Duration [h]	Seed	Results
1	Feasibility of conversion with shear-generators[5]	-	Sc237 263K	900	60/10	0; 15; 30; 45; 60; 75 krpm[5]	24	1:10	Figure 4.4, p. 70
2	Test of the SSA array Frequency range	-	Sc237 263K	900	60/60	40; 54; 72; 96; 129; 173; 232; 311; 417; 559; 749; 1,004	24	1:10	Figure 4.5, p. 72
3	Non-seeded reactions	-	-	900	60/10	54; 173; 417	22	-	Figure 4.5, p. 72
4	Cycle time	+	Sc237	1,150	5/5, 15, 30, 60, 90	1,000	40	1:50	Figure 4.6, p. 73
5	Frequency range	+	Sc237 263K	1,150	5/5	96; 119; 150; 189; 238; 300; 476; 600; 756; 953; 1,201	22	1:50	Figure 4.7, p. 75

[4] After ~1; 3; 6; 12; 24; 36 and 48 h samples of ~20 µl were taken from the reactions. The shape of the rotor blade edges was rounded down by manual grinding to avoid vibrations.

[5] These initial reactions were performed with non-modified hardware from Heidolph (Silent Crusher S, 3F dispersion tool). Speed of rotation was only adjustable by a built-in potentiometer with a rough rpm scale. All other experiments were performed with modified hardware (SSA array) giving the possibility to adjust the frequency precisely.

Experiment	Purpose	Kinetic[4]	Prion strain	Volume [ml]	Cycle time [sec/min] On/total	Frequency [Hz]	Duration [h]	Seed	Results
6	Continuously increased incubation time[6]	+	Sc237	1,150	Start value 5/5; end value 5/15	96; 119; 150; 189; 238; 300; 476; 600; 756; 953; 1,201	48	1:50	Figure 4.8, p. 77
7	Non-processed reaction	+	Sc237 263K	1,150	5/5	-	24	1:50	Figure 4.9, p. 80
8	Seed dilution	+	Sc237	1,150	5/5	600	24	1:25-1:225[7]	Figure 4.9, p. 80
9	Centrifugation of reaction mix[8]	+	Sc237	1,150	5/5	1,000	48	1:50	Figure 4.9, p. 80
10	Centrifugation of NBH[9]	+	Sc237	1,150	5/5	96; 119; 150; 189;	48	1:50	Figure 4.10, p. 81

[6] The increase of the cycle time is defined by $C(t) = C1 + (C2 - C1)(1 - exp(-\frac{1}{Ck*t})$. C1 represents the start cycle time (t=0). C2 is the final cycle time and Ck determines the initial slope. For the presented experiment a setting of C1 = 5 min, C2 = 10 min and Ck = 18 was used.

[7] A 10% (w/v) ScBH (Sc237) was diluted 1:25, 1:50, 1:75, 1:100, 1:125, 1:150, 1:175, 1:200 or 1:225 into a 10% (w/v) NBH.

[8] A mixture of 2% (v/v) ScBH in NBH was centrifuged with 2,000; 5,000; 10,000; 15,000 and 25,000 x g for 10 min at 4 °C (+ one non-centrifuged experiment). Supernatant was used for conversion reactions.

[9] Freshly prepared NBH was spinned at 25,000 x g for 10 min at 4 °C (splitted in two SS34 centrifugation tubes). Supernatant was mixed with ScBH and taken for the conversion experiment.

Experiment	Purpose	Kinetic[4]	Prion strain	Volume [ml]	Cycle time [sec/min] On/total	Frequency [Hz]	Duration [h]	Seed	Results
						238; 300; 476; 600; 756; 953; 1,201			
11	Effect of SDS (0, 1, 2.5, 5 mM)	+	Sc237	1,150	5/5	150; 1,201	48	1:50	Figure 4.11, p. 82

Abbreviations

139A	Mouse prion strain (Chandler strain)
22L	Mouse prion strain
263K	Hamster prion strain
79A	Mouse prion strain
Aβ	Alzheimer peptide
Bax	Bcl-2-associated protein x
Bcl-2	B-cell lymphoma 2
BH	Brain homogenate
BH2	Bcl-2 homologue domain 2
bPrP	Bovine prion protein
BSE	Bovine spongiform encephalopathy
CHAPS	3-[(3-Cholamidopropyl) dimethylammonio]-1-propanesulfonate
CHAPSO	3-[(3-Cholamidopropyl) dimethylammonio]-2-hydroxy-1-propanesulfonate
CJD	Creutzfeldt-Jakob disease
CMC	Critical micelle concentration
CMC	Critical micelle concentration
CPA	Cell panel assay

CWD	Chronic wasting disease
DHPC	Dihexanoylphosphatidylcholine
DMPC	Dimyristoylphosphatidylcholine
DMPS	Dimyristoylphosphatidylserine
DNA	Desoxyribonucleic acid
Dpl	Doppel protein
DY	Drowsy (hamster prion strain)
EDTA	Ethylenediaminetetraacetic acid
ER	Endoplasmic reticulum
fCJD	Familiar form of the Creutzfeldt-Jakob disease
FFI	Fatal familial insomnia
Fyn	A member of the Src tyrosine kinase family
GITC	Guanidinium thiocyanate
GPI	Glycosylphosphatidylinositol
GSS	Gerstmann Sträussler Scheinker syndrome
hPrP	Human prion protein
hPrP	Human prion protein
HY	Hyper (hamster prion strain)
HZI	Helmholtz-Centre for Infection Research, Braunschweig, Germany

HZI	Helmholtz centre for infection research (ger. : Helmholtz-Zentrum für Infektionsforschung; Braunschweig, Germany)
iCJD	Iatrogen form of the Creutzfeldt-Jakob disease
LB	Lysogeny broth
LDS	Lithium dodecyl sulfate
MHM2 PrP	Chimeric mouse hamster prion protein
mPrP	Mouse prion protein
mPrP(121-230)	Mouse prion protein (residues 121-230), recombinant
mPrP(23-231)	Mouse prion protein (residues 23-231), recombinant
$mPrP^{C}$	Cellular mouse prion protein
MS	Mass spectroscopy
MW	Molecular weight
MWCO	Molecular weight cut-off
NADPH	Nicotinamide adenine dinucleotide phosphate
NaPTA	Sodium (ger. : Natrium (Na)) phosphotungstic acid
NBH	Normal brain homogenate (healthy animal)
NBH	Normal brain homogenate
Ni-NTA	Nitrilotriacetic acid and Ni
NMR	Nuclear magnetic resonance
NOG	N-oxalylglycine

OD	Optical density
PBS	Phosphate buffered saline
PCR	Polymerase chain reaction
PK	Proteinase K
PK1[22L]	Mouse prion strain 22L adapted to PK1-cells
PK1-cells	Porcine kidney epithelia cells
PMCA	Protein misfolding cyclic amplification
PMCAb	Protein misfolding cyclic amplification with beads
PMSF	Phenylmethylsulfonylfluorid
Poly(A), poly(rA)	Polyadenylic acid, polyadenylic ribonucleic acid
POPG	1-palmitoyl-2-oleoyl-sn-glycero-3-phosphoglycerol
Prnd	Mouse gene encoding for doppel
Prnp	Mouse gene encoding for the prion protein
PrP	Prion protein
PrP*	A hypothetical intermediate form of the prion protein
PrP^{27-30}	Protease resistant core of protease K treated PrP^{Sc} or PrP^{res}
PrP^{res}	Partially protease K resistant form of the prion protein
PrP^{Sc}	Disease associated isoform of the prion protein (Sc = scrapie). Major or only part of the prion.
PrPβ	A β-sheet rich isoform of the prion protein

PrPβf	A β-sheet-rich and fibril forming isoform of the prion protein
PTFE	Polytetrafluoroethylene
QuIC	Quaking induced conversion
recPrP	Recombinant prion protein
recPrP-PMCA	Recombinant prion protein – protein misfolding cyclic amplification
RML	Rocky Mountain Laboratories prion strain (mouse)
RML	Rocky mountain laboratory mouse prion strain
RNA	Ribonucleic acid
$rPrP^{Sc}$	Protease K resistant form of PrP^{Sc}
RT	Room temperature
RT-QuIC	Real time-quaking induced conversion
RT-QuIC	Real-time Quaking-induced conversion
saPMCA	Serial automated protein misfolding cyclic amplification
Sc237	Hamster adapted prion strain
Sc237BH	Brain homogenate from Syrian golden hamsters which were infected with the hamster prion strain Sc237
ScBH	Scrapie brain homogenate
ScBH	Scrapie brain homogenate
sCJD	Sporadic form of the Creutzfeldt-Jakob disease
SDS	Sodium dodecyl sulfate

SDS	Sodium dodecyl sulfate
SDS-PAGE	Sodium dodecyl sulfate-poly acryl amide gel electrophoresis
shPrP	Syrian Golden hamster prion protein
shPrP(23-231)	Full length Syrian Golden hamster prion protein (residues 23-231), recombinant
SOD	Superoxide dismutase
$sPrP^{Sc}$	Protease K sensitive form of PrP^{Sc}
Src	Sarcoma tyrosine kinase
SSA	Selective shearing amplification
SSA	Selective shearing amplification
SSCA	Standard scrapie cell assay
Swa	Swainsonine, a Golgi α-mannosidase II inhibitor, which is capable to inhibit prion infections in cell culture
TBST	Tris-buffered saline and Tween 20
TSE	Transmissible spongiforme encephalopahty
vCJD	Variant form of the Creutzfeldt-Jakob disease
β_2m	β_2-microglobulin

Bibliography

1. Jucker, M. & Walker, L. C. Pathogenic protein seeding in Alzheimer disease and other neurodegenerative disorders. *Ann Neurol* **70,** 532–40 (2011).

2. Lansbury, P. T. Structural neurology: are seeds at the root of neuronal degeneration? *Neuron* **19,** 1151–4 (1997).

3. Prusiner, S. B. Prions. *Proc Natl Acad Sci U S A* **95,** 13363–13383 (1998).

4. Saa, P., Castilla, J. & Soto, C. Cyclic amplification of protein misfolding and aggregation. *Methods Mol Biol* **299,** 53–65 (2005).

5. Saborio, G. P., Permanne, B. & Soto, C. Sensitive detection of pathological prion protein by cyclic amplification of protein misfolding. *Nature* **411,** 810–813 (2001).

6. Wells, G. A. Pathology of nonhuman spongiform encephalopathies: variations and their implications for pathogenesis. *Dev Biol Stand* **80,** 61–69 (1993).

7. Budka, H. *et al.* Neuropathological diagnostic criteria for Creutzfeldt-Jakob disease (CJD) and other human spongiform encephalopathies (prion diseases). *Brain Pathol* **5,** 459–466 (1995).

8. MacDonald, S. T., Sutherland, K. & Ironside, J. W. Prion protein genotype and pathological phenotype studies in sporadic Creutzfeldt-Jakob disease. *Neuropathol Appl Neurobiol* **22,** 285–292 (1996).

9. Gray, F. *et al.* Neuronal apoptosis in Creutzfeldt-Jakob disease. *J Neuropathol Exp Neurol* **58,** 321–328 (1999).

10. Jeffrey, M., Goodbrand, I. A. & Goodsir, C. M. Pathology of the transmissible spongiform encephalopathies with special emphasis on ultrastructure. *Micron* **26,** 277–298 (1995).

11. Lührs, T. Structural and functional studies of monomeric and aggregated amyloidogenic forms of prion proteins. (2002).

12. Brown, P., Cathala, F., Castaigne, P. & Gajdusek, D. C. Creutzfeldt-Jakob disease: clinical analysis of a consecutive series of 230 neuropathologically verified cases. *Ann Neurol* **20,** 597–602 (1986).

13. Johnson, R. T. & Gibbs Jr., C. J. Creutzfeldt-Jakob disease and related transmissible spongiform encephalopathies. *N Engl J Med* **339,** 1994–2004 (1998).

14. Weber, T. Clinical and laboratory diagnosis of Creutzfeldt-Jakob disease. *Clin Neuropathol* **19,** 249–250 (2000).

15. Collinge, J. Prion diseases of humans and animals: their causes and molecular basis. *Annu Rev Neurosci* **24,** 519–550 (2001).

16. Prusiner, S. B. & Scott, M. R. Genetics of prions. *Annu Rev Genet* **31,** 139–175 (1997).

17. Kovacs, G. G. *et al.* Mutations of the prion protein gene phenotypic spectrum. *J Neurol* **249,** 1567–1582 (2002).

18. Brown, P. *et al.* Iatrogenic Creutzfeldt-Jakob disease at the millennium. *Neurology* **55,** 1075–1081 (2000).

19. Will, R. G. Acquired prion disease: iatrogenic CJD, variant CJD, kuru. *Br Med Bull* **66,** 255–265 (2003).

20. Zobeley, E., Flechsig, E., Cozzio, A., Enari, M. & Weissmann, C. Infectivity of scrapie prions bound to a stainless steel surface. *Mol Med* **5,** 240–243 (1999).

21. Bernoulli, C. *et al.* Danger of accidental person-to-person transmission of Creutzfeldt-Jakob disease by surgery. *Lancet* **1,** 478–9 (1977).

22. Frosh, A., Joyce, R. & Johnson, A. Iatrogenic vCJD from surgical instruments. *BMJ* **322,** 1558–1559 (2001).

23. Ironside, J. W. *et al.* A new variant of Creutzfeldt-Jakob disease: neuropathological and clinical features. *Cold Spring Harb Symp Quant Biol* **61,** 523–530 (1996).

24. NCJDRSU. Variant Creutzfeldt-Jakob disease - current data (August 2012). (2012). at <http://www.cjd.ed.ac.uk/vcjdworld.htm>

25. Collinge, J., Sidle, K. C., Meads, J., Ironside, J. & Hill, A. F. Molecular analysis of prion strain variation and the aetiology of "new variant" CJD. *Nature* **383,** 685–690 (1996).

26. Collinge, J. Variant Creutzfeldt-Jakob disease. *Lancet* **354,** 317–323 (1999).

27. Ironside, J. W. Neuropathological findings in new variant CJD and experimental transmission of BSE. *FEMS Immunol Med Microbiol* **21,** 91–95 (1998).

28. Will, R. G. *et al.* Diagnosis of new variant Creutzfeldt-Jakob disease. *Ann Neurol* **47,** 575–582 (2000).

29. Hill, A. F. *et al.* The same prion strain causes vCJD and BSE. *Nature* **389,** 448–50, 526 (1997).

30. Bruce, M. E. *et al.* Transmissions to mice indicate that "new variant" CJD is caused by the BSE agent. *Nature* **389,** 498–501 (1997).

31. Lasmezas, C. I. *et al.* BSE transmission to macaques. *Nature* **381,** 743–744 (1996).

32. Scott, M. R. *et al.* Compelling transgenetic evidence for transmission of bovine spongiform encephalopathy prions to humans. *Proc Natl Acad Sci U S A* **96,** 15137–15142 (1999).

33. Ghetti, B. *et al.* Gerstmann-Straussler-Scheinker disease and the Indiana kindred. *Brain Pathol* **5,** 61–75 (1995).

34. Yamazaki, M. *et al.* Variant Gerstmann-Straussler syndrome with the P105L prion gene mutation: an unusual case with nigral degeneration and widespread neurofibrillary tangles. *Acta Neuropathol* **98,** 506–511 (1999).

35. Scaravilli, F. *et al.* Sporadic fatal insomnia: a case study. *Ann Neurol* **48,** 665–668 (2000).

36. Cortelli, P., Gambetti, P., Montagna, P. & Lugaresi, E. Fatal familial insomnia: clinical features and molecular genetics. *J Sleep Res* **8 Suppl 1,** 23–29 (1999).

37. Budka, H. Fatal familial insomnia around the world. Introduction. *Brain Pathol* **8,** 553 (1998).

38. Gajdusek, D. C. Unconventional viruses and the origin and disappearance of kuru. *Science (80-)* **197,** 943–960 (1977).

39. Liberski, P. P. & Gajdusek, D. C. Kuru: forty years later, a historical note. *Brain Pathol* **7,** 555–560 (1997).

40. Detwiler, L. A. Scrapie. *Rev Sci Tech* **11,** 491–537 (1992).

41. Cullie P.L., J. and C. Experimental transmissions of trembling to the goat. *Rendus des Seances de l'Academie des Sciences* **208,** 1058–1160 (1939).

42. Chandler, R. L. An experimental mixed infection of mice with scrapie and an oncogenic virus. *J Comp Pathol* **75,** 323–326 (1965).

43. Chandler, R. L. & Fisher, J. Experimental Transmission of Scrapie to Rats. *Lancet* **2,** 1165 (1963).

44. Chandler, R. L. Experimental transmission of scrapie to voles and Chinese hamsters. *Lancet* **1,** 232–233 (1971).

45. Williams, E. S. & Miller, M. W. Chronic wasting disease in deer and elk in North America. *Rev Sci Tech* **21,** 305–316 (2002).

46. Wadsworth, J. D. *et al.* Tissue distribution of protease resistant prion protein in variant Creutzfeldt-Jakob disease using a highly sensitive immunoblotting assay. *Lancet* **358,** 171–180 (2001).

47. Glatzel, M. *et al.* Human prion diseases: epidemiology and integrated risk assessment. *Lancet Neurol* **2,** 757–763 (2003).

48. Head, M. W. *et al.* Peripheral tissue involvement in sporadic, iatrogenic, and variant Creutzfeldt-Jakob disease: an immunohistochemical, quantitative, and biochemical study. *Am J Pathol* **164,** 143–153 (2004).

49. Brown, P. *et al.* Human spongiform encephalopathy: the National Institutes of Health series of 300 cases of experimentally transmitted disease. *Ann Neurol* **35,** 513–529 (1994).

50. Brown, P. & Walker, J. M. in (Baker, H. F. & Ridley, R. M.) **3,** 139–154 (Springer New York, 1996).

51. Bruce, M. E., McConnell, I., Will, R. G. & Ironside, J. W. Detection of variant Creutzfeldt-Jakob disease infectivity in extraneural tissues. *Lancet* **358,** 208–209 (2001).

52. Wadsworth, J. D. *et al.* Prion infectivity in variant Creutzfeldt-Jakob disease rectum. *Gut* **56,** 90–94 (2007).

53. Notari, S. *et al.* Multiorgan detection and characterization of protease-resistant prion protein in a case of variant CJD examined in the United States. *PLoS One* **5,** e8765 (2010).

54. Llewelyn, C. A. *et al.* Possible transmission of variant Creutzfeldt-Jakob disease by blood transfusion. *Lancet* **363,** 417–421 (2004).

55. HPA. New case of variant CJD associated with blood transfusion. (2006). at <http://www.hpa.org.uk/hpa/news/articles/press_releases/2006/060209_cjd.htm>

56. Sutton, J. M., Dickinson, J., Walker, J. T. & Raven, N. D. Methods to minimize the risks of Creutzfeldt-Jakob disease transmission by surgical procedures: where to set the standard? *Clin Infect Dis* **43,** 757–764 (2006).

57. Peden, A. H., Head, M. W., Ritchie, D. L., Bell, J. E. & Ironside, J. W. Preclinical vCJD after blood transfusion in a PRNP codon 129 heterozygous patient. *Lancet* **364,** 527–529 (2004).

58. Peden, A. H., Ritchie, D. L. & Ironside, J. W. Risks of transmission of variant Creutzfeldt-Jakob disease by blood transfusion. *Folia Neuropathol* **43,** 271–278 (2005).

59. Bishop, M. T. *et al.* Predicting susceptibility and incubation time of human-to-human transmission of vCJD. *Lancet Neurol* **5,** 393–398 (2006).

60. Ironside, J. W. Variant Creutzfeldt-Jakob disease: risk of transmission by blood transfusion and blood therapies. *Haemophilia* **12 Suppl 1,** 8 (2006).

61. TSE-Koord. Akquirierte Creutzfeldt-Jakob Krankheit. (2012). at <http://www.prionforschung.de/flash_page.php>

62. Fichet, G. *et al.* Novel methods for disinfection of prion-contaminated medical devices. *Lancet* **364,** 521–526 (2004).

63. McLeod, A. H. *et al.* Proteolytic inactivation of the bovine spongiform encephalopathy agent. *Biochem Biophys Res Commun* **317,** 1165–1170 (2004).

64. Yan, Z. X., Stitz, L., Heeg, P., Pfaff, E. & Roth, K. Infectivity of prion protein bound to stainless steel wires: a model for testing decontamination procedures for transmissible spongiform encephalopathies. *Infect Control Hosp Epidemiol* **25,** 280–283 (2004).

65. Baxter, H. C. *et al.* Elimination of transmissible spongiform encephalopathy infectivity and decontamination of surgical instruments by using radio-frequency gas-plasma treatment. *J Gen Virol* **86,** 2393–2399 (2005).

66. Jackson, G. S. *et al.* An enzyme-detergent method for effective prion decontamination of surgical steel. *J Gen Virol* **86,** 869–878 (2005).

67. Peretz, D. *et al.* Inactivation of prions by acidic sodium dodecyl sulfate. *J Virol* **80,** 322–331 (2006).

68. WHO. WHO Infection control guidelines for transmissible spongiform encephalopathies. (1999).

69. Chandler, R. L. Encephalopathy in mice produced by inoculation with scrapie brain material. *Lancet* **1,** 1378–1379 (1961).

70. Beck, E., Daniel, P. M., Alpers, M., Gajdusek, D. C. & Gibbs Jr., C. J. Experimental “kuru” in chimpanzees. A pathological report. *Lancet* **2,** 1056–1059 (1966).

71. Gajdusek, D. C., Gibbs, C. J. & Alpers, M. Experimental transmission of a Kuru-like syndrome to chimpanzees. *Nature* **209,** 794–796 (1966).

72. Alper, T., Haig, D. A. & Clarke, M. C. The exceptionally small size of the scrapie agent. *Biochem Biophys Res Commun* **22,** 278–284 (1966).

73. Alper, T., Cramp, W. A., Haig, D. A. & Clarke, M. C. Does the agent of scrapie replicate without nucleic acid? *Nature* **214,** 764–766 (1967).

74. Cho, H. J. Requirement of a protein component for scrapie infectivity. *Intervirology* **14,** 213–216 (1980).

75. Prusiner, S. B. *et al.* Molecular properties, partial purification, and assay by incubation period measurements of the hamster scrapie agent. *Biochemistry* **19,** 4883–4891 (1980).

76. Hunter, G. D., Kimberlin, R. H., Millson, G. C. & Gibbons, R. A. An experimental examination of the scrapie agent in cell membrane mixtures. *Journal of Comparative Pathology* **81,** 23–32 (1971).

77. Kimberlin, R. H., Millson, G. C. & Hunter, G. D. An experimental examination of the scrapie agent in cell membrane mixtures. 3. Studies of the operational size. *J Comp Pathol* **81,** 383–391 (1971).

78. Millson, G. C., Hunter, G. D. & Kimberlin, R. H. An experimental examination of the scrapie agent in cell membrane mixtures. *Journal of Comparative Pathology* **81,** 255–265 (1971).

79. Semancik, J. S., Marsh, R. F., Geelen, J. L. & Hanson, R. P. Properties of the scrapie agent-endomembrane complex from hamster brain. *J Virol* **18,** 693–700 (1976).

80. Prusiner, S. B. *et al.* Evidence for hydrophobic domains on the surface of the scrapie agent. *Trans Am Neurol Assoc* **103,** 62–64 (1978).

81. Prusiner, S. B., Hadlow, W. J., Eklund, C. M., Race, R. E. & Cochran, S. P. Sedimentation characteristics of the scrapie agent from murine spleen and brain. *Biochemistry* **17,** 4987–4992 (1978).

82. Prusiner, S. B. *et al.* Partial purification and evidence for multiple molecular forms of the scrapie agent. *Biochemistry* **17,** 4993–4999 (1978).

83. Griffith, J. S. Self-replication and scrapie. *Nature* **215,** 1043–1044 (1967).

84. Kimberlin, R. H. Scrapie agent: prions or virinos? *Nature* **297,** 107–108 (1982).

85. Carp, R. I., Ye, X., Kascsak, R. J. & Rubenstein, R. The nature of the scrapie agent. Biological characteristics of scrapie in different scrapie strain-host combinations. *Ann N Y Acad Sci* **724,** 221–234 (1994).

86. Prusiner, S. B. Novel proteinaceous infectious particles cause scrapie. *Science (80-)* **216,** 136–144 (1982).

87. McKinley, M. P., Bolton, D. C. & Prusiner, S. B. A protease-resistant protein is a structural component of the scrapie prion. *Cell* **35,** 57–62 (1983).

88. Prusiner, S. B. Molecular biology of prion diseases. *Science (80-)* **252,** 1515–1522 (1991).

89. Gabizon, R., McKinley, M. P., Groth, D. & Prusiner, S. B. Immunoaffinity purification and neutralization of scrapie prion infectivity. *Proc Natl Acad Sci U S A* **85,** 6617–6621 (1988).

90. Kim, J. I. *et al.* Mammalian prions generated from bacterially expressed prion protein in the absence of any mammalian cofactors. *J Biol Chem* **285,** 14083–14087 (2010).

91. Basler, K. *et al.* Scrapie and cellular PrP isoforms are encoded by the same chromosomal gene. *Cell* **46,** 417–428 (1986).

92. Stahl, N. *et al.* Structural studies of the scrapie prion protein using mass spectrometry and amino acid sequencing. *Biochemistry* **32,** 1991–2002 (1993).

93. Pan, K. M. *et al.* Conversion of alpha-helices into beta-sheets features in the formation of the scrapie prion proteins. *Proc Natl Acad Sci U S A* **90,** 10962–10966 (1993).

94. Cohen, F. E. & Prusiner, S. B. Pathologic conformations of prion proteins. *Annu Rev Biochem* **67,** 793–819 (1998).

95. Hope, J. & Manson, J. The scrapie fibril protein and its cellular isoform. *Curr Top Microbiol Immunol* **172,** 57–74 (1991).

96. Cronier, S. *et al.* Detection and characterization of proteinase K-sensitive disease-related prion protein with thermolysin. *Biochem J* **416,** 297–305 (2008).

97. Nazor, K. E. *et al.* Immunodetection of disease-associated mutant PrP, which accelerates disease in GSS transgenic mice. *EMBO J* **24,** 2472–80 (2005).

98. Safar, J. *et al.* Eight prion strains have PrP(Sc) molecules with different conformations. *Nat Med* **4,** 1157–1165 (1998).

99. Tzaban, S. *et al.* Protease-sensitive scrapie prion protein in aggregates of heterogeneous sizes. *Biochemistry* **41,** 12868–75 (2002).

100. D'Castro, L. *et al.* Isolation of proteinase K-sensitive prions using pronase E and phosphotungstic acid. *PLoS One* **5,** e15679 (2010).

101. Bueler, H. *et al.* Normal development and behaviour of mice lacking the neuronal cell-surface PrP protein. *Nature* **356,** 577–582 (1992).

102. Oesch, B. *et al.* A cellular gene encodes scrapie PrP 27-30 protein. *Cell* **40,** 735–746 (1985).

103. Hsiao, K. K. *et al.* Spontaneous neurodegeneration in transgenic mice with mutant prion protein. *Science (80-)* **250,** 1587–1590 (1990).

104. Hsiao, K. K. *et al.* Serial transmission in rodents of neurodegeneration from transgenic mice expressing mutant prion protein. *Proc Natl Acad Sci U S A* **91,** 9126–9130 (1994).

105. Barron, R. M. & Manson, J. C. A gene-targeted mouse model of P102L Gerstmann-Straussler-Scheinker syndrome. *Clin Lab Med* **23,** 161–173 (2003).

106. Westaway, D. *et al.* Degeneration of skeletal muscle, peripheral nerves, and the central nervous system in transgenic mice overexpressing wild-type prion proteins. *Cell* **76,** 117–129 (1994).

107. Chesebro, B. BSE and prions: uncertainties about the agent. *Science (80-)* **279,** 42–43 (1998).

108. Narang, H. A critical review of the nature of the spongiform encephalopathy agent: protein theory versus virus theory. *Exp Biol Med (Maywood)* **227,** 4–19 (2002).

109. Derrington, E. A. & Darlix, J.-L. The Enigmatic Multifunctionality of the Prion Protein. *Drug News Perspect* **15,** 206–219 (2002).

110. Gabus, C. *et al.* The prion protein has RNA binding and chaperoning properties characteristic of nucleocapsid protein NCP7 of HIV-1. *J Biol Chem* **276,** 19301–19309 (2001).

111. Weiss, S. *et al.* RNA aptamers specifically interact with the prion protein PrP. *J Virol* **71,** 8790–7 (1997).

112. Deleault, N. R., Lucassen, R. W. & Supattapone, S. RNA molecules stimulate prion protein conversion. *Nature* **425,** 717–720 (2003).

113. Gajdusek, D. *Slow, latent, and temperate virus infections*. (U.S. National Institute of Neurological Diseases and Blindness; [for sale by the Supt. of Docs. U.S. Govt. Print. Off.], 1965). at <http://www.worldcat.org/title/slow-latent-and-temperate-virus-infections/oclc/51941>

114. Schatzl, H. M., Da Costa, M., Taylor, L., Cohen, F. E. & Prusiner, S. B. Prion protein gene variation among primates. *J Mol Biol* **245,** 362–374 (1995).

115. Wopfner, F. *et al.* Analysis of 27 mammalian and 9 avian PrPs reveals high conservation of flexible regions of the prion protein. *J Mol Biol* **289,** 1163–1178 (1999).

116. Prusiner, S. B. *et al.* Transgenetic studies implicate interactions between homologous PrP isoforms in scrapie prion replication. *Cell* **63,** 673–686 (1990).

117. Scott, M. *et al.* Propagation of prions with artificial properties in transgenic mice expressing chimeric PrP genes. *Cell* **73,** 979–988 (1993).

118. Collinge, J. *et al.* Unaltered susceptibility to BSE in transgenic mice expressing human prion protein. *Nature* **378,** 779–83 (1995).

119. Weissmann, C., Li, J., Mahal, S. P. & Browning, S. Prions on the move. *EMBO Rep* **12,** 1109–17 (2011).

120. Bruce, M. E. Scrapie strain variation and mutation. *Br. Med. Bull.* **49,** 822–838 (1993).

121. Collinge, J. & Clarke, A. R. A general model of prion strains and their pathogenicity. *Science (80-)* **318,** 930–936 (2007).

122. Kimberlin, R. H. & Walker, C. A. Evidence that the transmission of one source of scrapie agent to hamsters involves separation of agent strains from a mixture. *J Gen Virol* **39,** 487–96 (1978).

123. Kimberlin, R. H. & Walker, C. Characteristics of a short incubation model of scrapie in the golden hamster. *J Gen Virol* **34,** 295–304 (1977).

124. Bruce, M. *et al.* Transmission of bovine spongiform encephalopathy and scrapie to mice: strain variation and the species barrier. *Philos Trans R Soc Lond B Biol Sci* **343,** 405–11 (1994).

125. Fraser, H. & Dickinson, A. G. Scrapie in mice. *Journal of Comparative Pathology* **83,** 29–40 (1973).

126. Bessen, R. A. *et al.* Non-genetic propagation of strain-specific properties of scrapie prion protein. *Nature* **375,** 698–700 (1995).

127. Bessen, R. A. & Marsh, R. F. Distinct PrP properties suggest the molecular basis of strain variation in transmissible mink encephalopathy. *J. Virol.* **68,** 7859–7868 (1994).

128. Bessen, R. A. & Marsh, R. F. Biochemical and physical properties of the prion protein from two strains of the transmissible mink encephalopathy agent. *J. Virol.* **66,** 2096–2101 (1992).

129. Kuczius, T. & Groschup, M. H. Differences in proteinase K resistance and neuronal deposition of abnormal prion proteins characterize bovine spongiform encephalopathy (BSE) and scrapie strains. *Mol Med* **5,** 406–18 (1999).

130. Safar, J., Cohen, F. E., Prusiner, S. B., Groschup, M. H. & Kretzschmar, H. Quantitative traits of prion strains are enciphered in the conformation of the prion protein. 227–235 (2000). at <http://www.cabdirect.org/abstracts/20013068552.html;jsessionid=B7D4D8E2E8689160F6BF01B30390AF20>

131. Wadsworth, J. D. *et al.* Strain-specific prion-protein conformation determined by metal ions. *Nat Cell Biol* **1,** 55–9 (1999).

132. Telling, G. C. *et al.* Evidence for the conformation of the pathologic isoform of the prion protein enciphering and propagating prion diversity. *Science (80-)* **274,** 2079–2082 (1996).

133. Khalili-Shirazi, A. *et al.* PrP glycoforms are associated in a strain-specific ratio in native PrPSc. *J Gen Virol* **86,** 2635–2644 (2005).

134. Yull, H. M. *et al.* Detection of type 1 prion protein in variant Creutzfeldt-Jakob disease. *Am J Pathol* **168,** 151–7 (2006).

135. Polymenidou, M. *et al.* Coexistence of multiple PrPSc types in individuals with Creutzfeldt-Jakob disease. *Lancet Neurol* **4,** 805–14 (2005).

136. Béringue, V. *et al.* A bovine prion acquires an epidemic bovine spongiform encephalopathy strain-like phenotype on interspecies transmission. *J Neurosci* **27,** 6965–71 (2007).

137. Wadsworth, J. D. F. *et al.* Human prion protein with valine 129 prevents expression of variant CJD phenotype. *Science* **306,** 1793–6 (2004).

138. Asante, E. A. BSE prions propagate as either variant CJD-like or sporadic CJD-like prion strains in transgenic mice expressing human prion protein. *The EMBO Journal* **21,** 6358–6366 (2002).

139. Lloyd, S. E. *et al.* Characterization of two distinct prion strains derived from bovine spongiform encephalopathy transmissions to inbred mice. *J Gen Virol* **85,** 2471–8 (2004).

140. Li, J., Browning, S., Mahal, S. P., Oelschlegel, A. M. & Weissmann, C. Darwinian evolution of prions in cell culture. *Science* **327,** 869–72 (2010).

141. Taylor, D. M. *et al.* Decontamination studies with the agents of bovine spongiform encephalopathy and scrapie. *Archives of Virology* **139,** 313–326 (1994).

142. Taylor, D. M., Fernie, K., McConnell, I. & Steele, P. J. Observations on thermostable subpopulations of the unconventional agents that cause transmissible degenerative encephalopathies. *Vet Microbiol* **64,** 33–8 (1998).

143. Arjona, A., Simarro, L., Islinger, F., Nishida, N. & Manuelidis, L. Two Creutzfeldt-Jakob disease agents reproduce prion protein-independent identities in cell cultures. *Proc Natl Acad Sci U S A* **101,** 8768–73 (2004).

144. Arima, K. *et al.* Biological and biochemical characteristics of prion strains conserved in persistently infected cell cultures. *J Virol* **79,** 7104–12 (2005).

145. Bruce, M. E. TSE strain variation. *Br Med Bull* **66,** 99–108 (2003).

146. Kimberlin, R. H., Cole, S. & Walker, C. A. Temporary and permanent modifications to a single strain of mouse scrapie on transmission to rats and hamsters. *J Gen Virol* **68 (Pt 7),** 1875–81 (1987).

147. Jahn, T. R. & Radford, S. E. The Yin and Yang of protein folding. *FEBS J* **272,** 5962–70 (2005).

148. Guijarro, J. I., Sunde, M., Jones, J. A., Campbell, I. D. & Dobson, C. M. Amyloid fibril formation by an SH3 domain. *Proc Natl Acad Sci U S A* **95,** 4224–8 (1998).

149. Eisenberg, D. & Jucker, M. The amyloid state of proteins in human diseases. *Cell* **148,** 1188–203 (2012).

150. Toyama, B. H. & Weissman, J. S. Amyloid structure: conformational diversity and consequences. *Annu Rev Biochem* **80,** 557–85 (2011).

151. Sunde, M. & Blake, C. The structure of amyloid fibrils by electron microscopy and X-ray diffraction. *Adv Protein Chem* **50,** 123–59 (1997).

152. Tycko, R. Progress towards a molecular-level structural understanding of amyloid fibrils. *Curr Opin Struct Biol* **14,** 96–103 (2004).

153. Petkova, A. T. *et al.* Self-propagating, molecular-level polymorphism in Alzheimer's beta-amyloid fibrils. *Science* **307,** 262–5 (2005).

154. Oosawa, F. & Asakura, S. *Thermodynamics of the Polymerization of Protein (Molecular Biology)*. 204 (Academic Press Inc, 1975). at <http://www.amazon.com/Thermodynamics-Polymerization-Protein-Molecular-Biology/dp/012527050X>

155. Gibbs, J. W. *On the equilibrium of heterogeneous substances*. (Trans. comn. Acad Arts Sci., 1878).

156. Volmer, M. & Weber, A. Keimbildung in übersättigten Gebilden. *The Journal of Chemical Physics* (1926).

157. Avrami, M. Kinetics of Phase Change. I General Theory. *The Journal of Chemical Physics* **7,** 1103 (1939).

158. Oosawa, F. & Kasai, M. A theory of linear and helical aggregations of macromolecules. *Journal of Molecular Biology* **4,** 10–21 (1962).

159. Becker, R. & Döring, W. Kinetische Behandlung der Keimbildung in übersättigten Dämpfen. *Ann Phys* **416,** 719–752 (1935).

160. Kaischew, R. & Stranski, I. N. The theory of the linear rate of crystallisation. *The Journal of Chemical Physics* (1934).

161. Stranski, I. N. & Kaischew, R. Crystal growth and crystal nucleation. *The Journal of Physics* (1935).

162. DePace, A. H., Santoso, A., Hillner, P. & Weissman, J. S. A critical role for amino-terminal glutamine/asparagine repeats in the formation and propagation of a yeast prion. *Cell* **93,** 1241–52 (1998).

163. Serio, T. R. *et al.* Nucleated conformational conversion and the replication of conformational information by a prion determinant. *Science (80-)* **289,** 1317–1321 (2000).

164. Padrick, S. B. & Miranker, A. D. Islet amyloid: phase partitioning and secondary nucleation are central to the mechanism of fibrillogenesis. *Biochemistry* **41,** 4694–703 (2002).

165. Zerovnik, E. Amyloid-fibril formation. Proposed mechanisms and relevance to conformational disease. *Eur J Biochem* **269,** 3362–71 (2002).

166. Ross, C. A., Poirier, M. A., Wanker, E. E. & Amzel, M. Polyglutamine fibrillogenesis: the pathway unfolds. *Proc Natl Acad Sci U S A* **100,** 1–3 (2003).

167. Thirumalai, D., Klimov, D. K. & Dima, R. I. Emerging ideas on the molecular basis of protein and peptide aggregation. *Curr Opin Struct Biol* **13,** 146–59 (2003).

168. Ferrone, F. A., Hofrichter, J., Sunshine, H. R. & Eaton, W. A. Kinetic studies on photolysis-induced gelation of sickle cell hemoglobin suggest a new mechanism. *Biophys J* **32,** 361–80 (1980).

169. Bishop, M. F. & Ferrone, F. A. Kinetics of nucleation-controlled polymerization. A perturbation treatment for use with a secondary pathway. *Biophys J* **46,** 631–44 (1984).

170. Ferrone, F. A., Hofrichter, J. & Eaton, W. A. Kinetics of sickle hemoglobin polymerization. II. A double nucleation mechanism. *J Mol Biol* **183,** 611–31 (1985).

171. Wegner, A. Spontaneous fragmentation of actin filaments in physiological conditions. *Nature* **296,** 266–7 (1982).

172. Wegner, A. & Savko, P. Fragmentation of actin filaments. *Biochemistry* **21,** 1909–13 (1982).

173. Collins, S. R., Douglass, A., Vale, R. D. & Weissman, J. S. Mechanism of prion propagation: amyloid growth occurs by monomer addition. *PLoS Biol* **2,** e321 (2004).

174. Knowles, T. P. J. *et al.* An analytical solution to the kinetics of breakable filament assembly. *Science* **326,** 1533–7 (2009).

175. Xue, W.-F., Hellewell, A. L., Hewitt, E. W. & Radford, S. E. Fibril fragmentation in amyloid assembly and cytotoxicity: when size matters. *Prion* **4,** 20–5

176. Xue, W.-F. *et al.* Fibril fragmentation enhances amyloid cytotoxicity. *J Biol Chem* **284,** 34272–82 (2009).

177. Silveira. The most infectious prion protein particles. *Nature* **437,** 257–261 (2005).

178. Kayed, R. *et al.* Common structure of soluble amyloid oligomers implies common mechanism of pathogenesis. *Science* **300,** 486–9 (2003).

179. Reixach, N., Deechongkit, S., Jiang, X., Kelly, J. W. & Buxbaum, J. N. Tissue damage in the amyloidoses: Transthyretin monomers and nonnative oligomers are the major cytotoxic species in tissue culture. *Proc Natl Acad Sci U S A* **101,** 2817–22 (2004).

180. Lesné, S. *et al.* A specific amyloid-beta protein assembly in the brain impairs memory. *Nature* **440,** 352–7 (2006).

181. Shankar, G. M. *et al.* Amyloid-beta protein dimers isolated directly from Alzheimer's brains impair synaptic plasticity and memory. *Nat Med* **14,** 837–42 (2008).

182. Lasmezas, C. I. *et al.* Transmission of the BSE agent to mice in the absence of detectable abnormal prion protein. *Science (80-)* **275,** 402–405 (1997).

183. Hill, A. F., Antoniou, M. & Collinge, J. Protease-resistant prion protein produced in vitro lacks detectable infectivity. *J Gen Virol* **80 (Pt 1),** 11–14 (1999).

184. Hill, A. F. *et al.* Species-barrier-independent prion replication in apparently resistant species. *Proceedings of the National Academy of Sciences* **97,** 10248–10253 (2000).

185. Stöhr, J. *et al.* Purified and synthetic Alzheimer's amyloid beta (Aβ) prions. *Proc Natl Acad Sci U S A* **109,** 11025–30 (2012).

186. Meyer-Luehmann, M. *et al.* Exogenous induction of cerebral beta-amyloidogenesis is governed by agent and host. *Science* **313,** 1781–4 (2006).

187. Wolynes, P. G. Energy landscapes and solved protein-folding problems. *Philos Transact A Math Phys Eng Sci* **363,** 453–64; discussion 464–7 (2005).

188. Uversky, V. N. & Fink, A. L. Conformational constraints for amyloid fibrillation: the importance of being unfolded. *Biochim Biophys Acta* **1698,** 131–53 (2004).

189. Harrison, P. M., Chan, H. S., Prusiner, S. B. & Cohen, F. E. Thermodynamics of model prions and its implications for the problem of prion protein folding. *J Mol Biol* **286,** 593–606 (1999).

190. Soto, C. *Prions - The new biology of proteins*. (CRC - Taylor & Francis - Taylor & Francis group, 2006).

191. Eigen, M. Prionics or the kinetic basis of prion diseases. *Biophys Chem* **63,** A1–18 (1996).

192. Come, J. H., Fraser, P. E. & Lansbury Jr., P. T. A kinetic model for amyloid formation in the prion diseases: importance of seeding. *Proc Natl Acad Sci U S A* **90,** 5959–5963 (1993).

193. Jarrett, J. T. & Lansbury Jr., P. T. Seeding "one-dimensional crystallization" of amyloid: a pathogenic mechanism in Alzheimer's disease and scrapie? *Cell* **73,** 1055–1058 (1993).

194. Caughey, B. Interactions between prion protein isoforms: the kiss of death? *Trends Biochem Sci* **26,** 235–242 (2001).

195. Caughey, B. & Lansbury, P. T. Protofibrils, pores, fibrils, and neurodegeneration: separating the responsible protein aggregates from the innocent bystanders. *Annu Rev Neurosci* **26,** 267–298 (2003).

196. Telling, G. C. *et al.* Prion propagation in mice expressing human and chimeric PrP transgenes implicates the interaction of cellular PrP with another protein. *Cell* **83,** 79–90 (1995).

197. Kaneko, K. *et al.* Evidence for protein X binding to a discontinuous epitope on the cellular prion protein during scrapie prion propagation. *Proc Natl Acad Sci U S A* **94,** 10069–10074 (1997).

198. Saborio, G. P. *et al.* Cell-lysate conversion of prion protein into its protease-resistant isoform suggests the participation of a cellular chaperone. *Biochem Biophys Res Commun* **258,** 470–475 (1999).

199. Kocisko, D. A. *et al.* Cell-free formation of protease-resistant prion protein. *Nature* **370,** 471–474 (1994).

200. Cordeiro, Y. *et al.* DNA converts cellular prion protein into the beta-sheet conformation and inhibits prion peptide aggregation. *J Biol Chem* **276,** 49400–49409 (2001).

201. Saá, P. *et al.* Strain-specific role of RNAs in prion replication. *J Virol* **86,** 10494–504 (2012).

202. Atarashi, R. *et al.* Ultrasensitive detection of scrapie prion protein using seeded conversion of recombinant prion protein. *Nat Methods* **4,** 645–650 (2007).

203. Deleault, N. R., Harris, B. T., Rees, J. R. & Supattapone, S. Formation of native prions from minimal components in vitro. *Proc Natl Acad Sci U S A* **104,** 9741–9746 (2007).

204. Atarashi, R. *et al.* Simplified ultrasensitive prion detection by recombinant PrP conversion with shaking. *Nat Methods* **5,** 211–212 (2008).

205. Wang, F., Wang, X., Yuan, C. G. & Ma, J. Generating a prion with bacterially expressed recombinant prion protein. *Science (80-)* **327,** 1132–1135 (2010).

206. Raeber, A. J., Borchelt, D. R., Scott, M. & Prusiner, S. B. Attempts to convert the cellular prion protein into the scrapie isoform in cell-free systems. *J Virol* **66,** 6155–6163 (1992).

207. Castilla, J., Saa, P., Hetz, C. & Soto, C. In vitro generation of infectious scrapie prions. *Cell* **121,** 195–206 (2005).

208. Saa, P., Castilla, J. & Soto, C. Ultra-efficient replication of infectious prions by automated protein misfolding cyclic amplification. *J Biol Chem* **281,** 35245–35252 (2006).

209. Supattapone, S., Deleault, N. R. & Rees, J. R. Amplification of purified prions in vitro. *Methods Mol Biol* **459,** 117–130 (2008).

210. Soto, C., Saborio, G. P. & Anderes, L. Cyclic amplification of protein misfolding: application to prion-related disorders and beyond. *Trends Neurosci* **25,** 390–394 (2002).

211. Castilla Saá, P., and Soto, C., J. in *Techniques in prion research* (Grassi, S. L. and J.) (Birkhauser Verlag, 2004).

212. Castilla, J., Saa, P. & Soto, C. Detection of prions in blood. *Nat Med* **11,** 982–985 (2005).

213. Castilla, J. *et al.* Protein misfolding cyclic amplification for diagnosis and prion propagation studies. *Methods Enzymol* **412,** 3–21 (2006).

214. Lucassen, R., Nishina, K. & Supattapone, S. In vitro amplification of protease-resistant prion protein requires free sulfhydryl groups. *Biochemistry* **42,** 4127–4135 (2003).

215. Zhang, W., Wu, J., Li, Y., Carke, R. C. & Wong, T. The in vitro bioassay systems for the amplification and detection of abnormal prion PrP(Sc) in blood and tissues. *Transfus Med Rev* **22,** 234–242 (2008).

216. Deleault, N. R., Kascsak, R., Geoghegan, J. C. & Supattapone, S. Species-dependent differences in cofactor utilization for formation of the protease-resistant prion protein in vitro. *Biochemistry* **49,** 3928–3934 (2010).

217. Shi, S. *et al.* The propagation of hamster-adapted scrapie PrPSc can be enhanced by reduced pyridine nucleotide in vitro. *Febs J* **276,** 1536–1545 (2009).

218. Geoghegan, J. C., Miller, M. B., Kwak, A. H., Harris, B. T. & Supattapone, S. Trans-dominant inhibition of prion propagation in vitro is not mediated by an accessory cofactor. *PLoS Pathog* **5,** e1000535 (2009).

219. Patent US7871776 - Compositions and methods for enhancing the identification of prior protein PrPSc. at <http://www.google.de/patents?hl=de&lr=&vid=USPAT7871776&id=FOLwAAAAEBAJ&oi=fnd&dq=Compositions+and+methods+for+enhancing+the+identification+of+prior+protein+PrPSc&printsec=abstract#v=onepage&q=C

ompositions and methods for enhancing the identification of prior protein PrPSc&f=false>

220. Nishina, K., Deleault, N. R., Lucassen, R. W. & Supattapone, S. In vitro prion protein conversion in detergent-solubilized membranes. *Biochemistry* **43,** 2613–2621 (2004).

221. Murayama, Y. *et al.* Sulfated dextrans enhance in vitro amplification of bovine spongiform encephalopathy PrP(Sc) and enable ultrasensitive detection of bovine PrP(Sc). *PLoS One* **5,** (2010).

222. Nishina, K. A. *et al.* The stoichiometry of host PrPC glycoforms modulates the efficiency of PrPSc formation in vitro. *Biochemistry* **45,** 14129–14139 (2006).

223. Mays, C. E., Titlow, W., Seward, T., Telling, G. C. & Ryou, C. Enhancement of protein misfolding cyclic amplification by using concentrated cellular prion protein source. *Biochem Biophys Res Commun* **388,** 306–310 (2009).

224. Rigter, A. *et al.* Prion protein self-peptides modulate prion interactions and conversion. *BMC Biochem* **10,** 29 (2009).

225. Jackson, G. S. *et al.* Location and properties of metal-binding sites on the human prion protein. *Proc Natl Acad Sci U S A* **98,** 8531–8535 (2001).

226. Kim, N. H. *et al.* Effect of transition metals (Mn, Cu, Fe) and deoxycholic acid (DA) on the conversion of PrPC to PrPres. *Faseb J* **19,** 783–785 (2005).

227. Fujihara, A. *et al.* Hyperefficient PrP Sc amplification of mouse-adapted BSE and scrapie strain by protein misfolding cyclic amplification technique. *Febs J* **276,** 2841–2848 (2009).

228. Bieschke, J. *et al.* Autocatalytic self-propagation of misfolded prion protein. *Proc Natl Acad Sci U S A* **101,** 12207–12211 (2004).

229. Piening, N., Weber, P., Giese, A. & Kretzschmar, H. Breakage of PrP aggregates is essential for efficient autocatalytic propagation of misfolded prion protein. *Biochem Biophys Res Commun* **326,** 339–343 (2005).

230. Gonzalez-Montalban, N. *et al.* Highly efficient protein misfolding cyclic amplification. *PLoS Pathog* **7,** e1001277 (2011).

231. Morales, R., Duran-Aniotz, C., Diaz-Espinoza, R., Camacho, M. V & Soto, C. Protein misfolding cyclic amplification of infectious prions. *Nat Protoc* **7,** 1397–409 (2012).

232. Orrú, C. D. *et al.* Human variant Creutzfeldt-Jakob disease and sheep scrapie PrP(res) detection using seeded conversion of recombinant prion protein. *Protein Eng Des Sel* **22,** 515–21 (2009).

233. Orru, C. D. *et al.* Prion disease blood test using immunoprecipitation and improved quaking-induced conversion. *MBio* **2,** e00078–11 (2011).

234. Wilham, J. M. *et al.* Rapid end-point quantitation of prion seeding activity with sensitivity comparable to bioassays. *PLoS Pathog* **6,** e1001217 (2010).

235. Bueler, H. *et al.* Mice devoid of PrP are resistant to scrapie. *Cell* **73,** 1339–1347 (1993).

236. Legname, G. *et al.* Synthetic mammalian prions. *Science* **305,** 673–6 (2004).

237. Riek, R. *et al.* NMR structure of the mouse prion protein domain PrP(121-321). *Nature* **382,** 180–182 (1996).

238. Riek, R., Hornemann, S., Wider, G., Glockshuber, R. & Wuthrich, K. NMR characterization of the full-length recombinant murine prion protein, mPrP(23-231). *FEBS Lett* **413,** 282–288 (1997).

239. Cohen, F. E. Protein misfolding and prion diseases. *J Mol Biol* **293,** 313–320 (1999).

240. Stahl, N., Borchelt, D. R., Hsiao, K. & Prusiner, S. B. Scrapie prion protein contains a phosphatidylinositol glycolipid. *Cell* **51,** 229–240 (1987).

241. Vey, M. *et al.* Subcellular colocalization of the cellular and scrapie prion proteins in caveolae-like membranous domains. *Proc Natl Acad Sci U S A* **93,** 14945–14949 (1996).

242. Naslavsky, N., Stein, R., Yanai, A., Friedlander, G. & Taraboulos, A. Characterization of detergent-insoluble complexes containing the cellular prion protein and its scrapie isoform. *J Biol Chem* **272,** 6324–6331 (1997).

243. Simons, K. & Toomre, D. Lipid rafts and signal transduction. *Nat Rev Mol Cell Biol* **1,** 31–39 (2000).

244. Simons, K. & Ehehalt, R. Cholesterol, lipid rafts, and disease. *J Clin Invest* **110,** 597–603 (2002).

245. Parchi, P. *et al.* Typing prion isoforms. *Nature* **386,** 232–234 (1997).

246. Hill, A. F. *et al.* Molecular classification of sporadic Creutzfeldt-Jakob disease. *Brain* **126,** 1333–1346 (2003).

247. James, T. L. *et al.* Solution structure of a 142-residue recombinant prion protein corresponding to the infectious fragment of the scrapie isoform. *Proc Natl Acad Sci U S A* **94,** 10086–10091 (1997).

248. Zahn, R. *et al.* NMR solution structure of the human prion protein. *Proc Natl Acad Sci U S A* **97,** 145–150 (2000).

249. Liu, H. *et al.* Solution structure of Syrian hamster prion protein rPrP(90-231). *Biochemistry* **38,** 5362–5377 (1999).

250. Lopez Garcia, F., Zahn, R., Riek, R. & Wuthrich, K. NMR structure of the bovine prion protein. *Proc Natl Acad Sci U S A* **97,** 8334–8339 (2000).

251. Calzolai, L., Lysek, D. A., Perez, D. R., Guntert, P. & Wuthrich, K. Prion protein NMR structures of chickens, turtles, and frogs. *Proc Natl Acad Sci U S A* **102,** 651–655 (2005).

252. Kretzschmar, H. A., Prusiner, S. B., Stowring, L. E. & DeArmond, S. J. Scrapie prion proteins are synthesized in neurons. *Am J Pathol* **122,** 1–5 (1986).

253. Manson, J. C., Clarke, A. R., McBride, P. A., McConnell, I. & Hope, J. PrP gene dosage determines the timing but not the final intensity or distribution of lesions in scrapie pathology. *Neurodegeneration* **3,** 331–340 (1994).

254. Tobler, I. *et al.* Altered circadian activity rhythms and sleep in mice devoid of prion protein. *Nature* **380,** 639–642 (1996).

255. Brown, D. R., Nicholas, R. S. & Canevari, L. Lack of prion protein expression results in a neuronal phenotype sensitive to stress. *J Neurosci Res* **67,** 211–224 (2002).

256. Sakaguchi, S. *et al.* Loss of cerebellar Purkinje cells in aged mice homozygous for a disrupted PrP gene. *Nature* **380,** 528–531 (1996).

257. Moore, R. C. *et al.* Ataxia in prion protein (PrP)-deficient mice is associated with upregulation of the novel PrP-like protein doppel. *J Mol Biol* **292,** 797–817 (1999).

258. Rossi, D. *et al.* Onset of ataxia and Purkinje cell loss in PrP null mice inversely correlated with Dpl level in brain. *Embo J* **20,** 694–702 (2001).

259. Behrens, A. & Aguzzi, A. Small is not beautiful: antagonizing functions for the prion protein PrP(C) and its homologue Dpl. *Trends Neurosci* **25,** 150–154 (2002).

260. Shmerling, D. *et al.* Expression of amino-terminally truncated PrP in the mouse leading to ataxia and specific cerebellar lesions. *Cell* **93,** 203–214 (1998).

261. Tuzi, N. L., Gall, E., Melton, D. & Manson, J. C. Expression of doppel in the CNS of mice does not modulate transmissible spongiform encephalopathy disease. *J Gen Virol* **83,** 705–711 (2002).

262. Sailer, A., Bueler, H., Fischer, M., Aguzzi, A. & Weissmann, C. No propagation of prions in mice devoid of PrP. *Cell* **77,** 967–968 (1994).

263. Sakaguchi, S. *et al.* Accumulation of proteinase K-resistant prion protein (PrP) is restricted by the expression level of normal PrP in mice inoculated with a mouse-adapted strain of the Creutzfeldt-Jakob disease agent. *J Virol* **69,** 7586–7592 (1995).

264. Büeler, H. *et al.* High prion and PrPSc levels but delayed onset of disease in scrapie-inoculated mice heterozygous for a disrupted PrP gene. *Mol Med* **1,** 19–30 (1994).

265. Brown, D. R. *et al.* The cellular prion protein binds copper in vivo. *Nature* **390,** 684–687 (1997).

266. Kramer, M. L. *et al.* Prion protein binds copper within the physiological concentration range. *J Biol Chem* **276,** 16711–16719 (2001).

267. Pattison, I. H. & Jebbett, J. N. Clinical and histological recovery from the scrapie-like spongiform encephalopathy produced in mice by feeding them with cuprizone. *J Pathol* **109,** 245–250 (1973).

268. McCord, J. M. & Fridovich, I. Superoxide Dismutase. AN ENZYMIC FUNCTION FOR ERYTHROCUPREIN (HEMOCUPREIN). *J. Biol. Chem.* **244,** 6049–6055 (1969).

269. Brown, D. R. Copper and prion disease. *Brain Res Bull* **55,** 165–173 (2001).

270. Harris, D. A. Cellular biology of prion diseases. *Clin Microbiol Rev* **12,** 429–444 (1999).

271. Harris, D. A. Trafficking, turnover and membrane topology of PrP. *Br Med Bull* **66,** 71–85 (2003).

272. Pauly, P. C. & Harris, D. A. Copper stimulates endocytosis of the prion protein. *J Biol Chem* **273,** 33107–33110 (1998).

273. Waggoner, D. J. *et al.* Brain copper content and cuproenzyme activity do not vary with prion protein expression level. *J Biol Chem* **275,** 7455–7458 (2000).

274. Wong, B. S. *et al.* Increased levels of oxidative stress markers detected in the brains of mice devoid of prion protein. *J Neurochem* **76,** 565–572 (2001).

275. Thackray, A. M., Knight, R., Haswell, S. J., Bujdoso, R. & Brown, D. R. Metal imbalance and compromised antioxidant function are early changes in prion disease. *Biochem J* **362,** 253–258 (2002).

276. Wong, B. S. *et al.* Aberrant metal binding by prion protein in human prion disease. *J Neurochem* **78,** 1400–1408 (2001).

277. Qin, K. *et al.* Copper(II)-induced conformational changes and protease resistance in recombinant and cellular PrP. Effect of protein age and deamidation. *J Biol Chem* **275,** 19121–19131 (2000).

278. Mouillet-Richard, S. *et al.* Signal transduction through prion protein. *Science (80-)* **289,** 1925–1928 (2000).

279. Spielhaupter, C. & Schatzl, H. M. PrPC directly interacts with proteins involved in signaling pathways. *J Biol Chem* **276,** 44604–44612 (2001).

280. Kuwahara, C. *et al.* Prions prevent neuronal cell-line death. *Nature* **400,** 225–226 (1999).

281. Bounhar, Y., Zhang, Y., Goodyer, C. G. & LeBlanc, A. Prion protein protects human neurons against Bax-mediated apoptosis. *J Biol Chem* **276,** 39145–39149 (2001).

282. Nelson, R. *et al.* Structure of the cross-beta spine of amyloid-like fibrils. *Nature* **435,** 773–8 (2005).

283. Ritter, C. *et al.* Correlation of structural elements and infectivity of the HET-s prion. *Nature* **435,** 844–8 (2005).

284. Lührs, T. *et al.* 3D structure of Alzheimer's amyloid-beta(1-42) fibrils. *Proc Natl Acad Sci U S A* **102,** 17342–7 (2005).

285. Wasmer, C. *et al.* Amyloid fibrils of the HET-s(218-289) prion form a beta solenoid with a triangular hydrophobic core. *Science* **319,** 1523–6 (2008).

286. Laganowsky, A. *et al.* Atomic view of a toxic amyloid small oligomer. *Science* **335,** 1228–31 (2012).

287. Knowles, T. P. *et al.* Role of intermolecular forces in defining material properties of protein nanofibrils. *Science* **318,** 1900–3 (2007).

288. Sambrook, J. *Molecular Cloning: A Laboratory Manual, Third Edition (3 volume set)*. 999 (Cold Spring Harbor Laboratory Press, 2000). at

<http://www.amazon.com/Molecular-Cloning-Laboratory-Manual-Edition/dp/0879695773>

289. Dunn, B. M., Speicher, D. W. & Wingfield, P. T. *Short Protocols in Protein Science*. 810 (Wiley, 2003). at <http://www.amazon.com/Short-Protocols-Protein-Science-Dunn/dp/0471483389>

290. *Short Protocols in Molecular Biology, 4th Edition*. 1104 (Current Protocols, 1999). at <http://www.amazon.com/Short-Protocols-Molecular-Biology-Edition/dp/047132938X>

291. Sanders, C. R. & Prosser, R. S. Bicelles: a model membrane system for all seasons? *Structure* **6,** 1227–34 (1998).

292. Sanders, C. R., Hare, B. J., Howard, K. P. & Prestegard, J. H. Magnetically-oriented phospholipid micelles as a tool for the study of membrane-associated molecules. *Progress in Nuclear Magnetic Resonance Spectroscopy* **26,** 421–444 (1994).

293. Sanders, C. R. & Landis, G. C. Reconstitution of membrane proteins into lipid-rich bilayered mixed micelles for NMR studies. *Biochemistry* **34,** 4030–40 (1995).

294. Sanders, C. R. & Schwonek, J. P. Characterization of magnetically orientable bilayers in mixtures of dihexanoylphosphatidylcholine and dimyristoylphosphatidylcholine by solid-state NMR. *Biochemistry* **31,** 8898–905 (1992).

295. Sanders, C. R. Solid state 13C NMR of unlabeled phosphatidylcholine bilayers: spectral assignments and measurement of carbon-phosphorus dipolar couplings and 13C chemical shift anisotropies. *Biophys J* **64,** 171–81 (1993).

296. Sanders, C. R. & Prestegard, J. H. Magnetically orientable phospholipid bilayers containing small amounts of a bile salt analogue, CHAPSO. *Biophys J* **58,** 447–60 (1990).

297. Tjandra, N. Direct Measurement of Distances and Angles in Biomolecules by NMR in a Dilute Liquid Crystalline Medium. *Science (80-)* **278,** 1111–1114 (1997).

298. Bax, A. & Tjandra, N. High-resolution heteronuclear NMR of human ubiquitin in an aqueous liquid crystalline medium. *Journal of Biomolecular NMR* **10,** 289–292

299. Lührs, T., Zahn, R. & Wüthrich, K. Amyloid formation by recombinant full-length prion proteins in phospholipid bicelle solutions. *J Mol Biol* **357,** 833–41 (2006).

300. Hauser, H., Pascher, I., Pearson, R. H. & Sundell, S. Preferred conformation and molecular packing of phosphatidylethanolamine and phosphatidylcholine. *Biochimica et Biophysica Acta (BBA) - Reviews on Biomembranes* **650,** 21–51 (1981).

301. Burns, R. A., Roberts, M. F., Dluhy, R. & Mendelsohn, R. Monomer-to-micelle transition of dihexanoylphosphatidylcholine: carbon-13 NMR and Raman studies. *J Am Chem Soc* **104,** 430–438 (1982).

302. Ottiger, M. & Bax, A. Characterization of magnetically oriented phospholipid micelles for measurement of dipolar couplings in macromolecules. *Journal of Biomolecular NMR* **12,** 361–372

303. Lewis, B. A. & Engelman, D. M. Lipid bilayer thickness varies linearly with acyl chain length in fluid phosphatidylcholine vesicles. *Journal of Molecular Biology* **166,** 211–217 (1983).

304. Tanford, C. & Reynolds, J. A. Characterization of membrane proteins in detergent solutions. *Biochimica et Biophysica Acta (BBA) - Reviews on Biomembranes* **457,** 133–170 (1976).

305. Tausk, R. J. M., Van Esch, J., Karmiggelt, J., Voordouw, G. & Overbeek, J. T. G. Physical chemical studies of short-chain lecithin homologues. II. *Biophysical Chemistry* **1,** 184–203 (1974).

306. Deluweit, F. & Lührs, T. Device and method for production and analysis of prions. (2012).

307. Deluweit, F. & Lührs, T. Device and method for production and analysis of prions. (2012).

308. Peretz, D. *et al.* Inactivation of prions by acidic sodium dodecyl sulfate. *J Virol* **80,** 322–331 (2006).

309. Fichet, G. *et al.* Investigations of a prion infectivity assay to evaluate methods of decontamination. *J Microbiol Methods* **70,** 511–8 (2007).

310. Moser, M., Colello, R. J., Pott, U. & Oesch, B. Developmental expression of the prion protein gene in glial cells. *Neuron* **14,** 509–517 (1995).

311. Moudjou, M., Frobert, Y., Grassi, J. & La Bonnardière, C. Cellular prion protein status in sheep: tissue-specific biochemical signatures. *J Gen Virol* **82,** 2017–24 (2001).

312. Wadsworth, J. D. F. & Collinge, J. Molecular pathology of human prion disease. *Acta Neuropathol* **121,** 69–77 (2011).

313. Cohen, S. I. A., Vendruscolo, M., Dobson, C. M. & Knowles, T. P. J. Nucleated polymerization with secondary pathways. III. Equilibrium behavior and oligomer populations. *J Chem Phys* **135,** 065107 (2011).

314. Hill, E. K., Krebs, B., Goodall, D. G., Howlett, G. J. & Dunstan, D. E. Shear flow induces amyloid fibril formation. *Biomacromolecules* **7,** 10–3 (2006).

315. Eggersdorfer, M. L., Kadau, D., Herrmann, H. J. & Pratsinis, S. E. Fragmentation and restructuring of soft-agglomerates under shear. *J Colloid Interface Sci* **342,** 261–8 (2010).

316. Deluweit, F., Gupta, V., Ritter, C. & Lührs, T. Kinetic Selection of Prion Seed Populations. *in preparation* (2012).

317. Taylor, G. I. Stability of a Viscous Liquid Contained between Two Rotating Cylinders. *Philosophical Transactions of the Royal Society of London. Series A, Containing Papers of a Mathematical or Physical Character* **223 ,** 289–343 (1923).

318. Bird Steward, W. E., Lightfood, E. N., R. B. *Transport phenomena*. (Marcel Dekker, New York, 1960).

319. Dickinson, A. G. in *Frontiers of Biol. S* (Kimberlin, R. H.) 209–241 (Amsterdam: North-Holland 1976. (Frontiers of Biology), 1976). at <http://www.amazon.com/Virus-Diseases-Animals-Frontiers-Biol/dp/0720404185>

320. Chandler, R. L. Experimental scrapie in the mouse. *Research in Veterinary Science* 276–285 (1963).

321. Pattison, I. H. & Jones, K. M. Modification of a strain of mouse-adapted scrapie by passage through rats. *Res Vet Sci* **9,** 408–10 (1968).

322. Chandler, R. L. & Turfrey, B. A. Inoculation of voles, Chinese hamsters, gerbils and guinea-pigs with scrapie brain material. *Res Vet Sci* **13,** 219–24 (1972).

323. Kimberlin, R. H. & Marsh, R. F. Comparison of scrapie and transmissible mink encephalopathy in hamsters. I. Biochemical studies of brain during development of disease. *J Infect Dis* **131,** 97–103 (1975).

324. Hecker, R. *et al.* Replication of distinct scrapie prion isolates is region specific in brains of transgenic mice and hamsters. *Genes Dev* **6,** 1213–1228 (1992).

325. Scott, M. *et al.* Transgenic mice expressing hamster prion protein produce species-specific scrapie infectivity and amyloid plaques. *Cell* **59,** 847–57 (1989).

326. Bosque, P. J. & Prusiner, S. B. Cultured cell sublines highly susceptible to prion infection. *J Virol* **74,** 4377–4386 (2000).

327. Lehmann, S. Prion propagation in cell culture. *Methods Mol Biol* **299,** 227–34 (2005).

328. Nishida, N. *et al.* Successful transmission of three mouse-adapted scrapie strains to murine neuroblastoma cell lines overexpressing wild-type mouse prion protein. *J Virol* **74,** 320–5 (2000).

329. Rubenstein, R. *et al.* Demonstration of scrapie strain diversity in infected PC12 cells. *J Gen Virol* **73 (Pt 11,** 3027–31 (1992).

330. Schätzl, H. M. *et al.* A hypothalamic neuronal cell line persistently infected with scrapie prions exhibits apoptosis. *J Virol* **71,** 8821–31 (1997).

331. Vorberg, I., Raines, A., Story, B. & Priola, S. A. Susceptibility of common fibroblast cell lines to transmissible spongiform encephalopathy agents. *J Infect Dis* **189,** 431–9 (2004).

332. Klöhn, P.-C., Stoltze, L., Flechsig, E., Enari, M. & Weissmann, C. A quantitative, highly sensitive cell-based infectivity assay for mouse scrapie prions. *Proc Natl Acad Sci U S A* **100,** 11666–71 (2003).

333. Mahal, S. P. *et al.* Prion strain discrimination in cell culture: the cell panel assay. *Proc Natl Acad Sci U S A* **104,** 20908–13 (2007).

334. Browning, S. *et al.* Abrogation of complex glycosylation by swainsonine results in strain- and cell-specific inhibition of prion replication. *J Biol Chem* **286,** 40962–73 (2011).

335. Gonzalez-Montalban, N. & Baskakov, I. V. Assessment of strain-specific PrP(Sc) elongation rates revealed a transformation of PrP(Sc) properties during protein misfolding cyclic amplification. *PLoS One* **7,** e41210 (2012).

336. Danzer, K. M., Krebs, S. K., Wolff, M., Birk, G. & Hengerer, B. Seeding induced by alpha-synuclein oligomers provides evidence for spreading of alpha-synuclein pathology. *J Neurochem* **111,** 192–203 (2009).

337. Volpicelli-Daley, L. A. *et al.* Exogenous α-synuclein fibrils induce Lewy body pathology leading to synaptic dysfunction and neuron death. *Neuron* **72,** 57–71 (2011).

338. Luk, K. C. *et al.* Pathological α-synuclein transmission initiates Parkinson-like neurodegeneration in nontransgenic mice. *Science* **338,** 949–53 (2012).

339. Langer, F. *et al.* Soluble Aβ seeds are potent inducers of cerebral β-amyloid deposition. *J Neurosci* **31,** 14488–95 (2011).

340. Maa, Y. F. & Hsu, C. C. Effect of high shear on proteins. *Biotechnol Bioeng* **51,** 458–465 (1996).

341. Breyer, J. *et al.* Detergents modify proteinase K resistance of PrP Sc in different transmissible spongiform encephalopathies (TSEs). *Vet Microbiol* **157,** 23–31 (2012).